Multiport Broadband Matching and its Application in the Design of Feed Networks for Array Antennas

by

Clifford Richard Curry

A dissertation submitted in partial fulfillment

of the requirements for the degree of

Doctor of Philosophy

University of Washington

1997

Approved by F C Anderson

Chairperson of Supervisory Committee

Electrical Engineering Department

Date 1/28/97

In presenting this dissertation in partial fulfillment of the requirements for the Doctoral degree at the University of Washington, I agree that the Library shall make its copies freely available for inspection. I further agree that extensive copying of this dissertation is allowable only for scholarly purposes, consistent with "fair use" as described in the U. S. Copyright Law. Requests for copying or reproduction of this dissertation may be referred to University Microfilm, 1490 Eisenhower Place, P.O. Box 975, Ann Arbor, MI 48106, to whom the author has granted "the right to reproduce and sell (a) copies of the manuscript in microform and/or (b) printed copies of the manuscript made from microform."

Signature Clifford R. Cummings

Date 1/28/97

University of Washington

Abstract

Multiport Broadband Matching and its Application in the Design of Feed Networks for Array Antennas

by

Clifford Richard Curry

Chairperson of the Supervisory Committee: Professor Jonny Andersen
Department of Electrical Engineering

The design of 2N-port networks that allow good power flow between N isolated resistors and a general, passive, N-port network is discussed. A new design procedure is derived by first solving a multiport matching problem exactly for a particular class of load network. Then a strategy to extend this design to general load networks is presented. A congruence transformation that approximately diagonalizes the impedance matrix of a given multiport over a band of frequencies is found. It is shown how this congruence transformation can be practically implemented as a network at microwave frequencies. This 2N port transforming network is placed in front of the given multiport, so that the impedance looking into the transforming network consists of N approximately isolated impedances. Then N two port matching networks are designed to be placed between the isolated resistors and the input to the transforming network. These matching networks together with the

transforming network constitute a 2N port lossless coupling network with the desired performance. A specific multiport network model for array antennas is developed. A new expression for the power dissipated by a load with a Toeplitz immittance matrix, excited by a progressive phase signal, is derived. It is shown how the design of coupling networks at a particular frequency, and for a particular excitation pattern, is straightforward, but the performance can be unsatisfactory at other frequencies or with other excitation patterns. Results of several coupling network design techniques as applied to a feed network for a four element, linear array of slots at 3 GHz are presented.

Table of Contents

List of Figures

List of tables

ACKNOWLEDGMENTS

The author wishes to express sincere appreciation to Professor Jonny Andersen for his guidance and advice in the preparation of this manuscript. In addition, special thanks to Dr. W. Preston Geren for his support and valuable input during this research.

DEDICATION

To my children, Sarah and Paul, and to my wife, Susan Curry, for all the love, support, and encouragement they have shown me.

1.0 Introduction

This dissertation concerns the design of multiport coupling networks that provide good power flow between uncoupled resistive networks, and a general, complex, multiport. A design procedure for maximum power extraction from a multiport source at a particular frequency and excitation is presented, and then ways to generalize from these conditions to *ranges* of frequencies and arbitrary excitation patterns are given.

1.1 Research motivation

The motivation for these developments is the question of how to connect array antennas, often used in radar, radio, and ultrasound systems, to the electronics that constitute the receiver and transmitter parts of those systems. The designer of the antenna system needs to know how the received signal can be maximized, given a particular antenna, and incident wave. When transmitting, the ratio of the power delivered to the antenna divided by the maximum power available from the source excitation needs to be maximized to reduce the cost and complexity of the transmitting electronics.

The power flow into a multiport network is a function of the magnitude and phase pattern of the excitation source. Therefore, when a coupling network is designed to reduce the power reflected by the antenna, the success of the design will vary with the excitation. For example, a network which provides a

good match for a broadside beam may not do so well for a beam steered off broadside.

One exception to this situation is when the impedance matrix of the coupling network, as seen from the antenna, is the complex conjugate of the impedance matrix of the antenna. In this case, the power into the antenna is independent of the excitation pattern. However, perfect conjugate matching over a range of frequencies is not physically possible, therefore this solution is not applicable in the important broadband design condition. In applications, the perfect match and excitation pattern independence of conjugate loading will be sacrificed for approximate match and approximate excitation independence over a given band of frequencies. This dissertation provides design procedures for practical networks that provide good performance on both these dimensions.

1.2 Literature Review

The problems that mutual coupling causes in array antennas have been known for some time, and various solutions have been proposed [33], [34], [35], [43]. A paper by Bloch[1] views the antenna feed as multiport network, and identifies true conjugate loading as optimal. Several of these papers include techniques to cancel the reactive part of the mutual coupling, however, they do not mention the real coupling that exists between antenna elements.

The fact that conjugate loading is just one way to extract all the power from a multiport source was made clear by Desoer [8]. Other papers have made contributions to the field [12], [26], [5]. In general, finding useful optimum loads for multiport sources other than the conjugate load remains an unsolved problem.

Although broadband matching a single port load has many potential solutions, [21], [39], [40], [41], [42], the problem of extending match to a range of frequencies between two multiport loads, has not been addressed.

The realization that a physical element, the multiport transformer, can perform an arbitrary congruence transformation on multiport impedance and admittance matrices was probably reached sometime in the 1940's. Bellevitch [6] was one of the first to use the transformer explicitly.

Developments in this dissertation are an extension of work reported by Geren, Curry, and Andersen [7] this year.

1.3 The content of this dissertation

The necessary and sufficient conditions on a lossless two port coupling network that is placed between a resistive source and a known, complex load impedance to achieve a particular power gain vs. frequency response are known (Figure 1).

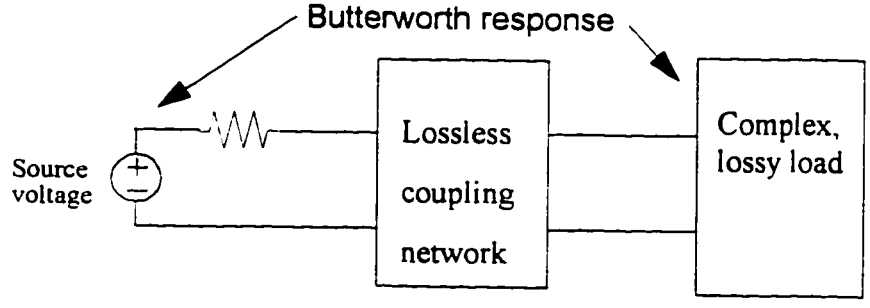

FIGURE 1. Necessary and sufficient conditions are known

Similar conditions on a lossless multiport coupling network are not known (Figure 2).

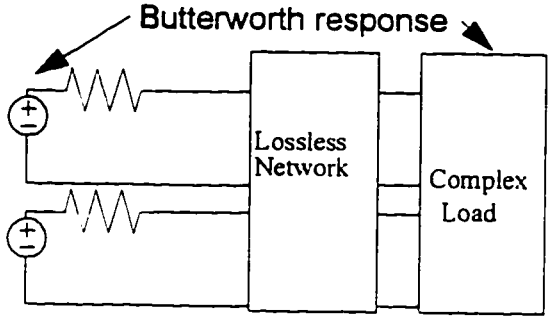

FIGURE 2. Necessary or sufficient conditions are unknown

One of the contributions of this dissertation is that sufficient conditions for a restricted class of complex multiport load impedances are found (Figure 3).

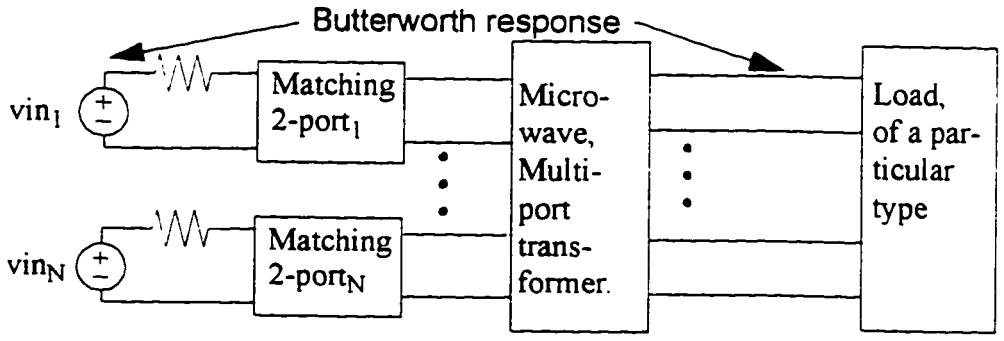

FIGURE 3. A sufficient design, for some loads.

The loads for which sufficient conditions are found are those whose impedance or admittance matrices can be diagonalized over all frequencies with a constant congruence transformation.

This dissertation asserts that finding a constant congruence transformation that *approximately* diagonalizes the impedance or admittance matrices of a load over a frequency band of interest will lead to a coupling network that *approximately* achieves a particular power gain vs. frequency response over that band. Evidence for this assertion is offered by way of an example design, using a four element linear array antenna as a load.

Two more of the contributions of this dissertation are in carrying out the steps necessary to test this assertion:

- A numerical procedure is developed to find a constant congruence transformation that approximately diagonalizes a load over a

frequency band. The procedure uses the singular value decomposition of a matrix of the load's impedance vs. frequency data.

- A design procedure is developed to implement the constant congruence transformation using combinations of two port transformers, four port directional couplers, and straight through connections. All of these components can be readily realized at microwave frequencies.

Less central to the main theme of the dissertation, but still significant achievements, are four other contributions to the general areas of multiport networks and broadband matching.

- Development of a network model for array antennas so that straightforward computation of antenna patterns and received signals is possible.

- Derivation of a new formula for scan-angle dependent power flow when transmitting with array antennas, derived entirely from the network model of the antennas.

- Introduction of a simple formula for designing the optimal decoupled load impedance for a multiport source, (for a given excitation, at a given frequency).

- Derivation of performance constraints and network requirements for Butterworth and Chebyshev bandpass matching into parallel and series resonant RLC loads.

1.4 Document organization

Although array antennas are modeled as multiport networks all the time, few articles make it clear that there is a relationship between the network model and common "wave domain" calculations performed with the antenna, such as the derivation of received signals from an incident wave, or the calculation of beam direction and shape when using the antenna to transmit. This connection is made explicit in Section 2.0, which discusses two different modeling techniques, and develops a network model that can easily be used for computation of antenna patterns and received signals.

Section 3.0 describes power flow into multiport loads, which is a model of the transmit mode with an array antenna. In this section, a new expression for power flow into multiports with Toeplitz describing matrices (like array antennas), with progressive phase excitation (again, like array antennas), is derived.

Power flow between two multiports, which is a good model for an array antenna in the receive mode, is analyzed in Section 4.0. A viable design procedure for broadband antenna feed networks is presented in Section 4.2. However, these feed networks are sensitive to the direction of the signals incident on the array, because they consist of uncoupled subnetworks. For the power flow to be independent of the direction of the incident signals, some kind

of coupling in the feed network is necessary to counteract the mutual coupling inherent in the array antenna.

Section 5.0 presents a classic solution to compensating for mutual coupling: an "ideal multiport transformer". This circuit component is the physical analog of a congruence transformation on impedance and admittance matrices of multiport networks. In Section 5.2 is the first presentation of a technique for designing a network with practical microwave devices that duplicates the congruence transformation performed by ideal multiport transformers.

Section 6.0 presents a new solution to the multiport matching problem, using decoupling and single port matching. This solution is not general, for it is only applicable when the source magnitude does not vary with frequency, and for multiports which can be diagonalized over all frequency.

A variation in the source magnitude is inherent in the antenna feed problem, because the source magnitude and phases change as the beam is steered or as the signal to the antenna is incident from a different direction. In section 6.1, many kinds of networks are identified that are inherently diagonalizable over all frequency, but a general array antenna is not of this class.

The first constraint of the theory of Section 6.0 is dealt with in Section 7.0. Through the use of gain equalization of the individual two port broadband matching networks used the multiport matching strategy, variations in source magnitude as frequency varies can be accommodated.

Section 8.0 shows how the solution of section 6.0 can be applied to general multiports, like those that represent array antennas, by *approximately* diagonalizing these networks. In order to find a network which cancels the mutual coupling of the antenna over a range of frequencies, a new design procedure is described, where measured data from the antenna is used in matrix form. This antenna data (over a band of frequencies), is then parameterized by two constant matrices and two frequency dependent functions. This parameterization is performed using the singular value decomposition of a matrix of antenna data. The two constant matrices are then used to design a network that approximately decouples the antenna over the entire frequency range.

The single port matching necessary for completion of the multiport broadband matching design is addressed in Section 9.0. Classical matching theory is applied to the kinds of resonant loads seen in typical antenna matching problems. Matching constraints for bandpass responses of the Butterworth and Chebyshev type are derived for parallel and series second order RLC loads in Section 9.2.

Numerical techniques for matching are both convenient and necessary for the multiport matching problem, and section 9.3 explains the technique, originated by Yarman [14], adopted in this dissertation. At times it is necessary to start from a close to optimum point to use the numerical technique effectively, and modifications of the technique to allow this are detailed in Section 9.4.

Section 10.0 illustrates the performance of various feed network strategies by showing the detailed results of several designs for a four element antenna.

Appendices I through VI are background information and reference material from other sources, helpful for understanding the developments in the body of the dissertation. Numerical examples of the use of singular value decomposition to find a diagonalizing congruence transformation, using a lossless scattering matrix to represent an impedance, and power flow into a multiport can be found in Appendices VII, VIII, and X. Appendix IX is a detailed derivation of the formula used to calculate power into networks with Toeplitz matrices presented in Section 3.1. Appendix XI contains the derivation of the matching conditions discussed in Section 9.2.

A note on notation: Most of the variables used in this dissertation are either matrices, identified with capital letters, or column vectors, identified

with lower case. Subscripted variables are components of a vector. An exception is the capital N, used as the integer number of ports of a general multiport network.

2.0 A network model for antennas

An array antenna with N elements has a lumped electrical model as an N+1 terminal network, with N ports that all share a common ground return. In this thesis, attention is restricted to reciprocal N-ports, for example, antennas in reciprocal media.

Antennas are, by nature, distributed rather than lumped systems. The object of an antenna is to launch or gather waves. Never the less, at some point the antenna connects to circuits and electronics that are modeled as lumped elements. From the point of view of these connections, an array antenna certainly can be thought of as a lumped, multiport network.

There is much to be gained by pushing the lumped network- distributed network border much further into the distributed network, both from a conceptual point of view and as an aide to computation of changes in antenna pattern resulting from changes in feed network design. Section 2.1 makes the case for antenna network models where the ports of the network correspond directly to the wave-launching part of the antenna.

Section 2.2 contains the results of the network analysis necessary to determine the performance of array feed networks.

Two important and common antenna array shapes, a linear array and a ring array, are discussed in Section 2.3.

2.1 The pattern of array antennas

The transmit and receive pattern for an array antenna at a particular frequency is often expressed as the product of two expressions: the *element pattern* and the *array factor*.

$$Pattern = \text{ElementPattern}*\text{ArrayFactor} = P_{ref}\sum_{m=1}^{N} a_m \exp(jk_0 r_m), \quad \text{(EQ 1)}$$

where P_{ref} is the pattern of the reference element and the summation of weighted exponentials expresses the time delay due to the relative element positions in the array. The complex numbers a_m are the antenna excitation. The fact that the pattern can be expressed as a product like this has been termed "factorization" [28], or principal of "pattern multiplication" [38]. The overall antenna pattern is then quite easy to compute. It is convenient to apply the same factorization technique to an array antenna modeled as a multiport network, but care must be taken in the modeling process if this is to be valid.

2.1.1 One network model for array antennas

An accurate way of analyzing antenna performance using a network model is to place inside the multiport the complete array antenna system, including enough of the feed network so that a lumped feed port is obvious. The

impedance at a port is then well defined, and the excitation at the ports can arbitrarily be taken as, for example, current, voltage, or some combination of the two. The electrical characteristics of the antenna, as viewed from the ports, are well defined by an impedance, admittance, or scattering matrix. For example, an antenna subsystem may consist of several copper patches etched on a printed circuit board, some stripline interconnections, and a coax connector for hookup to the associated circuits. This is shown schematically in Figure 4.

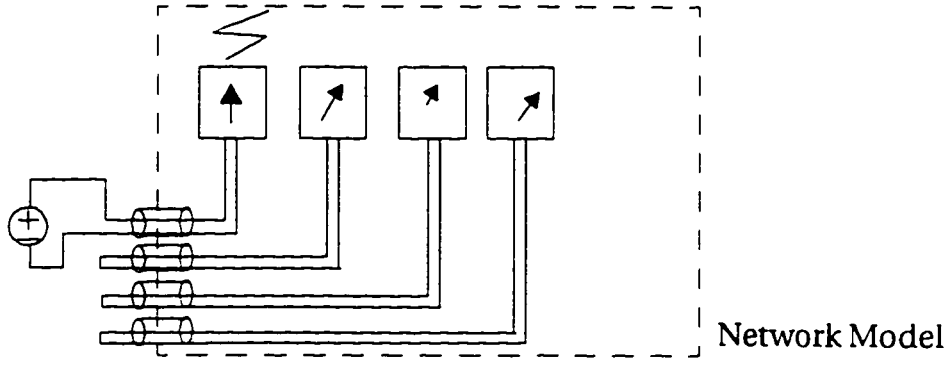

FIGURE 4. Excitation at one port causes every antenna to radiate.

A reasonable assumption is that, at the connector, there is one dominate waveguide mode of power transmission. Therefore, the voltage at the connector or current flowing in the center conductor of the connector are both equally fine choices for excitation of the antenna. A complete electromagnetic analysis (or a measurement) of the antenna subsystem results in a network model for the antenna that can accurately describe the antenna.

To predict the pattern of the antenna for arbitrary excitation, the pattern of the antenna when only one port is excited is computed or measured. However, the pattern resulting from excitation of one port will (in general), *not* be the same as the pattern resulting from excitation of another port. This is because excitation of a single port results in wave transmission from the antenna associated with the element at that port, as well as scattering and absorption by the other elements of the antenna. Since each element is in a different position in the array, to accurately predict the pattern for the entire antenna, the pattern of every port driven singly must be computed. Figure 4 illustrates that with this model, although excitation is applied at only one port, currents get induced into the other antennas, causing them to radiate.

With this network model for the antenna, it is not possible to compute the actual antenna element excitation, because that quantity is buried within the electromagnetic model of the antenna. Also, when receiving a plane wave signal from a particular direction, the output of the antenna cannot be calculated from the network model, but must be computed using electromagnetic simulation. Factorization (as applied at the ports of the network) fails here, although superposition of all the various port patterns gives the antenna pattern for an arbitrary excitation.

2.1.2 A more useful network model.

In order to allow the separation of the antenna pattern into in array pattern and an port pattern, the ports of the antenna network must be physically much closer to the antenna elements than in the previous network model discussed. Importantly, the port excitation must correspond directly with the antenna element excitation used to compute the element pattern. Thus excitation can no longer be *arbitrarily* chosen to be voltage or current. but must be appropriate with the antenna element type.

For example, consider an array of slots in ground plane (Figure 5). Because the pattern of a slot is computed from the electric field across the slot, the port excitation in the multiport model must be the voltage across the slots. "No excitation" means a zero voltage across a port, corresponding to a zero tangential electric field across the slots.

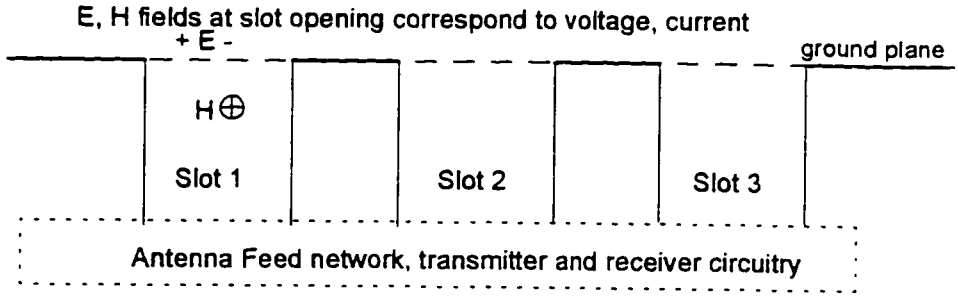

FIGURE 5. An array of slots in a ground plane

Because the excitation of a port corresponds with the excitation of an antenna element, the antenna pattern resulting from excitation of only one

port will be the same for all ports of the array. Zero excitation at the ports corresponds to zero excitation of the antenna elements, so that the pattern from excitation of one port is the same as the pattern of an element in isolation.

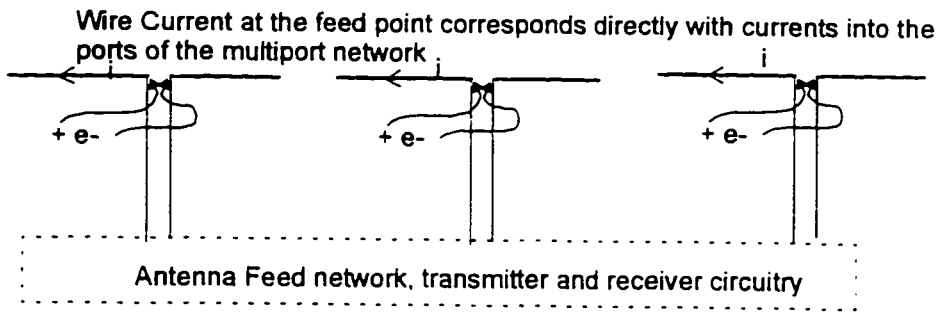

FIGURE 6. An array of dipoles

As another example, port current should correspond with the driving current in the center of the elements of an array of short, wire dipoles (Figure 6).

A problem with this formation arises when the elements are more complicated than simple slots or short wires. What does "excitation" mean for a particular element?

This question can be answered by the requirement that the element pattern part of the antenna pattern expression (Equation 1), be the same for all port excitations. The element pattern must be the pattern of the antenna when no other elements are excited. Therefore "no excitation" on an element must leave the element transparent to electromagnetic waves.

In several common circumstances, the other elements can be thought of as mostly transparent when they have no excitation. As well as the "slots in a ground plane" and the "array of short wire dipoles" examples, another example is an array of longer wire antennas, which can be made transparent by loading [33]. If the load impedance which leads to transparency is z, then when a port is loaded by z, the voltage across the port and the current through some port "m" are related by

$$v_m = -zi_m . \qquad \text{(EQ 2)}$$

Since this is the "no excitation" condition, the excitation at this port for this antenna can be expressed as

$$excitation_m = a_m = K(v_m + zi_m) , \qquad \text{(EQ 3)}$$

where K is a constant of proportionality.

When receiving from a particular direction, the signals that appear at this antenna's ports will not be solely currents or voltages, but will be a linear combination of the two as given in Equation 3. In the transmit mode, the excitation, as given by Equation 3, should be calculated at each port. Then the overall array antenna transmit pattern can be found directly using the form given by Equation 1, which shows a separation into a constant element pattern and an array factor.

In the network model for array antennas in this dissertation, the excitations used in the expression for array factor are the port excitations in the network model. Thus, array patterns can be straightforwardly computed from network analysis of the antenna system, (and knowledge of the array shape).

2.2 Calculating inputs and outputs from the antenna.

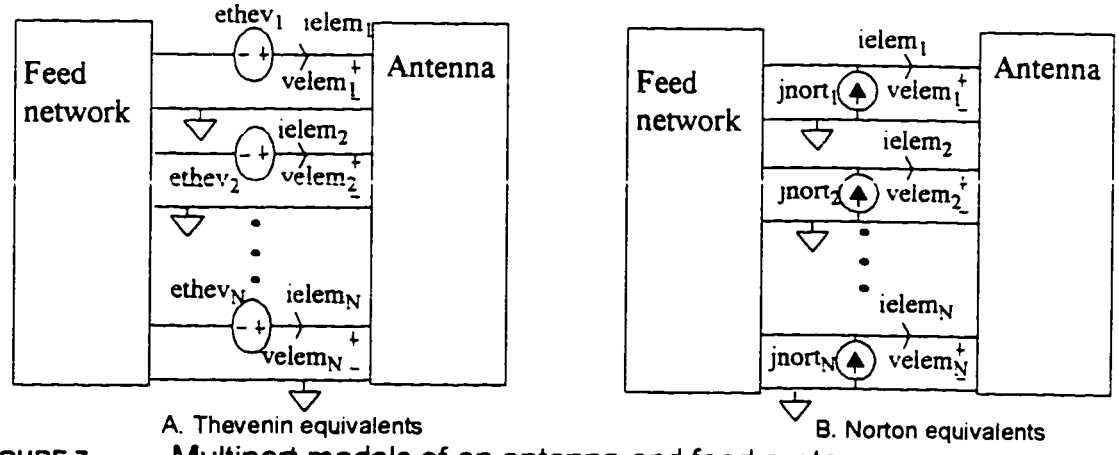

FIGURE 7. Multiport models of an antenna and feed system.

Figure 7 is a model of the N element antenna as a network, with N accessible ports. Both impedance and admittance representations are shown. The port voltages of the antenna network are called v_{elem}, (element voltages), and the port currents are identified as i_{elem}, (element currents).

The network of Figure 7A shows voltage sources in series with the antenna and the feed network. In a transmit situation, the voltages are the open circuit Thevenin equivalent voltages of the feed network, looking from the

antenna to the left. In a receive situation, the voltages are the output voltages from the antenna ports, when the antenna is open circuited. In the network of Figure 7B, the current sources in parallel with the antenna and feed network can be regarded as Norton short circuit equivalent sources from either the antenna, when receiving, or the feed network, when transmitting.

Because the excitation for aperture antennas is a voltage, when an aperture antenna is receiving, the Thevenin equivalent voltages from the antenna are independent of the antenna's impedance matrix, and are computable straightforwardly from the incident field and geometry of the antenna. A similar statement can be made for wire antennas and Norton equivalent currents. For more complex elements, an excitation that is some linear combination of currents and voltages is also independent of the describing matrix of the antenna. To compute Thevenin or Norton equivalents in this case, the antenna's impedance matrix must also be known.

Assuming Thevenin or Norton equivalents are known, referring to Figure 7, the antenna multiport voltages and currents due to an excitation can be calculated from the describing matrices of the various networks:

$$v_{elem} = (Z_{antenna}(Z_{feed} + Z_{antenna})^{-1})\, e_{thev} = (Y_{feed} + Y_{antenna})^{-1} j_{nort}$$

$$i_{elem} = (Y_{feed}(Y_{feed} + Y_{antenna})^{-1})\, j_{nort} = (Z_{feed} + Z_{antenna})^{-1} e_{thev} \qquad \text{(EQ 4)}$$

These formulas show the effect of mutual coupling, as commonly thought of in antenna problems. They make explicit how voltages and currents appear at all antenna elements, due to excitation of only one antenna element.

The transmitting situation is shown in Figure 8. During transmit, the excitation at the antenna ports is fixed by the choice of a desired transmit pattern. The transmit voltages or currents that produce these excitations can be obtained using Equations 5 through 8.

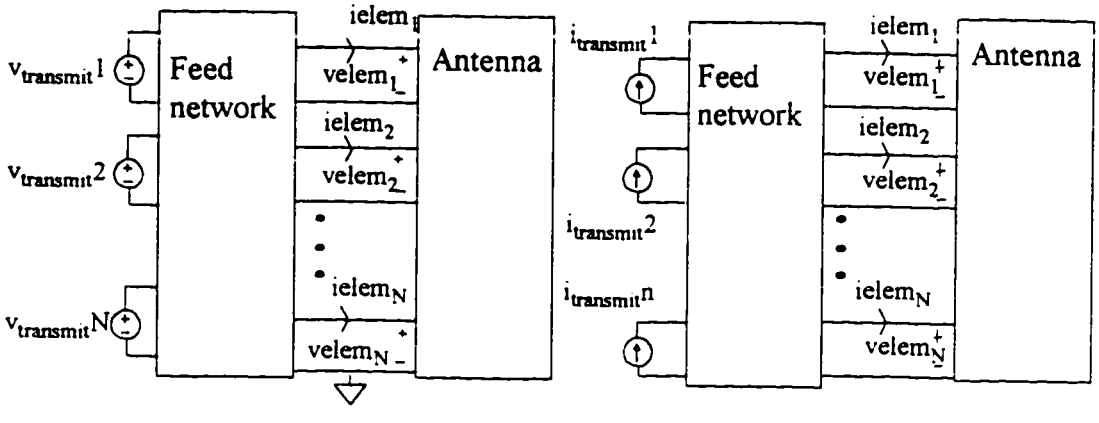

FIGURE 8. A schematic of the transmitting antenna

The feed network can be described in a partitioned form, where the partition corresponds to the input and output ports (usually of the same size). Let the feed open circuit impedance (or short circuit admittance), matrix be

$$Z_{feed} = \begin{bmatrix} Z_{11} & Z_{12} \\ Z_{21} & Z_{22} \end{bmatrix} \qquad Y_{feed} = \begin{bmatrix} Y_{11} & Y_{12} \\ Y_{21} & Y_{22} \end{bmatrix} \qquad \text{(EQ 5)}$$

The Thevenin equivalent voltages or Norton equivalent currents at the feed network output are then

$$e_{thev} = Z_{21} i_{transmit}$$
$$j_{nort} = Y_{21} v_{transmit} \qquad \text{(EQ 6)}$$

The impedance of the feed network as seen by the antenna, the feed impedance in Equation 4, is simply Z_{22}. The feed admittance in the second case is likewise Y_{22}. Substituting these values into the inverse of Equation 4, the transmit current needed to produce a particular aperture distribution, or the transmit voltage needed to produce a particular element current, in the presence of mutual coupling in the antenna and the feed network, can be written:

$$i_{transmit} = Z_{21}^{-1} (Z_{22} + Z_{antenna}) Z_{antenna}^{-1} v_{elem} = Z_{21}^{-1} (Z_{22} + Z_{antenna}) i_{elem}$$
$$v_{transmit} = Y_{21}^{-1} (Y_{22} + Y_{antenna}) v_{elem} = Y_{21}^{-1} (Y_{22} + Y_{antenna}) Y_{antenna}^{-1} i_{elem} \qquad \text{(EQ 7)}$$

Figure 9 shows the antenna system in the receive mode.

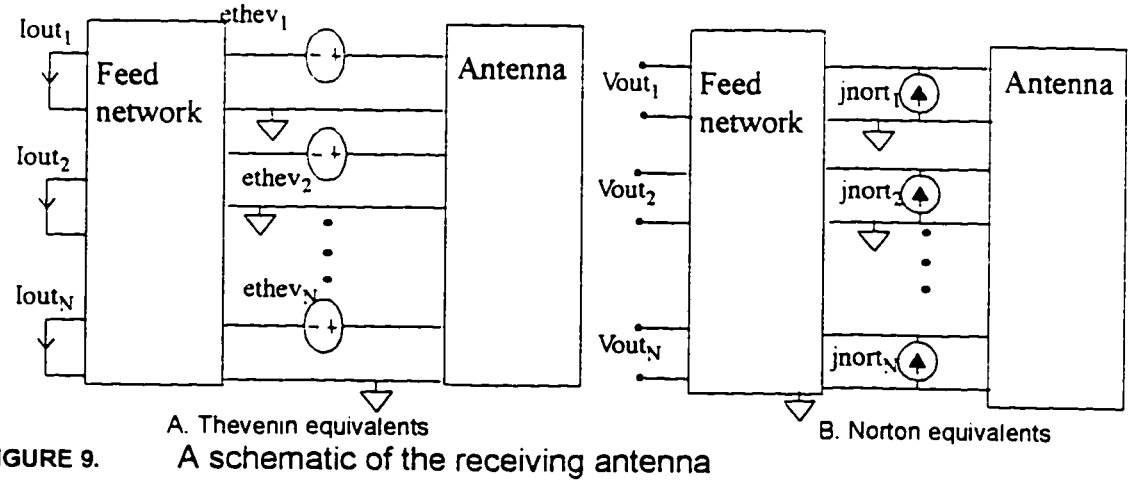

FIGURE 9. A schematic of the receiving antenna

Depending on the use of the Thevenin or Norton equivalents, the output from the antenna into the receiver can be calculated as

$$V_{out} = Z_{12}(Z_{22} + Z_{antenna})^{-1} e_{thev} = Z_{12} Y_{22} (Y_{22} + Y_{antenna})^{-1} j_{nort}$$

$$I_{out} = Y_{12}(Y_{22} + Y_{antenna})^{-1} j_{nort} = Y_{12} Z_{22} (Z_{22} + Z_{antenna})^{-1} e_{thev} \quad \text{(EQ 8)}$$

2.3 Describing matrices of particular array antennas

Because typical array antennas are very regular in shape, the impedance and admittance matrices that describe them are also regular. Two important array shapes are the uniformly spaced linear array, and the uniformly spaced ring array.

The elements of a linear array are mutually coupled because they are close to one another. One would expect the coupling factor between adjacent elements to be about the same, no matter where the element is in the array. Similarly, the coupling between elements separated by two spaces is probably

close to the same, and so on for the other spacings of the elements. For an N element array, there are N-1 different spacings. With the "self" term included, it would seem that the entire N by N describing matrix of the array depends on only N different terms. This is approximately the case. For an antenna where the excitation of an element is a current, the *impedance* matrix has this special form. For voltage-driven elements, the *admittance* matrix has this special form:

$$DescribingMatrix = \begin{bmatrix} t_1 & t_2 & t_3 & \cdots & t_N \\ t_2 & t_1 & t_2 & \cdots & t_{N-1} \\ t_3 & t_2 & t_1 & \cdots & t_{N-2} \\ \cdots & \cdots & \cdots & & \cdots \\ t_N & t_{N-1} & t_{N-2} & \cdots & t_1 \end{bmatrix}, \qquad \text{(EQ 9)}$$

where t_1 is the self term, t_2 is the coupling between adjacent elements, t_3 is the coupling between elements separated by two spaces, and so on. Matrices with the pattern of Equation 9 are called *symmetric Toeplitz matrices.*

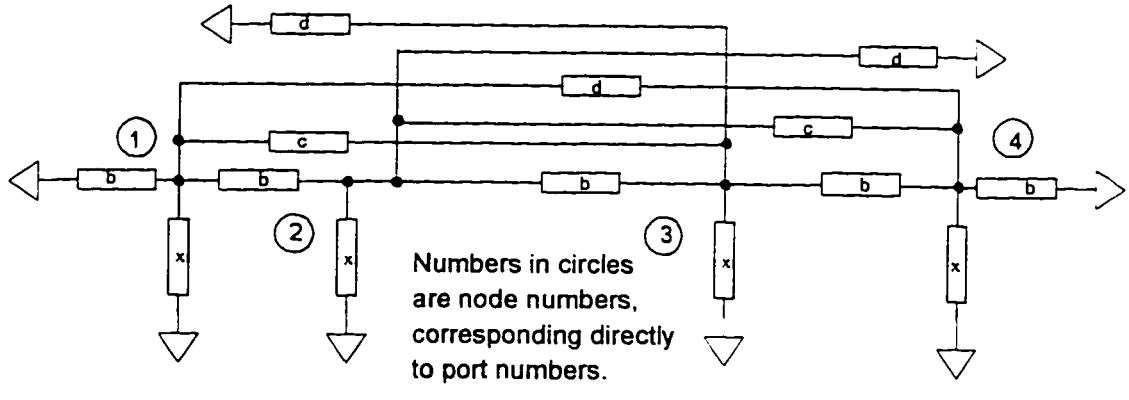

FIGURE 10. Schematic of a four element linear array antenna.

The nodal admittance matrix of Figure 10 can be written by inspection as

$$Y_{nodal} = \begin{bmatrix} x+2b+c+d & -b & -c & -d \\ -b & x+2b+c+d & -b & -c \\ -c & -b & x+2b+c+d & -b \\ -d & -c & -b & x+2b+c+d \end{bmatrix} = Y_{shortcircuit}, \quad \text{(EQ 10)}$$

where a, b, c, d, and x are the admittance values of the circuit components. If the node to ground voltages of Figure 10 represent the port voltage of a multiport network, then the short circuit admittance matrix and the nodal admittance matrix of the network are the same. This multiport network with a symmetric Toeplitz admittance matrix is an equivalent circuit for a four element, voltage excited antenna.

The elements at the ends of linear arrays are in a slightly different environment than elements in the middle of the antenna, and therefore matrices describing *finite* antennas are not exactly symmetric Toeplitz, but are almost so.

The second array shape presented here is the ring array. One can think of this antenna as a linear array with the ends curved around to meet each other. The describing matrix for this array is symmetric Toeplitz also. However, with N elements in a circle, element number 1 is adjacent to element 2 and element N. Elements two away from 1 are elements 3 and N-1, and so on.

Therefore, there are only integer(N/2)+1 different mutual couplings in the describing matrix. This symmetric Toeplitz matrix, with some elements repeated, is called a symmetric circulant matrix. In general, it looks like

$$Matrix = \begin{bmatrix} a & b & c & d & \dots & d & c & b \\ b & a & b & c & \dots & e & d & c \\ c & b & a & b & \dots & f & e & d \\ d & c & b & a & \dots & g & f & e \\ \dots & \dots & \dots & \dots & \dots & \dots & \dots & \dots \\ d & e & f & g & \dots & a & b & c \\ c & d & e & f & \dots & b & a & b \\ b & c & d & e & \dots & c & b & a \end{bmatrix}. \qquad \text{(EQ 11)}$$

It is readily shown that the inverse of a symmetric circulant matrix is also symmetric circulant, so both the impedance and admittance matrices of ring array antennas have this pattern.

2.4 Conclusion

By demanding that the signal at the ports of a network model for array antennas be directly related to the excitation of the antenna used to compute the array transmit and receive pattern, the connection between the electromagnetic behavior of the antenna and its circuit model is clear. For example, describing matrices for simple array shapes like linear arrays or ring arrays can be intuitively derived. Also, equivalent circuit models for some antennas are easily found. A characteristic of this formulation is that there are "natural' models for antennas with particular kinds of elements. Norton

equivalent circuits for wire antennas and Thevenin equivalent circuits for aperture antennas are two examples.

3.0 Power flow into a driven multiport

In this section, the idea of power flow into a network with more than one connection port is explored. In the single port case, real power always flows into the terminals of a passive network, but with multiple connection ports, power can be flowing in some terminals and out others. The power flow depends strongly on the *excitation pattern*, or the relative magnitudes and phases of the excitations at all the ports.

In section 3.1, new, simple expressions for power flow into antenna-like multiports under what is called "progressive phase" excitation conditions are derived, based entirely on network models for the antenna.

When applying a signal to a multiport network, the power into the network can be expressed from the scattering, admittance, or impedance matrix of the multiport as

$$ComplexPower = a^{t*}(I - S^{t*}S)\,a = v^{t*}Yv = i^{t*}Zi\ , \qquad \text{(EQ 12)}$$

where a, v, and i are 1 by n column vectors of complex phasors." a" is the incident wave, v is the port voltage, and i is the port current. When the phasors represent exponentials on the j-axis, the real part of the complex power is the average power dissipated over a period of the wave. In the following development, admittance matrices are used, although another type of describing matrix would serve just as well.

For an admittance, the real power dissipated in the network is

$$\Re\left(v^{t^*} Y v\right) = v^{t^*}\left(\frac{Y + Y^{t^*}}{2}\right) v = \sum_{k,m=1}^{N} \left(y_H\right)_{km} v_k^* v_m \qquad \text{(EQ 13)}$$

where y_H are the elements of the Hermitian part of the admittance.

If the network is passive, the real power flowing into it is always non-negative. This does not mean, however, that power always flows *into* each port of the network. Depending on the voltages on the ports, power can be flowing out of some ports and into others. In the literature associated with antenna arrays, the term "active impedance" is often used to represent the relation between voltage and current at a single port under certain conditions of excitation.

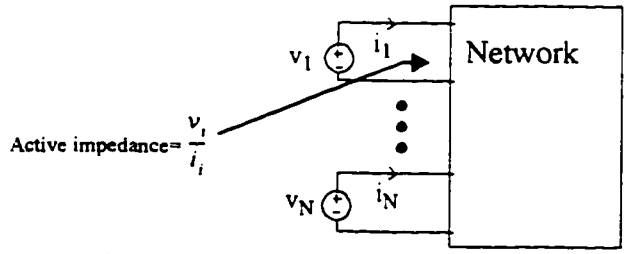

FIGURE 11. A multiport, driven by voltage sources

The real part of this "active impedance" can be positive, negative, or zero. In other words, when the ports are looked at individually, they can seem to be active or passive or lossless, even though the network is strictly passive. When looking at the "active impedance" of a multiport as the excitation

changes, odd responses that look like resonances occur, but they have nothing to do with the dynamics of the network. This is demonstrated in an example of power flow into a multiport network with a high degree of mutual coupling, presented in appendix X.

3.1 Excitations for antenna arrays

In order to arrange for a particular transmit pattern from array antennas, the magnitudes and phases of the port excitations are controlled. Although different design procedures can lead to all sorts of excitation, a common excitation for equally spaced arrays is called progressive phasing. In this technique, the transmit beam of the array is steered from broadside to endfire by applying an excitation to the elements that exhibits a constant phase shift from element to element. Because of the phasing difference and the slightly different distance waves from each element have to travel to reach a far away target, the wavefronts all add up in phase for a particular direction.

When the excitation has a progressive phase shift from port to port, the v_k terms in Equation 13 are of the form

$$v_k = \upsilon_k \exp(jk\theta) , \qquad \text{(EQ 14)}$$

where the υ_k are constants, and the port to port phase shift is θ. With N ports, k ranges from 0 to N-1. Converting the exponential to sines and cosines, one can see from Equation 13 that power into the admittance takes the form a

weighted sum of sines and cosines of multiples of the excitation phase shift. The highest multiple is one less than the number of the ports in the multiport.

More can be said about the power into the network as the port to port phase shift changes in the special case of a symmetric Toeplitz admittance. In the following, an expression for the power in terms of a sum of cosine terms is developed. For a detailed derivation, please refer to appendix IX.

If the admittance is symmetric Toeplitz, then the Hermitian part of the admittance is symmetric Toeplitz, also. Denote the first row or column of the Hermitian part of the admittance as $[Y_1, Y_2, Y_3,...Y_N]$. Then the main diagonal is all Y_1, the first superdiagonal and the first subdiagonal are Y_2, and so on.

A symmetric Toeplitz matrix with entries Y_{km} is as a matrix where

$$Y_{km} = Y_{k-m+1}. \qquad \text{(EQ 15)}$$

When the voltages display progressive phase, (Equation 14), with υ and θ real, then

$$v_k^* v_m = \upsilon_k \upsilon_m \exp(-jk\theta) \exp(jm\theta) = \upsilon_k \upsilon_m \exp(-j\theta(k-m)). \qquad \text{(EQ 16)}$$

As k and m range from 1 to n, their difference will range from n-1 to -(n-1). For every k, m combination with difference i=k-m, there will be another with difference -i=m-k. For every exponential with a positive exponent, there will be one with a negative exponent, with the same multipliers. The two

exponentials add up, with the sine terms cancelling and the cosine terms adding.

The real power that flows into the multiport under these conditions is a sum of cosines. Each diagonal of the admittance matrix contributes a cosine term to the power. The power into such an admittance, under progressive phasing, can be written

$$Power(\theta) = \Re(Y_1)\sum_{k=1}^{n} v_k^2 + \sum_{i=1}^{n-1}\left(\sum_{k=1}^{n-i} v_k v_{k+i}\right) 2\Re(Y_{i+1})\cos(i\Theta) \qquad \text{(EQ 17)}$$

For example, when the excitation is uniform, that is, the magnitude of the voltage at each port is constant (set to unity), and only the phase changes, the power into the admittance as a function of excitation angle takes a simple form of

$$Power(\theta) = NY_1 + \sum_{j=2}^{N} k_j Y_j \cos((j-1)\theta), \qquad \text{(EQ 18)}$$

where $k_j = (2(N+1-j))$. Thus, each diagonal of the matrix contributes a cosine term to the power into the admittance. The weighting of each term falls off linearly with movement away from the main diagonal. This is illustrated in Figure 12, where the total power into a four port multiport is decomposed of a sum of four weighted cosines.

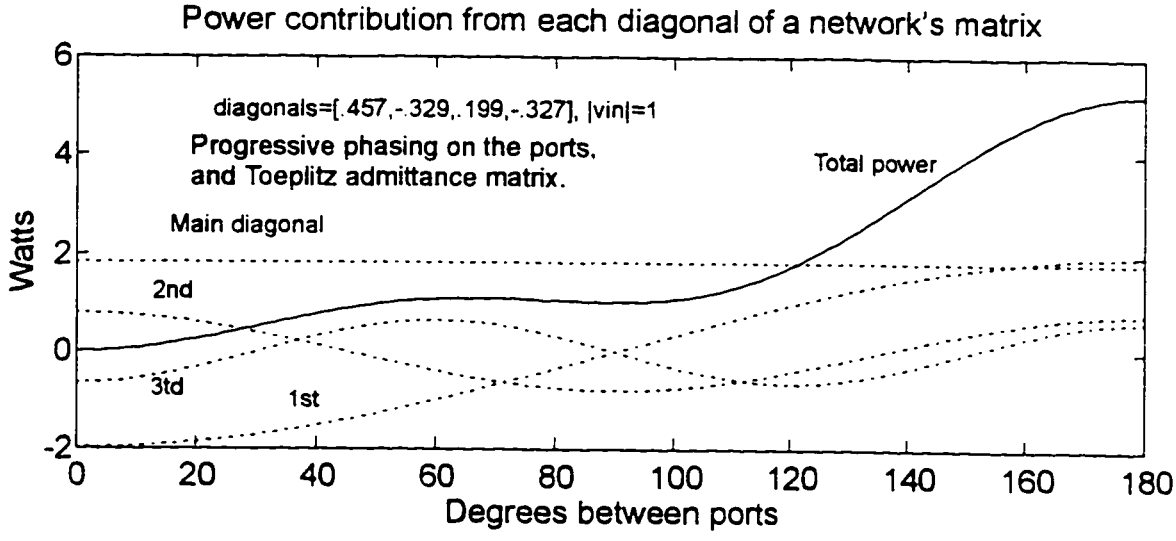

FIGURE 12. The power into a network is a sum of cosine terms

If the admittance matrix is positive real, the power will, of course, never be less than zero as the phasing changes.

The fact that the antenna is passive and has a describing matrix with a positive semidefinite Hermitian part limits the kinds of $Y_1 ... Y_N$ that will appear in Equation 17. This, in turn, limits the kinds of shapes that the power vs. angle between the ports curve will have. The positive semi-definiteness of the Y matrix can be expressed as a set of nonlinear expressions that all are non-negative[1]. Unfortunately, it is difficult to solve these equations in a way that sheds light on how they constrain the power curve vs. angle, in detail.

1.Two different procedures lead to these equations, (1), setting all the principal minors of Y_H to be greater than or equal to zero, or (2) setting all of the eigenvalues of Y_H to be greater than or equal to zero. Both techniques lead to complicated equations, even for matrices as small as 3 by 3.

3.2 Conclusion

Power into the network changes with changes in phase shift between the ports (or changes with *scanning*, if the network is an antenna), because there are non-zero entries off the main diagonal of the describing matrix of the multiport. As the beam of an antenna is steered, the power into the antenna may drop to very low levels for some scan directions. This is called *scan blindness* [43]. An example of a resistive network that exhibits this scan blindness effect is given in Appendix X.

In this section, we have shown how the power into a network described by a symmetric Toeplitz admittance matrix, with progressive phase excitation, varies with the cosine of multiples of the phase shift between ports. Thus, scan dependent power flow in array antennas can be understood as a consequence of the nature of the antenna's mutual coupling, which in turn, is a consequence of the physical shape of the array.

4.0 Power flow between a multiport source and multiport load

Section 3.0 developed the ideas of power flow when a multiport is driven by external sources, for example, an array antenna in transmit. In this section, the concentration is on power flow in the receive situation. It is shown that N isolated loads can be optimum at a single frequency and source distribution. A new, simple technique to find these loads is presented. Then, design of coupling networks where each port is isolated is analyzed.

To maximize the gain of an array antenna there must be optimum power flow between the antenna itself and the feed network. When the antenna is in the receiving mode, it can be modeled as a multiport source with Thevenin equivalent sources connected in series with each of its ports, or with Norton sources in parallel (Figure 9). A natural question to ask in this situation is "What is the receiver load that extracts the most power from the array antenna?" This problem of maximal power transfer for N-ports was addressed by Desoer [8], and Vidyaser [12]. They showed that, at any single frequency, the complex conjugate transpose of the antenna impedance extracts all of the available power from the antenna source. Their proof involves determining the port currents, i_{opt}, that flow for optimal power transfer. For details see appendix I.

They also pointed out that, for a particular excitation voltage, there are many different loads that will also extract all the available power from the

antenna. This is due the fact that the N^2 parameters of Z_{load} are constrained by only N equations. If N_{iopt} denotes the (N^2-N) dimensional subspace consisting of all matrices that map i_{opt} into the zero vector, then the matrices Z_{load} which satisfy these equations, and therefore optimal for power transfer, can be expressed as

$$(Z_{load} = \overline{Z^t_{source}} + Z_{null}), \quad Z_{null} \in N_{iopt} \qquad \text{(EQ 19)}$$

The best load is the conjugate of the source: however, this is only one of an infinite number of loads of extract the same power from the source, given a particular voltage excitation. One way to find Z_{null} matrices is to set up an orthonormal basis for R^n that includes the excitation vector, i_{opt}, as one of the basis vectors. Then, any linear combination of the other N-1 vectors in the basis, excluding i_{opt}, can be used to form the columns of Z_{null}.

Although Equation 19 is a description of all the loads that are optimal in a particular situation, finding loads that are optimal and have other desirable characteristics, (for example, simplicity), is generally an unsolved problem. (For in interesting attempt, see Flanders [5]).

4.1 "N" isolated impedances can form the optimal load

Knowing that many loads can act just like a conjugate load for a particular excitation, consider the observable voltages and currents flowing in the circuit when the conjugate load is connected. Regarding the antenna and

feed network (load), as black boxes, only the port currents i_{opt}, and the port voltages v_{opt}, are observable, so that any load which results in these voltages and currents, regardless of its internal structure, will extract the optimal power from the source. In particular, each port current and voltage defines an isolated, uncoupled impedance, given by $Z_{port} = \frac{v_{port}}{i_{port}}$, that can be substituted for the conjugate load without changing the voltages and currents of the circuit.

At a single frequency, given a particular excitation vector, there exists N isolated loads that extract all of the available power from an N-port source. The impedance of these loads can be calculated as the ratio of the voltages and currents on the ports of a conjugate load connected to the source. This important observation was made by Bloch [1].

For these conditions, designing the optimum load for a multiport source simplifies into designing N single port loads, as shown in Figure 13. It is not necessary to include mutual coupling in the load to extract the maximum power from the source.

The following three paragraphs make statements about the optimum diagonal load that are, in the author's opinion, quite fascinating. It is important to keep in mind, while reading the following, that these statements

are true for single frequency conditions, and are even true when the multiports in question are purely resistive.

Since the N numbers of the diagonal load are determined by N linear equations, the optimal diagonal load is unique. However, when the source network is passive, the diagonal load that extracts the same power as the conjugate load is not necessarily passive. A formula for the diagonal load that is passive and extracts the most power from a particular source is not known[8].

It has been mentioned in Section 3.0 that the impedance looking into a port of a multiport load, when considered in isolation, is sometimes called the active impedance. A multiport source can be considered a passive multiport network with Thevenin or Norton equivalent sources, and so the active impedance of a multiport source is well defined, as the ratio of voltage to current at a port of the passive multiport of the source (Figure 11). Interestingly, the diagonal load that extracts the most power from a multiport source is not the conjugate of the active impedance of the source. Thus, the best loading of a source does not lead to individual best loadings of its ports.

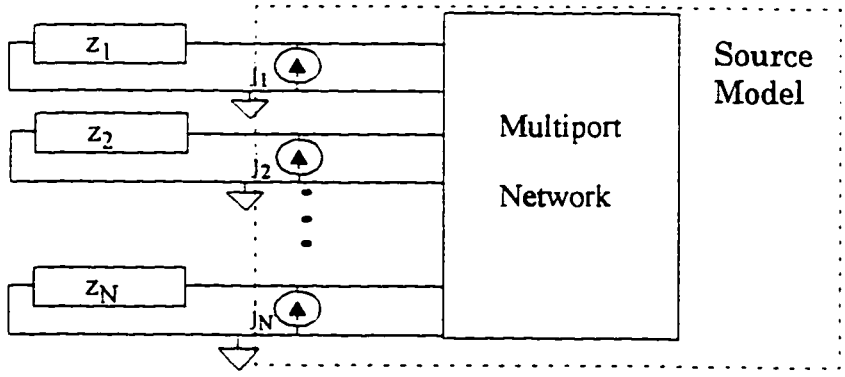

FIGURE 13. The optimum load can be simple, isolated impedances.

Consider a passive multiport in parallel with Norton equivalent sources, as shown in Figure 13. The N impedances can be found which extract all the available power from the source, following the procedure just discussed. Now, consider the same circuit, with the role of source and load reversed. The N impedances along with the current sources form a diagonal multiport source. The power extracted from this new source by the original multiport is not, in general, all the available power. This is in contrast to the conjugate-matched case, where reversing the roles of source and load lead to the optimum match in both situations.

When the excitation differs from the excitation used to design the load, the amount of power extracted from the source will not necessarily be all of the available power. The degree that the load becomes suboptimal for other excitations depends strongly on the original source. For example, the passive, resistive source in Figure 14 accepts very different power as the excitation

phasing changes, and also exhibits a high degree of variation of transducer power gain with excitation phasing. (If this multiport were a linear array antenna, it would be said to exhibit a high degree of *scan blindness* at broadside and at an angle corresponding to 90° between ports). Figure 14 shows the power gain that results from two different designs that are optimal at one particular phasing: one with no phase shift between the ports, and one with 60° between the ports. The 60° design has more gain over a broad range of input phasings, but still exhibits very low gain (or "blind spots") at some phasings.

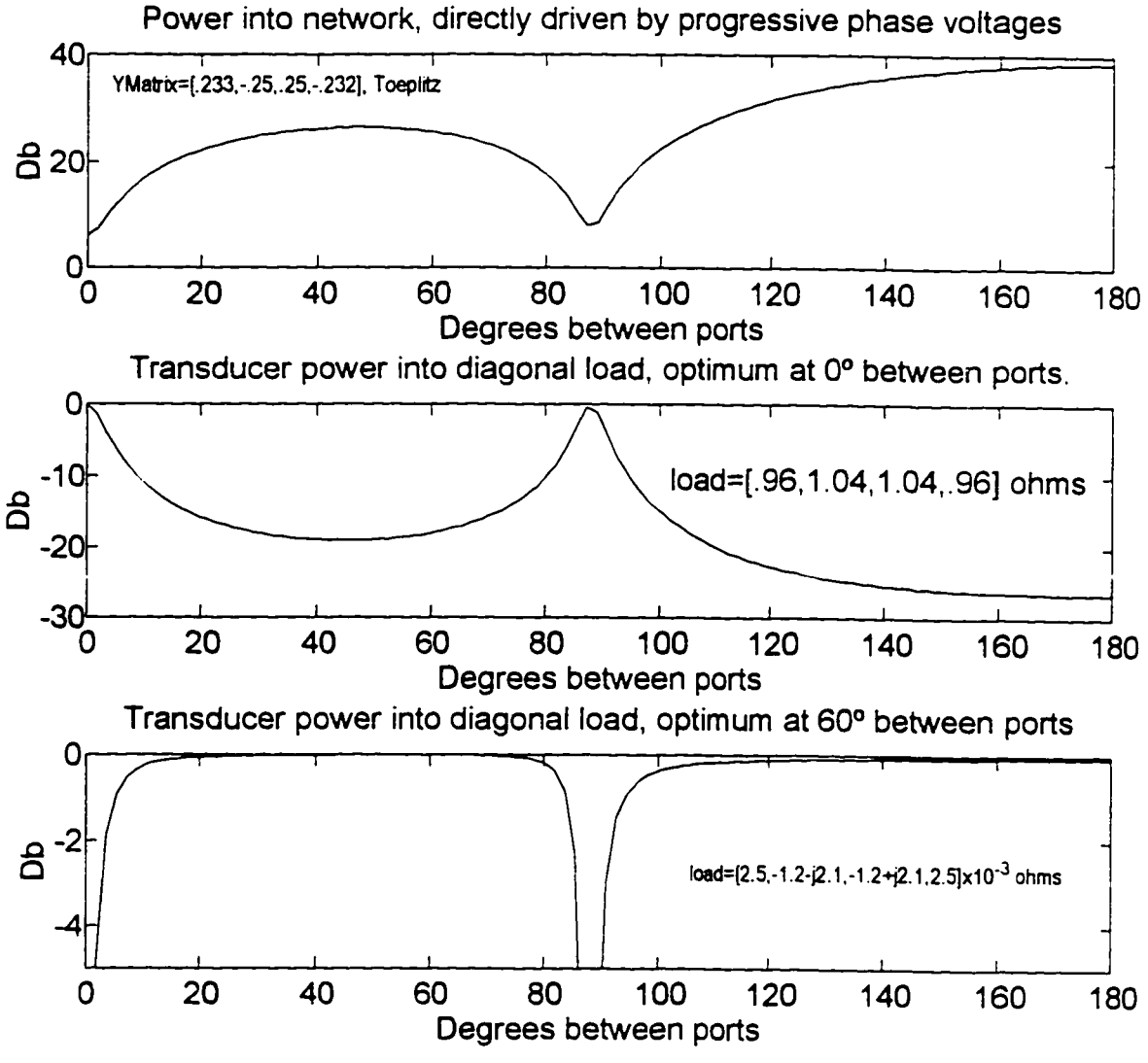

FIGURE 14. Power into two different loads from a source.

In contrast, the passive resistive network of Figure 15 shows minimal change in transducer power gain for changes in excitation phase, and also shows less variation of power into the network when driven by voltage sources. Thus, the suboptimal performance of a diagonal load as the excitation changes must be evaluated for each particular source.

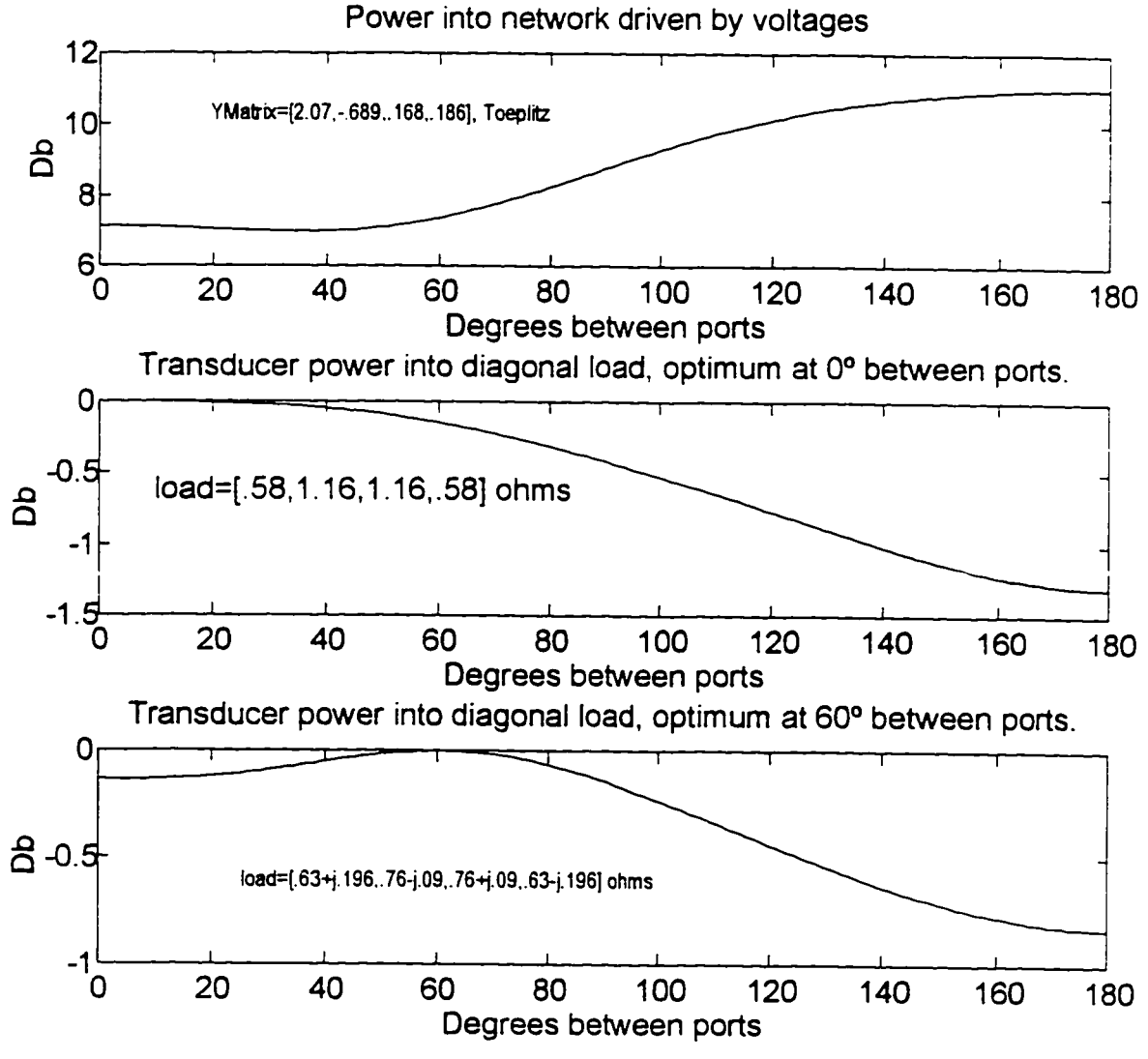

FIGURE 15. Power into two different loads from another source.

4.2 Using uncoupled feed networks

When an equally spaced array antenna is receiving from a far away source at a particular direction, the elements will be excited approximately equally in magnitude, with a progressive phase shift. This is an example of a situation where the excitation pattern of the source is known. For this case, a

specification for simple feed network design that results in optimal power extraction from the array antenna can be found by

- Conceptually connecting the conjugate load to the antenna source.
- For all frequencies, computing the current and voltages that exist at the load terminals.
- Computing the ratio of voltage to current at each port, which defines N isolated impedances that extract the most power possible from the antenna.

The problem remains to realize some (not too complicated), passive impedances that come close the specification over the band of frequencies.

After design of the isolated loads, an analysis of the overall system will reveal the performance of the antenna with sources at other locations. If the performance is acceptable, this "single scan angle" based design may be all that is needed. Figures 14 and 15 indicate that the antennas that exhibit a lot of scan blindness effect will probably not be good candidates for this technique.

For example, optimum uncoupled loads for a four element multiport with moderately low changes in power with scan were calculated in a band of frequencies for an excitation of progressive phase with 60 degrees between the

ports. Then, a numerical optimization routine was used to approximate the optimum loads with fourth order, positive real loads.

The approximation was performed in this way: For each load, at each frequency, the complex conjugate of the optimum load was computed. Then, a numerical broadband matching routine was used to find the best source impedance for delivering power over the given frequency band to the conjugate of the optimum load. This source impedance is then an approximation to the optimum load that is, in some "power" sense, a good approximation.

The total power out of the antenna into the realized load was calculated for various progressive phasings, over the frequency band. The four optimum loads are shown in Figure 16. (This multiport is actually the four element slot antenna used the examples of the section 10.0).

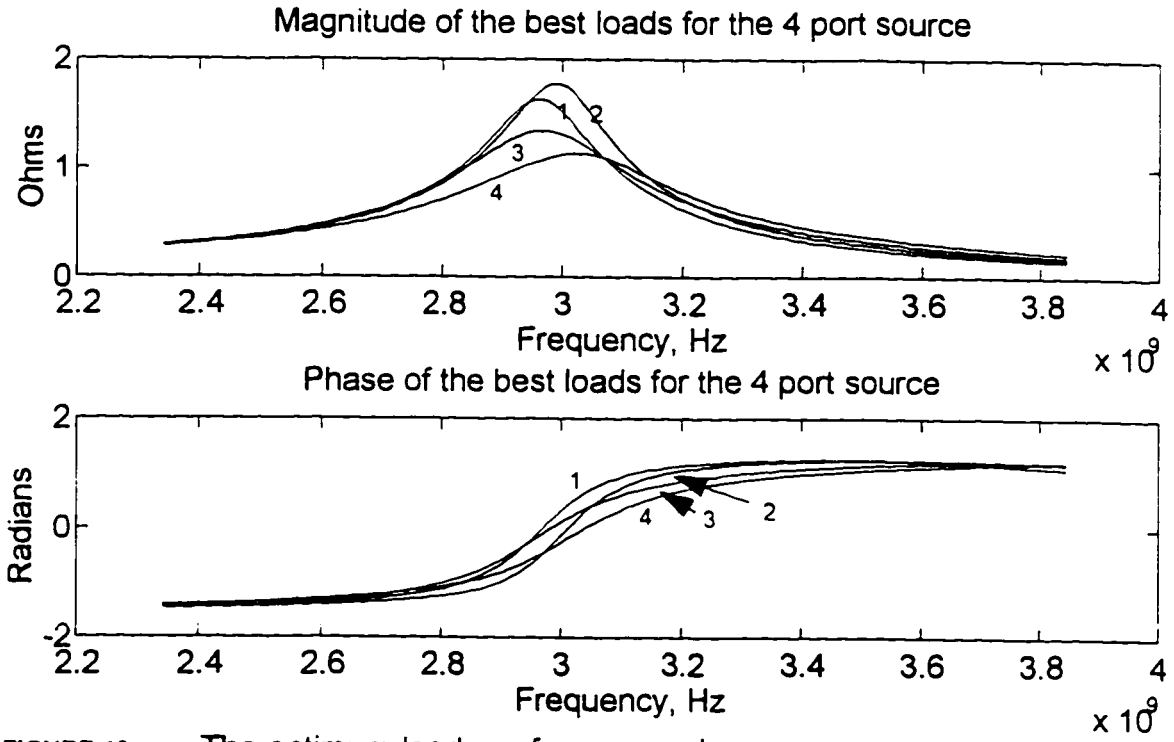

FIGURE 16. The optimum loads as frequency changes.

The four optimum loads are approximated using the networks of Figure 17. The result of the numerical approximation is a rational function. Cascade synthesis was then used on the rational functions to find the circuits of Figure 17.

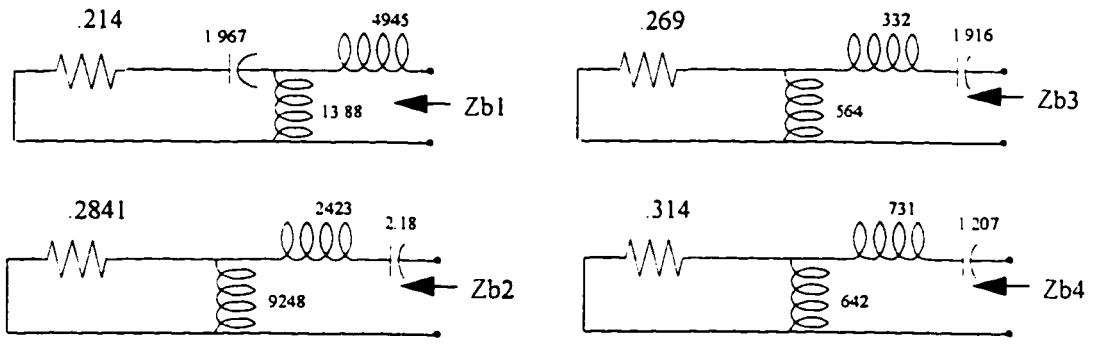

FIGURE 17. Designed matching networks

These networks produce the impedances of Figure 18.

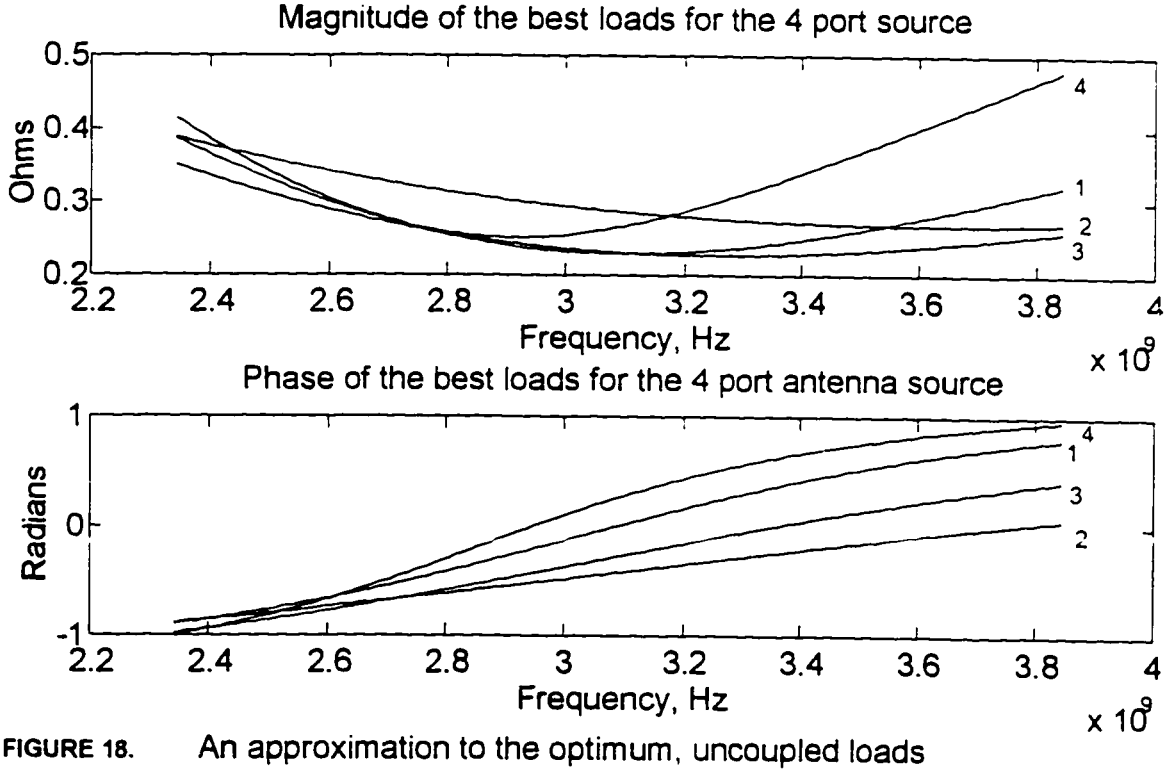

FIGURE 18. An approximation to the optimum, uncoupled loads

Note that the approximating impedances and the optimum loads have very different magnitude variation with frequency. However, the phase of the approximating and optimum impedances are similar.

The power gain into the realized networks, for antenna output voltages with progressive phasing, is shown in Figure 19. The power gain is quite flat, and quite high, also. The power gain changes with phasing, and is shown for several values of progressive phase signals from the source. As can be seen, the change in power gain as the excitation phasing differs from the design value is

nothing like the variations of Figure 14, it is more on the order of the variations in Figure 15. Since the variation in power gain with frequency and the variation in power gain with phasing are of the same order of magnitude in this case, this variation with excitation may be acceptable. This would mean that the design is good enough. If not, the following sections of this dissertation show how the variation in excitation can be reduced.

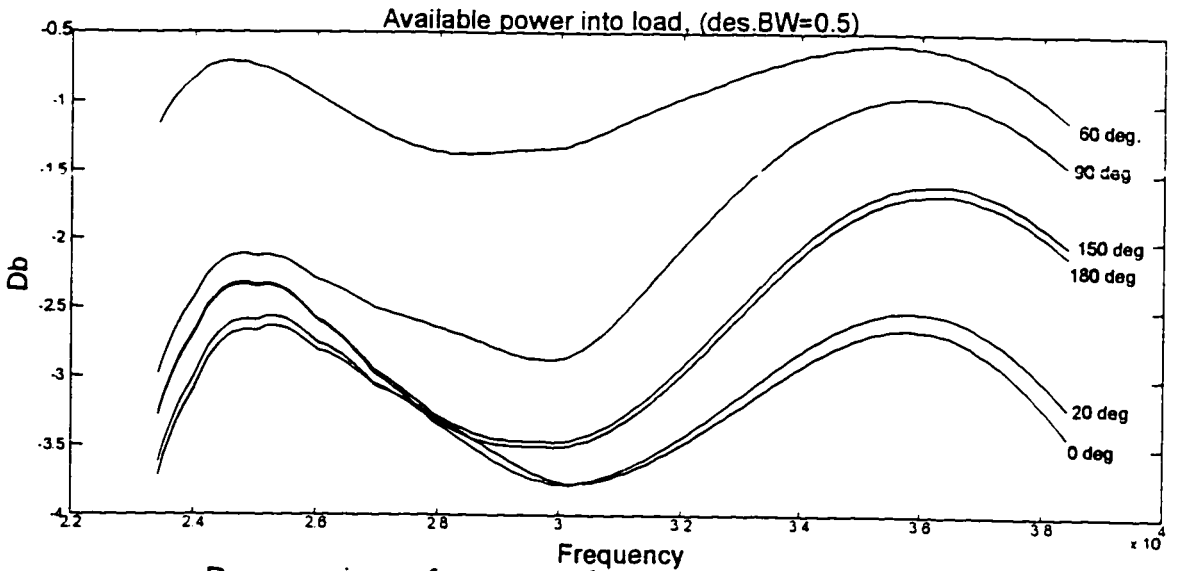

FIGURE 19. Power gain vs. frequency, for several excitation phasings.

4.3 Conclusion

Because there exists an optimum load for any N-port source that consists of N isolated loads, in this section, the viability of design with feed networks which consists of decoupled subnetworks is explored. An example design is actually carried out. It is quite possible that a design based on

uncoupled networks will have acceptable performance. This will depend on the nature of the multiport source.

5.0 Allowing mutual coupling in the feed network

Although an uncoupled feed network may provide a good match for a particular excitation, the only way to remove the match dependence on direction of reception is to compensate for the mutual coupling in the array. Also, in the transmit situation, the impedance change of the antenna with scan angle makes the driving of the antenna difficult, and a compensation for this scan dependence would reduce this impedance change. In this section, it is shown how, ideally, it is possible to completely compensate for the mutual coupling in a multiport. A design procedure for practical microwave circuits that carry out this compensation is introduced.

A scheme for compensation for the mutual coupling in an array antenna is suggested by Figure 10 on page 24. First, assume that all the admittances cross coupling the four nodes are reactive. Then assume that reactances of opposite signs, but the same magnitude, are substituted for those cross terms. The resulting network has an admittance matrix which is symmetric Toeplitz, and has cross terms which are exactly the negative of the original matrix. This compensation network can now be placed in parallel with the antenna, and the resulting input admittance does not vary with scan angle. Thus, the reactive part of the antenna admittance can be dealt with.

There is a considerable literature associated with reducing the scan dependence of an array antenna by connecting another network in parallel with the antenna [34], [35], [36]. However, this scheme can only work by cancelling the reactive part of the mutual coupling with reactances of the opposite sign. The real part of the mutual coupling cannot be cancelled by placing a positive real network in parallel with the antenna.

5.1 Decoupling the ports by a congruence transformation

At a single frequency, a passive multiport network can have all of its mutual coupling compensated for by a transformer network. This is because two matrices, one of which is positive definite, can be simultaneously diagonalized with a real congruence transformation. An impedance is completely described by its real and imaginary parts. Since the real part of the impedance matrix is positive definite (because the multiport is passive), the real and imaginary parts can be simultaneously diagonalized.

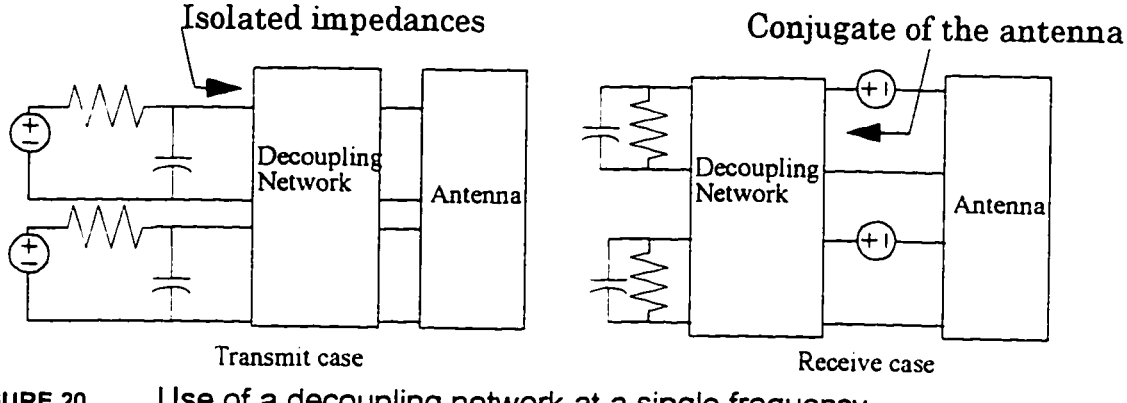

FIGURE 20. Use of a decoupling network at a single frequency.

It can be shown that the placing of a so called "multiport transformer" in front of a load described by its impedance matrix, has the effect of causing the transformer's input ports to have an impedance given by the congruence transformation of the load impedance by the transformer's turns ratio matrix [43].

An explanation of the multiport transformer ideal circuit element is available in appendix II.

In Figure 20, consider a transformer with a turns ratio matrix calculated by the simultaneous diagonalization of the real and imaginary antenna impedance used as the decoupling network. In the transmit mode, the transformer, when terminated in the antenna, will show isolated complex impedances at its input ports. These can be matched at a single frequency with a reactance and a resistor. In the receive mode, the transformer, when terminated with a resistance and a reactance, can show an exact conjugate of the antenna impedance to the antenna. Then all the available power can be extracted from the antenna.

The transformer provides a matched situation in both transmit and receive, but so does terminating the antenna in the optimum diagonal loads. The diagonal load, though, maintains a match only for a particular excitation. Because the transformer, along with the resistors and reactances, provides for

a true conjugate load at a single frequency, the match will be maintained by any excitation at that frequency. Thus, on transmit, high reflected power when scanning to particular beam directions will no longer occur. On receive, the maximum available power will be extracted from the antenna, regardless of the transmitter location.

5.2 A microwave multiport transformer

The above discussion seems academic because of the difficulty of making the multiport transformer. However, it is demonstrated here that at microwave frequencies, networks which act like multiport transformers (over a limited frequency range), can be practically constructed.

In the paper by Geren, Curry, and Andersen, [7], it has been shown that an "orthogonal transformer", that is, a multiport transformer with an orthogonal turns ratio matrix, can be constructed by a combination of microwave directional couplers with the correct coupling factors.

This result can be extended. In this section, it is shown that *any* turns ratio matrix, orthogonal or not, can be similarly constructed at microwave frequencies.

The formula for the scattering matrix of a transformer with turns ratio T is [2], [25]

$$S_{TRANSFORMER} = \begin{bmatrix} (I + T^t T)^{-1}(T^t T - I) & 2(I + T^t T)^{-1} T^t \\ 2T(I + T^t T)^{-1} & (I + TT^t)^{-1}(I - TT^t) \end{bmatrix} \quad \text{(EQ 20)}$$

If a transformer happens to have a turns ratio matrix which is orthogonal, then the upper left and lower right sub-matrices of its scattering matrix, (Equation 20), are zero, indicating the network is "matched" at all ports. Such a transformer is called an "orthogonal transformer." Its scattering matrix is

$$S_{\text{ORTHOGONAL TURNS MATRIX}} = \begin{bmatrix} 0 & T^t \\ T & 0 \end{bmatrix} \quad \text{(EQ 21)}$$

Any reciprocal, lossless network that is matched at all ports can be considered to be an orthogonal transformer [1]. Transformer networks that are not matched do not have orthogonal turns ratio matrices.

The cascade connection of a chain of multiport transformers is a multiport transformer, as shown in Figure 21. If the turns ratio matrices of the cascaded transformer networks are $T_1, T_2, T_3 \ldots T_n$, the overall network has a turns ratio matrix equal to the reversed product of the individual turns ratio matrices, that is

$$Turns_{BIG-TRANSFORMER} = T_n \times T_{n-1} \times \ldots \times T_2 \times T_1 \quad \text{(EQ 22)}$$

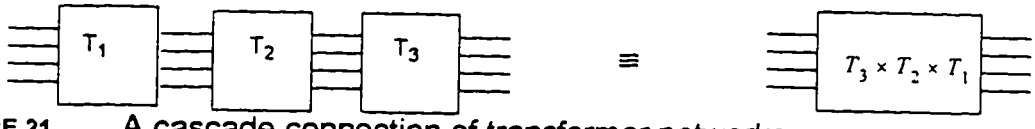

FIGURE 21. A cascade connection of transformer networks.

Equation 22 suggests that decomposition of a complicated transformer network into a cascade of simpler, (or more desirable), transformer networks can be accomplished by factoring the turns ratio matrix.

For example, it is possible to design "orthogonal transformer" networks at microwave frequencies using combinations of four port directional couplers and straight through connections [7]. Therefore, it is of interest to look at factorizations that result in orthogonal parts. Especially, the singular value decomposition (SVD), is useful because it creates two orthogonal factors and a diagonal factor. The orthogonal factors can be realized with a network of directional couplers, as already mentioned, while the diagonal factor represents uncoupled, two winding transformers. These simple transformers can be realized with quarter wave sections at microwave frequencies. The singular value decomposition is given by

$$SVD(Turns) = U \cdot S \cdot V^{T} . \qquad \text{(EQ 23)}$$

Here, U and V are orthogonal matrices, while S is a diagonal matrix with nonnegative entries.

The singular value decomposition is the only decomposition into orthogonal matrices and a nonnegative diagonal matrix. The non-negativeness of the diagonal parts is not necessary in order for realization with two port, quarter wave impedance transformers, so the SVD is not the only

decomposition that results in an easily realized network. It is suggested here because it is easy to compute (it is a standard library routine for most linear algebra packages), and the SVD exists for every matrix [9]. The singular value decomposition will be referred to later in this paper. A derivation of the SVD, from references [9] and [10] is presented in appendix III.

A feed network for array antennas that compensates for the mutual coupling between the elements at a single frequency can be implemented by a cascade of the three networks: an orthogonal transformer with turns ratio V^t, followed by isolated transformers whose primary turns are the diagonal elements of S, followed by an orthogonal transformer with turns ratio U. This is shown in Figure 22. In turn, each of the three ideal elements has a microwave circuit analog with a rich collection of design techniques associated with it [31]. A brief discussion of directional couplers is presented in the next section.

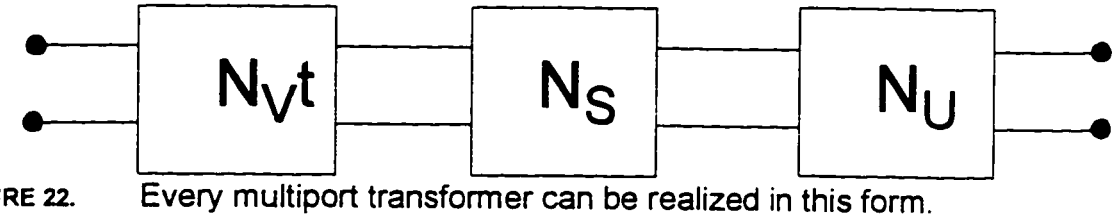

FIGURE 22. Every multiport transformer can be realized in this form.

5.2.1 Realizations with directional couplers

A matched, lossless four port at microwave frequencies is often called a directional coupler. So called "antisymmetical" couplers have a scattering matrix like [23]

$$S_{DIRECTIONAL-COUPLER} = \begin{bmatrix} 0 & 0 & \alpha & \beta \\ 0 & 0 & -\beta & \alpha \\ \alpha & -\beta & 0 & 0 \\ \beta & \alpha & 0 & 0 \end{bmatrix}, \quad \text{(EQ 24)}$$

where the orthogonal condition holds, $\alpha^2 + \beta^2 = 1$. Evidently, such a network is a four port orthogonal transformer with a turns ratio of

$$Turns_{DIRECTIONAL-COUPLER} = \begin{bmatrix} \alpha & -\beta \\ \beta & \alpha \end{bmatrix}. \quad \text{(EQ 25)}$$

Although no practical design technique exists to make directional couplers that are frequency independent, networks can be constructed that behave ideally over wide bandwidths.

Orthogonal transformers of any number of ports can be constructed from combinations of directional couplers and straight through connections. This is accomplished by factoring the orthogonal turns ratio matrix of the transformer into a product of "rank two corrections to the identity" of the form [24]

$$G(i,k,\theta) = \begin{bmatrix} 1 & \dots & 0 & \dots & 0 & \dots & 0 \\ \dots & \dots & \dots & \dots & \dots & \dots & \dots \\ 0 & \dots & \cos\theta & \dots & \sin\theta & \dots & 0 \\ \dots & \dots & \dots & \dots & \dots & \dots & \dots \\ 0 & \dots & -\sin\theta & \dots & \cos\theta & \dots & 0 \\ \dots & \dots & \dots & \dots & \dots & \dots & \dots \\ 0 & \dots & 0 & \dots & 0 & \dots & 1 \end{bmatrix} \begin{matrix} \\ \\ i \\ \\ k \\ \\ \\ \end{matrix} \qquad \text{(EQ 26)}$$

$\qquad\qquad\qquad\qquad\qquad\qquad\qquad\qquad\qquad\qquad\qquad\qquad\qquad\qquad\qquad\qquad\quad i \qquad k$

These matrices are called Givens rotations. As can be seen by the similarity of Equations 25 and 26, there a connection between the Givens rotations and directional couplers. Details of the design procedure for orthogonal turns ratio matrices are given in [7]. The results of that paper can now be extended.

Any multiport transformer, orthogonal or not, can be realized by combinations of directional couplers, straight through connections, and simple two port transformers.

Thus, in some sense, design of networks at microwave frequencies may be the only *practical* application of the extensive design procedures for arbitrary multiport networks built on the use of multiport transformers, such as those discussed by Newcomb [25].

5.3 Conclusion

A new way to implement constant congruence transformations with two port transformers, four port directional couplers, and straight through

connections has been presented here. All of these components are readily realized at microwave frequencies [31].

Directional couplers and impedance transformers behave ideally only around their design frequency, that is, they are band limited devices. The microwave multiport transformer approaches its ideal only within a limited band.

6.0 The Solution to a Multiport matching problem

Presented here is a solution to one kind of multiport broadband matching problem. The solution only works for

- loads that are diagonalizable over all frequency, and
- excitations which are constant with frequency.

Subsequent sections generalize these results to other conditions, and apply this theory to the antenna feed network design problem.

Consider a given N-port load, and N isolated, resistive sources, (Figure 23), where the excitation pattern of the sources does not vary with frequency.

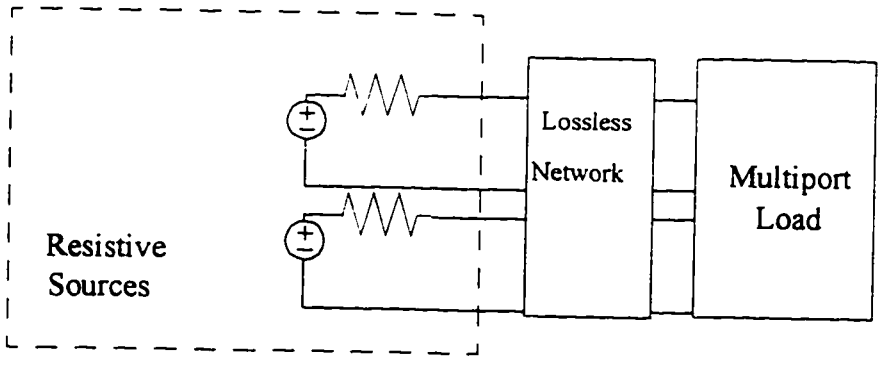

FIGURE 23. A matching problem.

The following paragraphs show how to find a lossless coupling network that will allow a given power gain vs. frequency specification to be realized between the resistive sources and the given load. Power gain, refers to the ratio

between the total power delivered to the load to the power available from the source. The power available from the source is independent of frequency for this particular problem.

This multiport matching problem would be solved if a congruence transformation that diagonalized the impedance matrix of the load over all frequencies could be found. Then the transformer which performs this congruence transformation could be placed in front of the load. At the transformer inputs, the circuit's impedance would be a diagonal matrix, and the multiport matching problem would be converted into N single port matching problems.

Fano[21] and Youla [22] derived the necessary and sufficient conditions for the solution of the single port matching problems. If a congruence transformation of the right kind is found, a solution is available for the multiport matching problem, shown in Figure 24. It may be that this is not the only solution, but it does provide one way to design a matching network to achieve Butterworth or Chebyshev power gain.

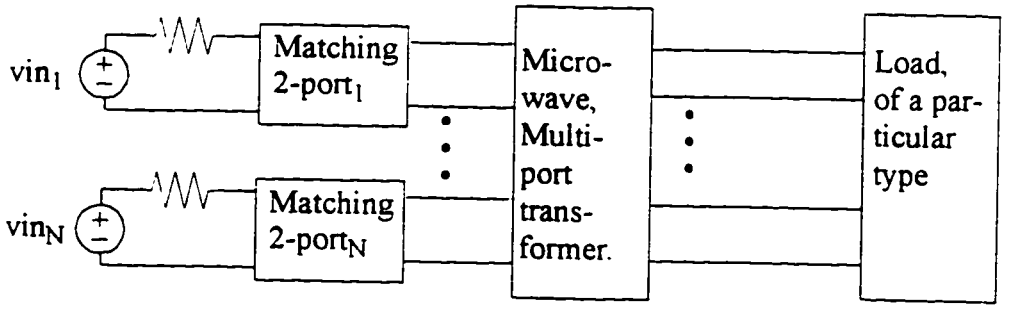

FIGURE 24. A solution, using a transformer

The magnitude of the excitation must remain constant as frequency varies. The individual ports of the transformer terminated in the load look like uncoupled impedances. Therefore, the power gain from the individual sources into these ports is independent of the individual excitation. However, the power gain into a given port will, in general, have a different *constant multiplier*[1] associated with it than the power gain into another port. The *overall* power gain, from *all of* the sources into the transformer and load, depends on which port is delivering power, and so depends on the magnitude of the excitation. The magnitude of the excitation does not matter to the overall power gain of the matching networks when the constant multiplier of each of the individual matches is the same.

1.The power gain at all of the ports is of the same shape, (for example Butterworth or Chebyshev), but the constant multiplier associated with the match depends on the particular load matched to, which will be different from port to port.

This solution to a multiport matching problem supposes that there is a congruence transformation that can diagonalize the impedance matrix of the multiport load over all frequency ranges.

6.1 Complete Decoupling over all frequency ranges.

Diagonalization over all frequency ranges is possible for the five types of load network discussed in this section: one element kind networks, two element kind networks with all ports accessible, systems with circular symmetry, systems with adjacent element coupling only, and three element kind networks with particular topologies.

6.1.1 One element kind networks

Conventional, lumped network theory is the study of the interconnection of two terminal elements with wires and ideal transformers. The three different types of elements normally used are resistors, capacitors, and inductors. These types are fixed: the designer is allowed to choose the values of the elements, but not their functional form. Networks can be classified in terms of the number of types of elements available for their design. Networks with the usual lumped elements are called *three element kind;* if only lossy capacitors are available for network synthesis, the networks are called *one element kind,* and so on.

For a one element kind network the impedance of the individual element can be factored out of the impedance matrix of the network, leaving a symmetric, real matrix multiplying a scalar impedance. A real and orthogonal matrix of eigenvectors of the symmetric real matrix acts to diagonalize the impedance matrix under a congruence transformation. This matrix of eigenvectors can be used as the turns ratio matrix of a diagonalizing transformer.

6.1.2 Special two element kind networks

Foster showed how to realize LC impedances by partial fraction expansion in 1924 [29]. Through the use of frequency transformations, RC and LR impedances can be realized in the same way. Taking this idea further, suppose the designer has available two different kinds of elements, whose impedance can be represented as some multiple of the basic elements Z1(s) and Z2(s). Any network consisting of two different kinds of two terminal elements can be transformed into an inductor capacitor network by dividing all impedances by some factor (called impedance leveling), and by replacing the complex variable s by some other function (called frequency translation). For example, Z1, Z2 networks can be transformed into LC networks in the following way:

- divide all impedances by Z1, (converting Z1 elements to resistors and Z2 elements into elements of type (Z2/Z1)(s)),

- replace Z1/Z2 everywhere with s^2, (converting the Z1/Z2's to super-inductors, and leaving the resistors unchanged),

- divide all impedances by s (converting all resistors to capacitors and all super-inductors to inductors).

All two element kind networks are therefore equivalent to LC networks.

The poles and zeros of any two element kind network will lie on a contour in the s-plane. This contour can be found as the solution to the equation

$$1 + k\frac{Z_1}{Z_2} = 0 \text{ for } k \geq 0 \qquad \text{(EQ 27)}$$

For example, critical frequencies of LC networks lie on the contour $ks^2 = -1$, for k positive and real, or the j-axis, in the s-plane. The critical frequencies of networks made of parallel LC tank circuits and resistors lie on the contour

$$1 + k\frac{R}{Ls + \frac{1}{Cs}} = 1 + \frac{kRCs}{LCs^2 + 1} = 0, \qquad \text{(EQ 28)}$$

which is a half circle, centered at the origin of the s-plane, and a portion of the negative real axis, (see Figure 25).

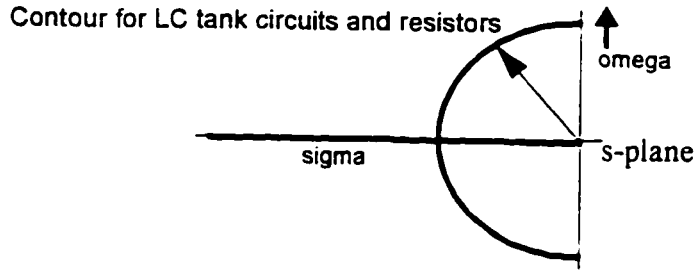

FIGURE 25. Critical frequencies of a two-element kind network

6.1.2.1 Multiport two element kind networks

Impedance or admittance matrices of reciprocal lossless N-port networks can be put into the form[25]

$$_{lc}(s) = A_o\frac{1}{s} + A_\infty s + \sum_{i=1}^{m}\frac{sA_i}{s^2 + w_i^2}, \qquad \text{(EQ 29)}$$

where the A matrices are N by N, symmetric, and positive semidefinite, and the w's are real. Each of the terms in Equation 29 can be realized by a transformer network terminated in isolated LC impedances.

Through the use of impedance leveling and frequency translation, it can be seen that impedance and admittance matrices of reciprocal two element kind N-port matrices can be put into the form

$$Z(s) = A_oZ_1(s) + A_\infty Z_2(s) + Z_1(s)\sum_{i=1}^{m}\frac{A_i}{\frac{Z_1(s)}{Z_2(s)} + w_i^2}. \qquad \text{(EQ 30)}$$

where the A matrices are N by N, symmetric, and positive semidefinite, and the w's are real and positive.

6.1.2.2 Sufficient conditions for a matching solution

It is instructive to consider a special type of two element kind network. Consider a multiport network where each of the node to datum voltages of the electrical network is directly accessible as a port voltage in the multiport. The definite admittance matrix of the electrical network can be expressed as $A_o Y_1(s) + A_\infty Y_2(s)$, where A_1 and A_2 can be found by inspection. The diagonal entries of A are positive and each a_{ii} can be found as the sum of all y's connected to node i. The off diagonal entries, a_{ij}, are the negative of the sum of all the y's connected between nodes i and j, and so on. The multiport short-circuit admittance matrix for this kind of network (which can be called a network with *all nodes accessible*) can be expressed using only the first two terms of Equation 30. (A similar argument could be made for the open circuit impedance matrix of two element kind networks with no internal, non-accessible loops). For networks with all nodes accessible to the ports, the multiport admittance is parameterized by two positive semidefinite matrices.

When the source network can be accurately modeled as a two element kind network with all of its nodes connected to a port, then the impedance of the source can be written

$$Ztotal = [Matrix1]\,Z_1(s) + [Matrix2]\,Z_2(s). \qquad \text{(EQ 31)}$$

Here, the two matrices are real, constant matrices, and all the frequency variation in the network is in the two scalar impedances, Z1 and Z2. In this case, a non-orthogonal congruence transformation can be found that diagonalizes both matrices simultaneously, as in the single frequency case.

6.1.2.3 A multiport matching example.

This section illustrates how the broadband multiport matching problem of section 6.0 can be completely solved for a limited class of networks.

Consider the network of Figure 26, with two ports. It would seem that this network is a RLC network, with internal nodes and loops. However, this can also be thought of as a two element kind network, where one element is a lossy capacitor, and the other is an inductor. This network can be matched exactly with a Butterworth response to a resistive source.

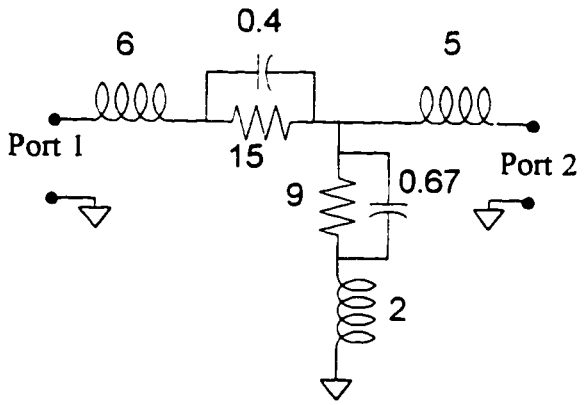

FIGURE 26. Example network for exact multiport matching.

The open circuit impedance matrix of the two port is

$$Z_{oc} = \begin{bmatrix} \frac{48s^2 + 8s + 24}{6s + 1} & \frac{12s^2 + 2s + 9}{6s + 1} \\ \frac{12s^2 + 2s + 9}{6s + 1} & \frac{18s^2 + 3s + 9}{6s + 1} \end{bmatrix} . \quad \text{(EQ 32)}$$

This can be written

$$Z_{oc} = \begin{bmatrix} 8 & 2 \\ 2 & 3 \end{bmatrix} s + \begin{bmatrix} 8 & 3 \\ 3 & 3 \end{bmatrix} \frac{3}{6s + 1} . \quad \text{(EQ 33)}$$

A transformer with a turns ratio matrix

$$T = \begin{bmatrix} 0.522 & -0.522 \\ 0.853 & 0.853 \end{bmatrix} , \quad \text{(EQ 34)}$$

can be placed in front of the given network. Then, looking into the transformer, the impedance seen is

$$Z_{in} = \begin{bmatrix} \frac{36.9s^2 + 6.15s + 21.1}{6s + 1} & 0 \\ 0 & \frac{15.5s^2 + 2.58s + 5.07}{6s + 1} \end{bmatrix} . \quad \text{(EQ 35)}$$

An equivalent circuit can be drawn for the input impedance of Equation 35. Figure 27 illustrates the view looking into the four port transformer. Now the multiport of Figure 26 is no longer coupled.

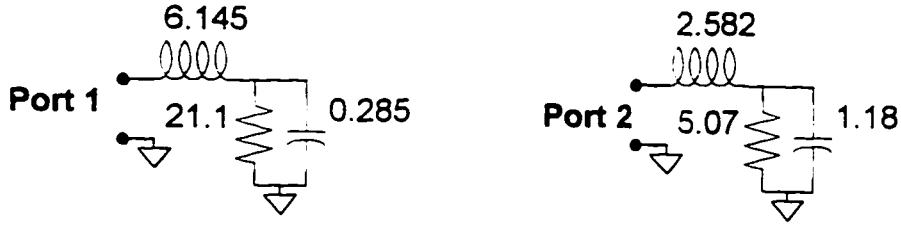

FIGURE 27. Uncoupled impedances looking into the transformer.

Networks to match the impedances of Equation 35 can be found using the classical matching theory of Youla. The maximum transducer gain for a fourth order Butterworth response shape with a cutoff of omega=1 is 0.6643 for port 1 and 0.6048 for port 2. The ratio of power delivered to the load to the available power from the source is maximum when port 1 is delivering all the power and port 2 none. For any constant magnitude excitation from source 1 and source 2, the power is Butterworth. The complete design of the Butterworth matching network is shown in Figure 28.

Although the first impedance could be matched with a ladder network, the second requires coupled inductors. Note, too, that the transformer turns ratios can be scaled to accommodate any particular source impedance.

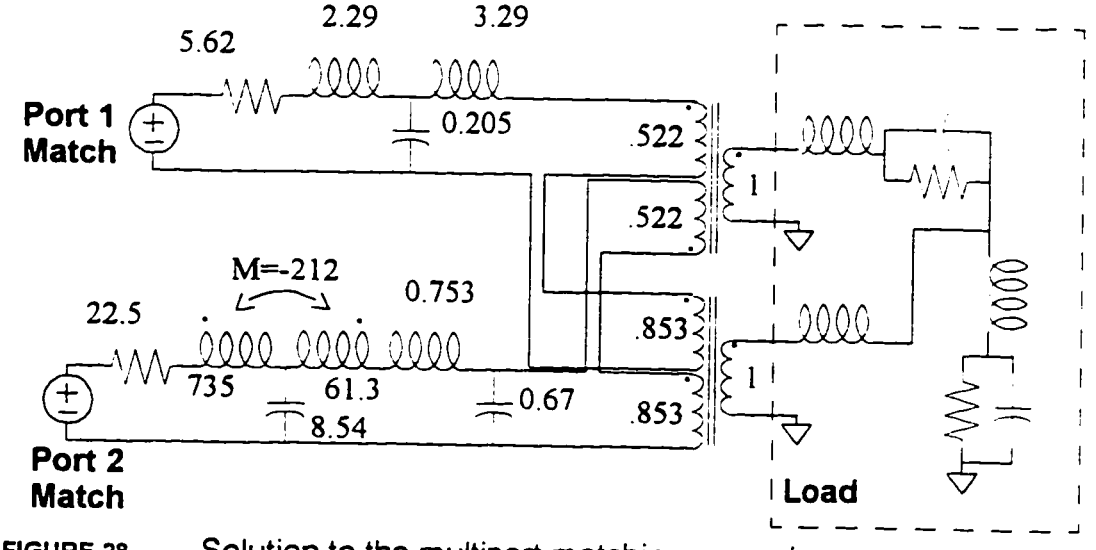

FIGURE 28. Solution to the multiport matching example.

6.1.3 Systems with circular symmetry

Another situation where a constant transformer turns ratio can decouple the multiport load completely is when the impedance matrix possesses a certain structure, for example, if Z is constrained to be circulant. All circulant matrices can be diagonalized by the same (unitary) transformation. Circulant matrices arise in situations where there is circular symmetry, such as a ring antenna array mentioned in section 2.3. For more information about circulant matrices, see appendix IV.

6.1.4 Systems with adjacent element coupling only

If the mutual coupling between antenna elements were to be modeled as insignificant, except for the adjacent couplings, the describing matrix for the antenna would be a symmetric, Toeplitz tri-diagonal matrix. These matrices e

are like circulant matrices, in that they also can all be diagonalized by one (unitary) transformation. For details of the diagonalizing matrix, see appendix VI.

6.1.5 Three element kind networks with particular topologies

Networks whose multiport describing matrices can be can be expressed as the sum of three terms, each one of which is a constant matrix times a scalar function of frequency, can sometimes be completely decoupled. If the three constant matrices are called A, B, and C, and if

$$BA^{-1}C = CA^{-1}B, \qquad \text{(EQ 36)}$$

then the three matrices can be simultaneously diagonalized. For more information about simultaneous diagonalization, see appendix IV.

6.2 Conclusion

In this section, the multiport matching problem has been solved for a limited class of load networks, as long as the source excitation pattern does not vary as frequency varies.

7.0 Application to the array feed problem

The multiport matching problem discussed in section 6.0 and illustrated in Figure 23 is a little different than the antenna feed problem shown in Figure 20. This section shows how to reconcile one of the differences.

The two problems are similar in the transmit situation, where resistive sources drive the coupling network that is terminated in the antenna. However, the aim in the transmitting situation is to drive the antenna ports with a particular excitation pattern, which is derived from the desired beam shape and direction. To produce such an excitation, the amplitude and phase of the sources (transmitters) changes as the beam is steered, and as the frequency changes. In general the power gain of the matching network will vary when the source magnitude varies. However, this will not be true if the power gain of each of the individual ports is the same.

Referring to Figure 24 on page 61, a design strategy that will produce a given power gain while transmitting (for the conditions of section 6.0), can be summarized as follows:

- Find the transformer which diagonalizes the antenna over all frequencies.

- Design matching networks for the impedances that are observed at the input ports of the diagonalizing transformer.

- Equalize the gain on all of the ports by lowering the gain of the better matches to the gain of the worst match.

- The resulting network will have an overall power gain that is independent of the magnitude of the source and so realizes the desired power gain, independent of scan angle or frequency of operation.

This strategy can be illustrated using the example of Figures 26-28. The load of Equation 32, the "two element kind" example, is taken as a model for a two element antenna. Let omega be fixed at unity. For this example, assume the load has progressive phasing on the ports, so that

$$V_{ports} = \begin{bmatrix} 1 \\ \exp(j\theta) \end{bmatrix}, \ \theta = 0 \ldots \pi . \qquad \text{(EQ 37)}$$

This means that the sources will be changing their magnitude and phase in order to create this voltage on the load ports. The power gain between the source and load in this case is shown as the top curve of Figure 29. When the load is driven in phase, port 1, the higher gain port, is used more. As the load voltage changes to exactly out of phase, port 2 comes to dominate. Since port 2 has less gain, this causes a variation in power gain with phasing. To eliminate the variation, the gain of port 1 must be equalized to the gain of port 2. When this is done, the variation in power gain is shown in lower curve of Figure 29. By lowering the gain of port 1, a "scan independent" power gain has been achieved.

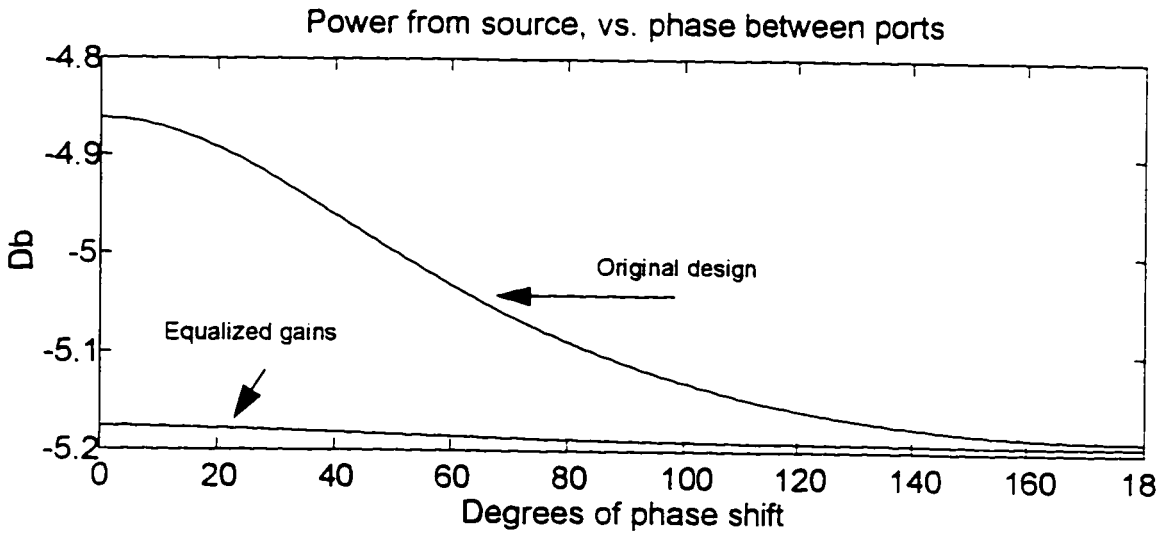

FIGURE 29. The result of equalizing the gains of the individual ports

7.1 Conclusion

In this example, lowering the gain of port 1 necessitated a more complex matching network, as shown in Figure 30.

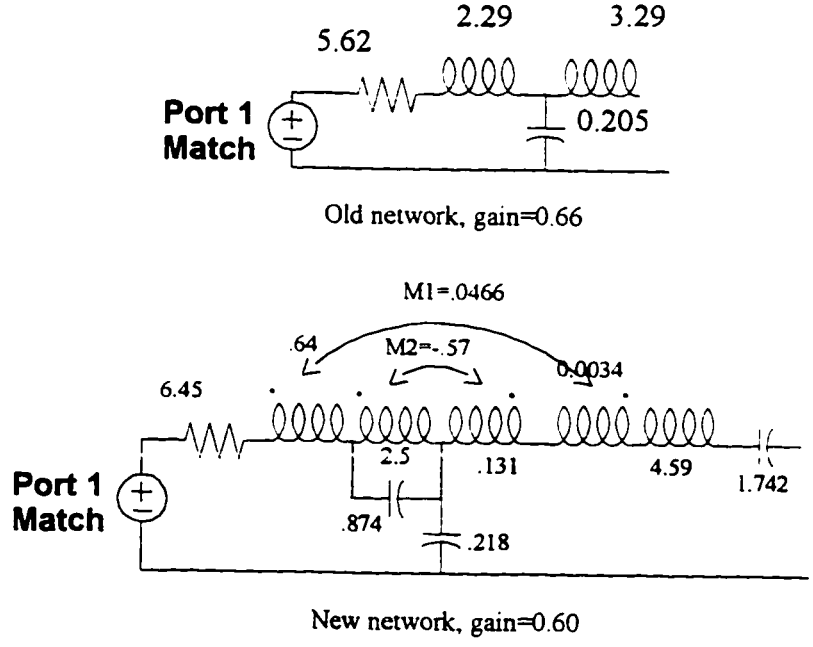

FIGURE 30. The matching network for port 1.

The matching network does not always become more complex, it depends on the particular matching situation. In this section, it has been shown that a given power gain (for example, Butterworth or Chebyshev), that is independent of the incident wave direction in the receive case, or the beam direction in the transmit case, can be achieved in the antenna matching situation. The price paid for scan independence is a lowering of the overall gain of the match.

8.0 A general diagonalizing transformation

The above sections have shown that several different types of load networks are diagonalizable over all frequencies. With the diagonalization and broadband matching, a scan independent match can be achieved over a wide bandwidth. Also, it has been demonstrated that at a single frequency, any passive load can be matched with scan independence. This section presents a formulation for designing scan independent matching networks over a broad band of frequencies, for general antenna-like load networks.

The motivation for this is that a two element kind network with all ports accessible is diagonalizable over all frequencies, and a linear array with a Toeplitz admittance matrix can be represented by an equivalent circuit, where each node is brought out as a port, (that is, all ports are accessible in this case).

It is these two facts that lead us to suspect that one frequency independent congruence transformation may do a good job of diagonalization over a large frequency range. In the following section, it is shown how such a congruence transformation can be found

8.1 Modeling for diagonalization

Matching a multiport load over a wide bandwidth involves reducing the mutual coupling between ports with a coupling network placed in front of the load. The admittance matrix of the given multiport can be expressed as

$$Y_{TOTAL} = \begin{bmatrix} A_{1,1} & A_{1,2} & \cdots & A_{1,N} \\ A_{2,1} & A_{2,2} & \cdots & A_{2,N} \\ \cdots & \cdots & \cdots & \cdots \\ A_{N,1} & A_{N,2} & \cdots & A_{N,N} \end{bmatrix} Y_1(s) + \begin{bmatrix} B_{1,1} & B_{1,2} & \cdots & B_{1,N} \\ B_{2,1} & B_{2,2} & \cdots & B_{2,N} \\ \cdots & \cdots & \cdots & \cdots \\ B_{N,1} & B_{N,2} & \cdots & B_{N,N} \end{bmatrix} Y_2(s), \qquad \text{(EQ 38)}$$

where the elements of the two matrices are real constants. By parameterizing the "spatial" aspect of this admittance with two constant matrices, it is possible to approximately diagonalize the admittance of the multiport source, by simultaneously diagonalizing both matrices.

The following sections present a method for modeling the multiport in the form of Equation 38. The method assumes that numerical data from an N port is available. The object is to find a good diagonalizing transformation that will work over the entire band of the data. A numerical example is presented in appendix VII.

For an N port like a linear array antenna, the matrices are symmetric Toeplitz, which are defined by N numbers, and the problem is to determine two admittances (the Y(s)), and 2*N constants that are the entries in the two arrays of Equation 39.

$$Y_{ANTENNA} = \begin{bmatrix} Y_{11} & Y_{12} & \cdots & Y_{1N} \\ Y_{12} & Y_{11} & \cdots & Y_{1N} \\ \cdots & \cdots & \cdots & \cdots \\ Y_{1N} & Y_{1N} & \cdots & Y_{NN} \end{bmatrix} = \begin{bmatrix} a_1 & a_2 & \cdots & a_N \\ a_2 & a_1 & \cdots & a_{N-1} \\ \cdots & \cdots & \cdots & \cdots \\ a_N & a_{N-1} & \cdots & a_1 \end{bmatrix} Y_1(s) + \begin{bmatrix} b_1 & b_2 & \cdots & b_N \\ b_2 & b_1 & \cdots & b_{N-1} \\ \cdots & \cdots & \cdots & \cdots \\ b_N & b_{N-1} & \cdots & b_1 \end{bmatrix} Y_2(s) \qquad \text{(EQ 39)}$$

Apparently,

$$\begin{aligned} Y_{11} &= a_1 Y_1(s) + b_1 Y_2(s) \\ Y_{12} &= a_2 Y_1(s) + b_2 Y_2(s) \\ &\cdots \\ Y_{1N} &= a_N Y_1(s) + b_N Y_2(s) \end{aligned} \qquad \text{(EQ 40)}$$

8.2 Using the data directly

The available data are N vectors of complex numbers, each one representing one of the N admittances on the left hand side of Equation 40. The length of these vectors is equal to the number of frequency points used in the multiport simulation. In terms of vectors of complex numbers, Equation 40 can be written

$$\begin{bmatrix} Y_{11} & Y_{12} & \cdots & Y_{1N} \end{bmatrix} = \begin{bmatrix} Y_1 & Y_2 \end{bmatrix} \begin{bmatrix} a_1 & a_2 & \cdots & a_N \\ b_1 & b_2 & \cdots & b_N \end{bmatrix}. \qquad \text{(EQ 41)}$$

Here the Y's are columns of complex numbers: the right hand side is known data, and the vectors Y1 and Y2, together with the real coefficient matrix, are unknown.

8.2.0.1 A Solution using the Singular Value Decomposition

Equation 41 could only have a solution if there is some degeneracy in the data vectors on the left hand side. It demands that N vectors be represented by a linear combination of only two. In fact, if the rank of the matrix on the left hand side of Equation 41 exceeds two, there will be no solution to the equations. However, an approximate solution can be found through the use of a singular value decomposition of the left hand side of Equation 41. The SVD yields a decomposition of the data matrix in this form:

$$SVD(Y) = U \cdot S \cdot V^t , \qquad \text{(EQ 42)}$$

where U and V are orthogonal matrices and S is a diagonal matrix with non-negative entries.

The aim is to find real coefficients that multiply the two complex basis vectors to approximate the N complex admittance vectors. To get *real* results, the dimension of the complex problem is doubled and the problem made real by representing the column vectors of data as [real, imaginary]^t. The columns of the matrix U form an orthonormal basis of the space that is spanned by the original data vectors. The N data vectors are then expressible as a linear combination of the columns of U. The entries in the columns of S are the weights that each of the U columns have in the reconstruction of the original data. For example, the (1,1) entry of S indicates the weight for reconstructing the data that is given to the first column of U. The size of the entries of S

indicate the relative contribution of the columns of U to a reconstruction of the original data. The values in each column of V^t, also contribute to the weights given to the columns of U. In general, however, the large value of S(1,1) indicates that the first column of U is the dominant basis vector for reconstruction of the data values.

For this N port, Toeplitz matrix problem the two columns of U with the largest weights in the corresponding columns of S are the two best basis vectors to use in an attempt to reconstruct all N of the original data vectors. The weights for the reconstruction are simply the corresponding two rows of the matrix product $S*V^t$ that involve the two largest entries in S. Most SVD routines return the matrices sorted so that the largest values in S are in the first columns, and smaller values follow. This means that the two basis vectors for the best approximation to the data are the first two columns of U. The weights are given by the first two rows of $S*V^t$.

Through the use of SVD, j-axis values of two admittances that most closely can approximate the N admittances that comprise the original data have been found. It is more important, though, that the set of weights for the two admittances have been found. These 2*N weights are the entries in the matrices of Equation 39.

8.2.0.2 Diagonalization with a congruence transform.

The entire admittance matrix of the multiport has now been parameterized with two constant matrices. Both matrices can be diagonalized simultaneously with a congruence transformation. This mathematical operation corresponds to the physical act of adding a lossless coupling network to the front of the antenna. This network is ideally a multiport transformer. A transformation matrix, "Trans", is found such that

$$Trans^{t} Y_{ANTENNA} Trans = \begin{bmatrix} x_1 & 0 & \dots & 0 \\ 0 & x_2 & \dots & 0 \\ \dots & \dots & \dots & \dots \\ 0 & 0 & \dots & x_N \end{bmatrix} Y_1(s) + \begin{bmatrix} y_1 & 0 & \dots & 0 \\ 0 & y_2 & \dots & 0 \\ \dots & \dots & \dots & \dots \\ 0 & 0 & \dots & y_N \end{bmatrix} Y_2(s), \qquad \text{(EQ 43)}$$

where the x_i and y_i are some real numbers. If a transformer with a turns ratio matrix given by "Turns" is loaded with a network that has an admittance matrix "Y_L", the admittance looking into the transformer is

$$Y_{in} = Turns^{-1} Y_L (Turns^{t})^{-1}. \qquad \text{(EQ 44)}$$

Therefore, the multiport admittance matrix can be approximately diagonalized with a multiport transformer coupling network. The multiport transformer should have a turns ratio of

$$Turns = (Trans^{t})^{-1}. \qquad \text{(EQ 45)}$$

This transformer does not exactly diagonalize the multiport. However, the mutual coupling effects are greatly reduced.

When the network which cancels the mutual coupling effects of the multiport is frequency independent, it will be more or less effective as frequency varies. Figure 31 illustrates the performance of four different frequency independent decoupling networks. The multiport used in this example is a four element linear array slot antenna. The ratio of the magnitudes of the diagonal elements of the admittance at the input of the feed network to the magnitudes of the off diagonal elements is plotted.

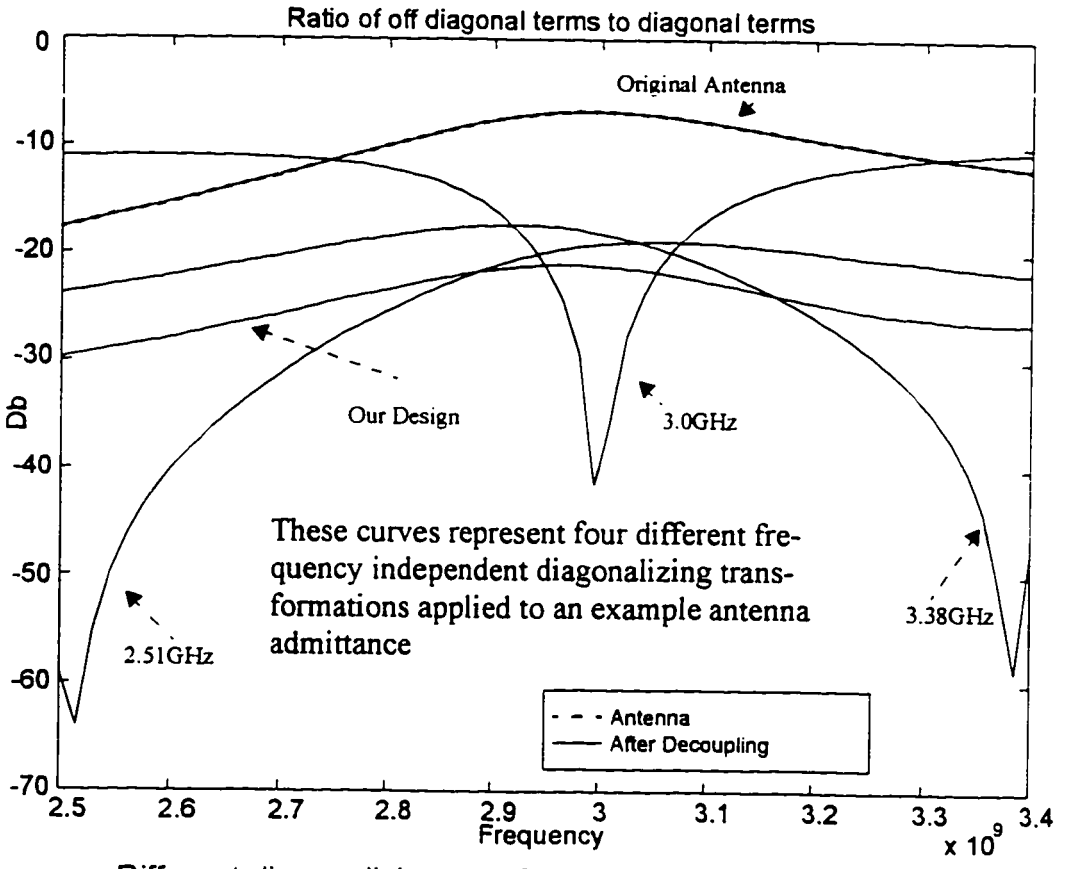

FIGURE 31. Different diagonalizing transformations.

The top curve shows the behavior of the multiport without a decoupling network. The antenna has a diagonal that is larger than its off diagonal elements by 8 to 18 db, over the frequency range. Three other curves show the performance of three designs based on perfect decoupling at a single frequency. These single frequencies are chosen at the low end of the frequency range, (2.51GHz), in the center (3.0GHz), and at the high end of the frequency range (3.38GHz). The decoupling is very large at the design frequency, but is unsatisfactory at other frequencies in the band. A fourth curve shows the results of the design procedure that uses the singular value decomposition of the data matrix to find the decoupling network. This procedure shows an improvement over the antenna alone of 12 to 15 db over the entire frequency band. Good performance is achieved over all frequencies.

8.3 Conclusion

In this section, a numerical procedure has been developed to find a constant congruence transformation that approximately diagonalizes a given multiport impedance or admittance matrix over a frequency band.

9.0 After Compensation for the Mutual Coupling Effects.

In order to reduce the dependence of the power flow into and out of the antenna on the excitation pattern, a procedure to find a decoupling network was presented in Section 8.2. Because the input impedance of this network, when it is loaded by the antenna, approximately consists of N isolated one port impedances, a broadband match to the antenna can be realized by designing N two port lossless coupling networks that connect the resistive transmitter and receiver to the decoupling network. Figure 32 shows that the two port broadband matching networks appear between the uncoupled resistors and the decoupling network in the overall matching scheme.

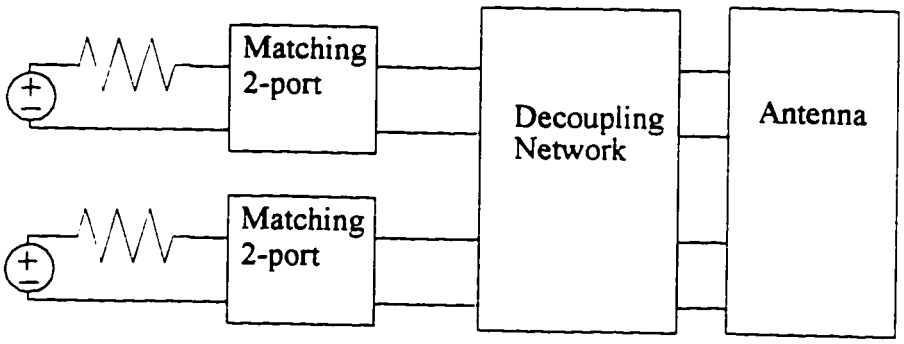

FIGURE 32. Lossless two port networks for broadband matching

To the extent that the decoupling network really does work, the matching two-ports can be designed by classical broadband matching theory, which details how to design a lossless two-port network to match a given single-port load impedance.

9.1 Matching over a wide range of frequencies

For antennas with simply shaped elements, one would expect the decoupled ports of the feed network to be broadly resonant impedances, with center frequencies at the antenna design frequency. For wire dipole elements, a series resonance seems likely, while apertures should be parallel resonant. Broadband elements, which are more complicated in structure, exhibit more complex frequency behavior. Simple element shapes are an important case to consider, however, because most arrays will use these kinds of elements.

The analytic theory of Youla [21] for the design of matching networks is a good starting point for numerical optimization techniques like the real frequency technique of Carlin[13]. Youla's theory has been applied in detail to *one load*, an inductor in series with a resistor and capacitor in parallel [39], [40], [41], [42]. Formulas have been derived for lowpass and bandpass matching networks with Butterworth and Chebyshev response shapes for this load. In the following section, Youla's theory is applied to bandpass matching of RLC series and parallel resonant loads.

9.2 Broadband Matching to resonant loads

The classical matching procedure starts with finding complex frequencies where the load can accept no power. For a parallel resonant load, given by

$$Z = \frac{1}{C}\frac{s}{\left(s^2 + \frac{w_0}{Q}s + w_0^2\right)} \quad \text{(EQ 46)}$$

the frequencies where the load are can accept no power are on the j-axis, at DC and infinity. Since the "usual" prototype responses like Butterworth and Chebyshev bandpass functions have their zeros at DC and infinity, these responses will be compatible with this load. The same can be said for the series resonant load,

$$Z = \frac{L}{s}\left(s^2 + \frac{w_0}{Q}s + w_0^2\right). \quad \text{(EQ 47)}$$

Because these loads have "zeros of power acceptance" at DC and infinity, the reflection coefficient at the load to matching network interface must reach a magnitude of unity at these frequencies. The other requirement that these loads place on the reflection coefficient has to do with how fast or how strong this movement to unity must be for the reflection coefficient to be compatible with the load. This is the requirement that really limits the gain obtainable for a specified bandwidth of response into the load. A detailed derivation of the gain bandwidth constraints for these loads is presented in Appendix XI. Only some results are shown here.

These loads are the simplest bandpass circuits, and a bandpass response is desired for the power gain into these loads. Intuitively, the gain possible for a particular bandwidth of response will decrease as the Q factor of the load

increases (see Figure 33). This is because the Q factor of the load is an indication of the load's natural bandwidth. Also, the possible gain must be greatest when the center frequency of the desired response corresponds to the center frequency of the load resonance. This is shown in Figure 34. Figures 33 and 34 are for Chebyshev power gains. Appendix XI also derives the matching constraints for Butterworth power gains. An example of these results is shown in Figure 35, which graphs the maximum gain vs. the bandwidth of the resulting power response, when the Q of the load changes.

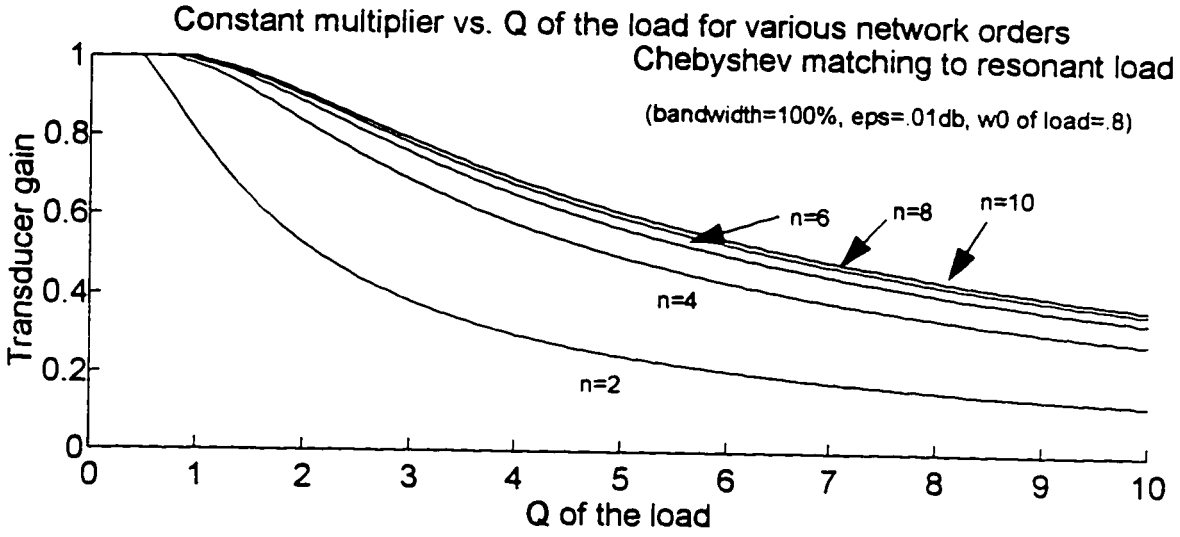

FIGURE 33. Matching best when the load is broad band

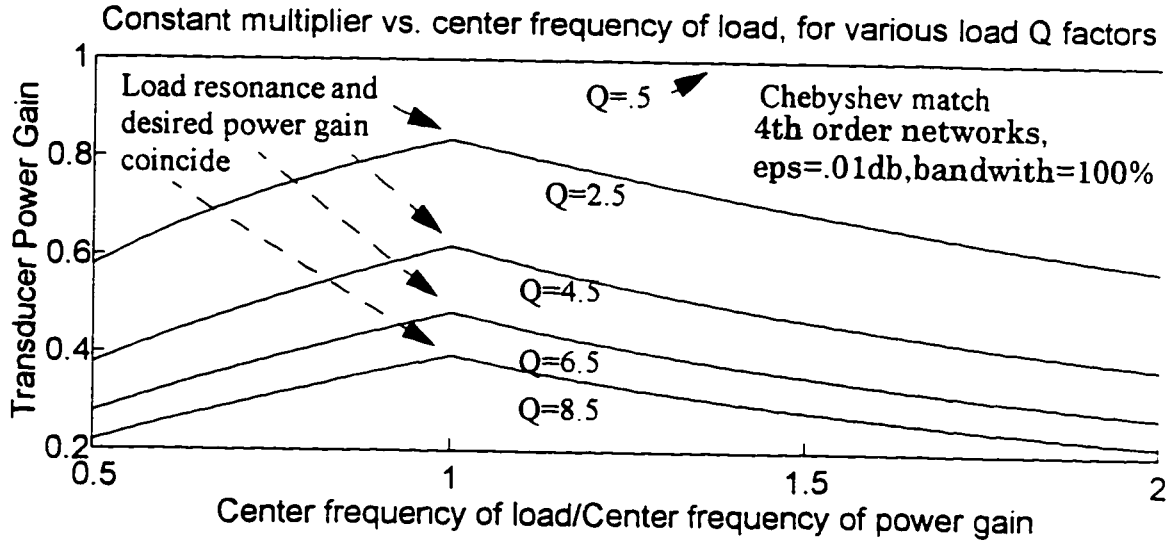

FIGURE 34. Max gain occurs for compatible load and power gains

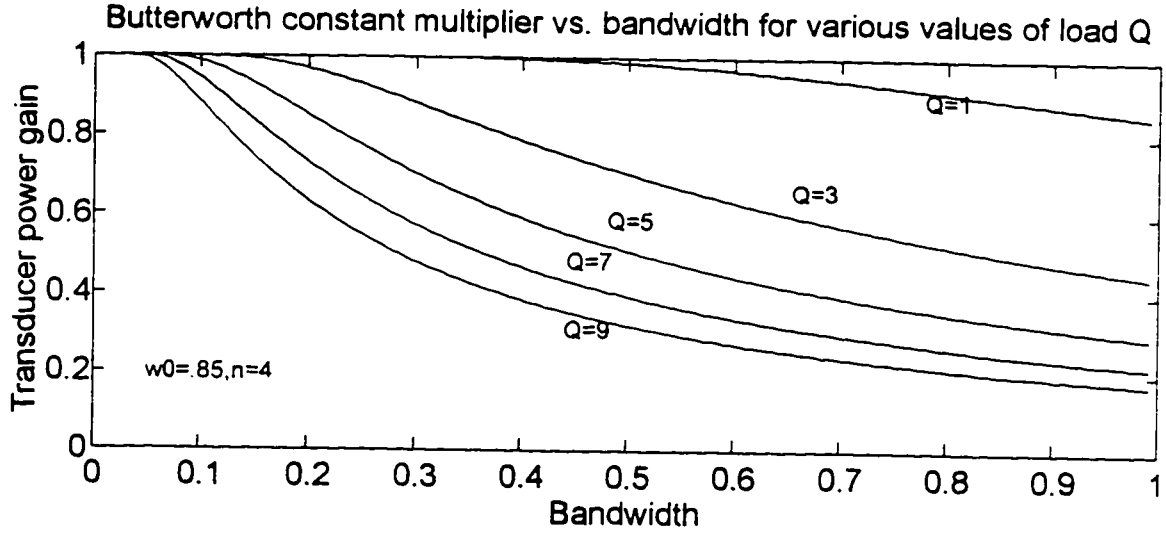

FIGURE 35. Gain vs. bandwidth for various Q's of the load

9.3 Carlin and Yarman's numerical matching technique

The classical theory of matching provides the necessary and sufficient conditions for realization of a matching network for a particular load and a

particular power gain. One of its main disadvantages is that the load must be known over the entire range of complex frequencies for the theory to be applied. In many practical situations, the load is only known at discrete frequencies on a portion of the j-axis in the s-plane. Thus, some modeling must be done to create a load, defined over all frequencies, that has the tabulated response.

Another potential disadvantage of the classical theory is the need to choose a power gain response, a priori. The classical responses: Butterworth and Chebyshev, come from filter design theory and are perhaps not the most appropriate for a matching application. Specifically, the filter responses have stopband requirements that are often not an issue for matching, where the passband response is of sole interest.

Some sort of numerical optimization technique is appropriate here, where the load's tabulated data can be used directly, and a passband only error criterion can be employed in the optimizing routine.

Carlin published a two part numerical procedure for single port matching that has had a significant impact on practical matching design[13]. First, the real part of the back end impedance of the matching network is modeled as a piecewise linear function (see Figure 36). The imaginary part is then calculated from the real part using the Hilbert transform. An optimization is performed on the resistive excursions of the real part of the back end

impedance. As the back end impedance changes, the transducer power gain into the load is computed, and eventually the back end impedance with the best transducer power gain is converged to.

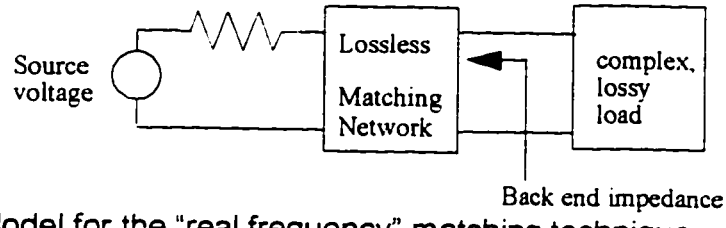

FIGURE 36. Model for the "real frequency" matching technique.

The second part of Carlin's procedure is converting the piecewise linear back end impedance into a positive real rational function. This curve fit involves a second optimization technique. Finally, the back end impedance is used to synthesize a matching network as a lossless network terminated in a resistor (which is the source impedance).

Carlin and Yarman have also published a second technique, which they call "simplified"[14]. It is a one-step optimization, that finds a rational back end impedance. This technique starts with the fact that a lossless 2-port network terminated in a resistor can realize any positive real input impedance. Since any real power that flows into the terminated two-port must be dissipated in the resistor, there is a connection between the transfer function of the lossless two port network and the real part of the input impedance.

The numerical matching technique used in this work is based on this simplified real frequency technique. The key to understanding this technique is the representation of the most general form of the scattering matrix for a lossless, reciprocal two port that was derived by Bellevitch [2].

The lossless two port is described by a rational, unit normalized scattering matrix. A lossless scattering matrix is para-unitary, or $S^t(-s)S(s) = 1_n$, and so it can take only two forms, depending on whether the transfer polynomial is even or odd [2, p. 278]. This is described in Table 1.

TABLE 1. Lossless, reciprocal scattering matrices take two possible forms

Condition	tran(s) is an even polynomial	tran(s) is an odd polynomial
Scattering Matrix	$S = \frac{1}{den(s)}\begin{bmatrix} num(s) & tran(s) \\ tran(s) & -num(-s) \end{bmatrix}$ **(EQ 48)**	$S = \frac{1}{den(s)}\begin{bmatrix} num(s) & tran(s) \\ tran(s) & num(-s) \end{bmatrix}$ **(EQ 49)**
$s_{11}s_{11}^{*+}$ $s_{12}s_{12}^{*}=1$	$num(s)num(-s) + tran(s)tran(s) = den(s)den(-s)$	$num(s)num(-s) - tran(s)tran(s) = den(s)den(-s)$
	$tran(s)tran(s) = den(s)den(-s) - num(s)num(-s)$	$tran(s)tran(s) = num(s)num(-s) - den(s)den(-s)$

This scattering matrix is used in the simplified real frequency technique to define the back end impedance of the matching network. If num(s) and tran(s) are known, one can see from Table 1 that the entire scattering matrix is known. Consequently, the impedance which results from terminating the lossless network with a unit resistor is also known.

Darlington showed how a driving point impedance can be realized by a lossless coupling network terminated in a unit resistor [31]. His formulation used the impedance parameters of the lossless network. The discussion above is really just the Darlington theory in terms of the scattering parameters rather than the impedance parameters.

The scattering formulation is used by Yarman in a numerical procedure. First, the degree of the num polynomial, "n", and the transfer polynomial, "tran", are chosen a priori. This determines the kind of network that will be used to realize the impedance. It is especially desirable that the transfer polynomial be chosen to be of the form $tran=s^k$, where k is some integer. Then the network realized will be a ladder network, with k zeros of transmission at DC and n minus k at infinity. Second, a numerator, num(s), is chosen and a denominator, den(s), is calculated using the equations in Table 1. In this way, one is able to determine an impedance, over all frequencies, by choosing the n coefficients of the num(s) polynomial.

Since the scattering matrix is normalized to unity, when it is terminated in a unit resistor, the input reflection coefficient is $\frac{num}{den}$. The terminated network is then used to realize the back end impedance of the matching network, as shown in Figure 36. At each iteration, the n coefficients

of the num polynomial are varied, and the power gain is computed. Eventually the procedure converges to define a maximum of the power gain.

9.4 From impedance to num(s)

In order to use a starting point for the numerical iteration that is derived from the analytic theory, the conversion of a known back end impedance to the scattering matrix of a lossless coupling network must be performed.

If the impedance is specified, the reflection coefficient can be calculated using

$$\Gamma = \frac{Z-1}{Z+1}. \qquad \text{(EQ 50)}$$

Equation 50 specifies $\frac{num}{den}$. However, num and den may not be acceptable as polynomials in Table 1. The num and den must result in $tran^2$ which is a perfect square, and a resulting tran that is either even or odd.

Therefore num and den sometimes must be augmented, (as are the polynomials of regular Darlington synthesis), to result in a scattering matrix of the form of Table 1.

For example, an impedance $Z = \frac{s^2+s+1}{s^2+s+2}$ results in a reflection coefficient of $\Gamma = \frac{-0.5}{s^2+s+1.5}$. This numerator and denominator implies a $tran^2$

polynomial of $tran^2(s) = s^4 + 2s + 2$. But, tran must be an even or odd polynomial. Therefore the numerator and denominator of the reflection coefficient must be augmented in order to insure that their magnitude square sum or difference is a perfect square of an even or odd polynomial. For example, if one were to multiply both num and den by $s^6 + 2.91s^5 + 7.235s^4 + 9.47s^3 + 10.64s^2 + 6.29s + 3.18$, then their magnitude squared difference is $tran^2(s) = s^{16} + 8s^{14} + 32.5s^{12} + 83s^{10} + 145.1s^8 + 176.2s^6 + 146.5s^4 + 76.5s^2 + 20.25$. This implies that tran is $tran(s) = s^8 + 4s^6 + 8.25s^4 + 8.5s^2 + 4.5$, which is even. The scattering matrix in the form of Table 1 corresponding to this impedance is then

$$S_{lossless} = \frac{1}{s^8 + 3.91s^7 + 11.64s^6 + 21.1s^5 + 31s^4 + 31s^3 + 26s^2 + 12.6s + 4.77} \times \begin{bmatrix} -0.5s^6 - 1.45s^5 - 3.6s^4 - 4.7s^3 - 5.3s^2 - 3.15s - 1.6 & s^8 + 4s^6 + 8.25s^4 + 8.5s^2 + 4.5 \\ s^8 + 4s^6 + 8.25s^4 + 8.5s^2 + 4.5 & -0.5s^6 + 1.45s^5 - 3.6s^4 + 4.7s^3 - 5.3s^2 + 3.15s - 1.6 \end{bmatrix} \quad \text{(EQ 51)}$$

The impedance in the above example cannot be realized as a lossless ladder terminated in a resistor. It was chosen as an example because it needs two coupled inductors and two capacitors in a lossless network terminated in a resistor [18]. Thus, as a representation for ladder structures, Table 1 is quite useful, however, more general matching networks are not simply represented by the scattering matrix of Table 1. Another example is given in Appendix VIII.

9.5 Comparison of the numerical and analytic results

Design of a matching network for a parallel RLC load impedance is used as an example of this numerical technique and the analytic technique developed in the last section. The load is of the form of Equation 46. Specifically, it is

$$Z_{load} = \frac{0.133s}{s^2 + 0.0665s + 1.003} \qquad \text{(EQ 52)}$$

The power gains that result from an analytical design and two different numerical designs are shown in Figure 37, with a 50% bandwidth as the target power gain response. The performances of the three designs are not significantly different, although the realizations of the designs are a bit different, as shown in Figure 38.

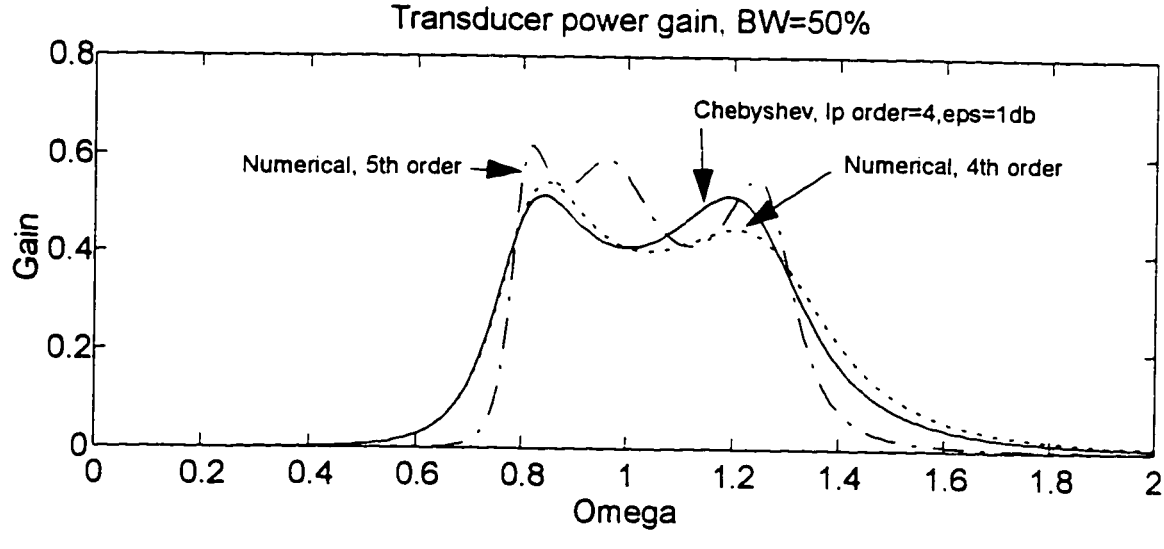

FIGURE 37. Match to a parallel resonant load

The result of all the matching procedures is a rational function, and the realizations shown in Figure 38 are the result of applying cascade synthesis to the rational functions. The performance improvement resulting from increasing the order used in the numerical procedure is slight to nonexistent, even though the matching network for n=5 is quite a bit more complicated.

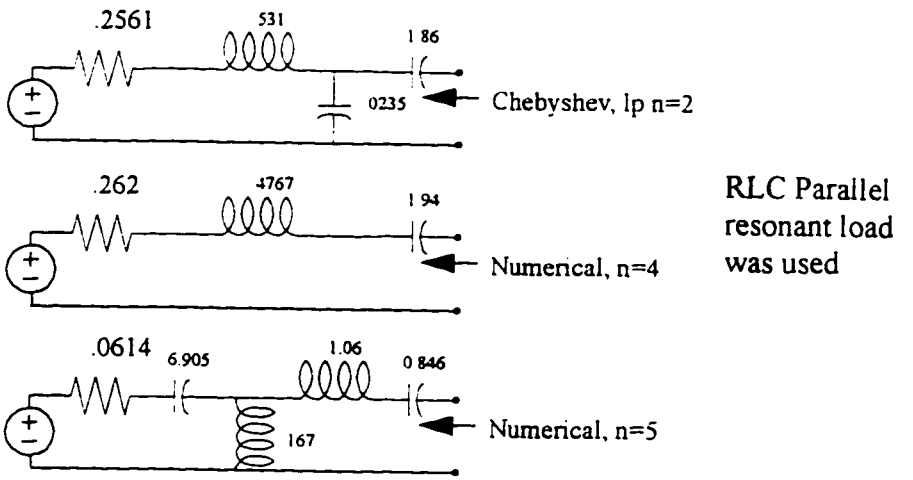

FIGURE 38. Three bandpass matching network designs.

9.6 Conclusion

This comparison used a load whose rational form was known. This is necessary for the analytical technique. For the numerical technique, the rational form was simply used to generate a data vector at equally spaced points across the matching band. Thus, the numerical technique is practical in matching measured or simulated loads, while the analytical technique requires a second type of numerical procedure to form a rational approximation. The ripple of the analytic technique is specified in advance, but the ripple resulting

from the numerical technique is unknown. Here, 1 db ripple was chosen so that the analytic technique would look similar to the numerical results.

The numerical design technique for matching that is presented here is attractive because of its simplicity. Carlin's original real frequency technique is a general technique that does not presuppose the form of the resulting matching network. This is because of the two step nature of the approximation: In the first step a curve of the real and imaginary parts of the impedance vs. frequency is found that is both stable (because of the Hilbert relation between the two). and positive real (because the optimization is constrained not to allow the real part to go below zero). It is only in the second step, (e.g., moving from the back end impedance curve vs. frequency to a rational approximation), that the realization of the network has to come in.

In contrast Yarman's technique is not general. A rational form for the matrix is presupposed, and the transmission zeros of the back end impedance network are chosen a priori. A major advantage of this technique, however, is that there is no need for a constrained optimization, since the numerator of the reflection coefficient, which is the polynomial changed at every iteration, is not necessarily Hurwitz.

10.0 Example

10.1 Four element linear array

To find a congruence transformation that compensates for the mutual coupling of a four element linear array, the SVD technique was applied to data collected from a numerical electromagnetic simulation of the antenna. Designs were performed for several bandwidths. One hundred and fifty data points of the antenna admittance were taken across the desired bandwidth of the design. Linear interpolation was used to fill in for frequencies that were not simulated.

When a plane electromagnetic wave impinges on a uniform linear array antenna from a particular direction, voltages appear at the antenna ports. It is assumed that the amplitude of the voltages is uniform, and they differ in phase depending on the direction of the source. For elements separated by a distance *spacing*, and wave incident from an angle θ, the waves travel $spacing \cos(\theta)$ farther for each element which is at a multiple of *spacing* from the reference element. The phase shift between ports is then

$$PhaseBetweenPorts = 2\pi d\cos\theta, \qquad \text{(EQ 53)}$$

where d is the spacing between elements in wavelengths, and theta is the angle of the incident wave. Here theta=0° is endfire and theta=90° is broadside to the array. In the following examples, the frequency response of the various power

gains is plotted for several different wave directions, and at each frequency the equivalent excitation phase is calculated from Equation 53.

10.2 Characteristics of the antenna

The antenna is four, quarter wave slots on a ground plane, with a spacing of 0.7 wavelengths, oriented broadside to the axis of the array. These slots are cavity backed, and the feed point has been adjusted so that the slot admittance is purely real at the center frequency of the design, which is 3.0GHz. This admittance is normalized to unity.

The variation in input power for a constant magnitude voltage excitation with progressive phase is shown in Figure 39. Curves are shown at five different frequencies. This multiport exhibits a moderate variation, with about 4 db of change over all scan angles. The variation shape is different as frequency varies, but shows about the same order of magnitude change.

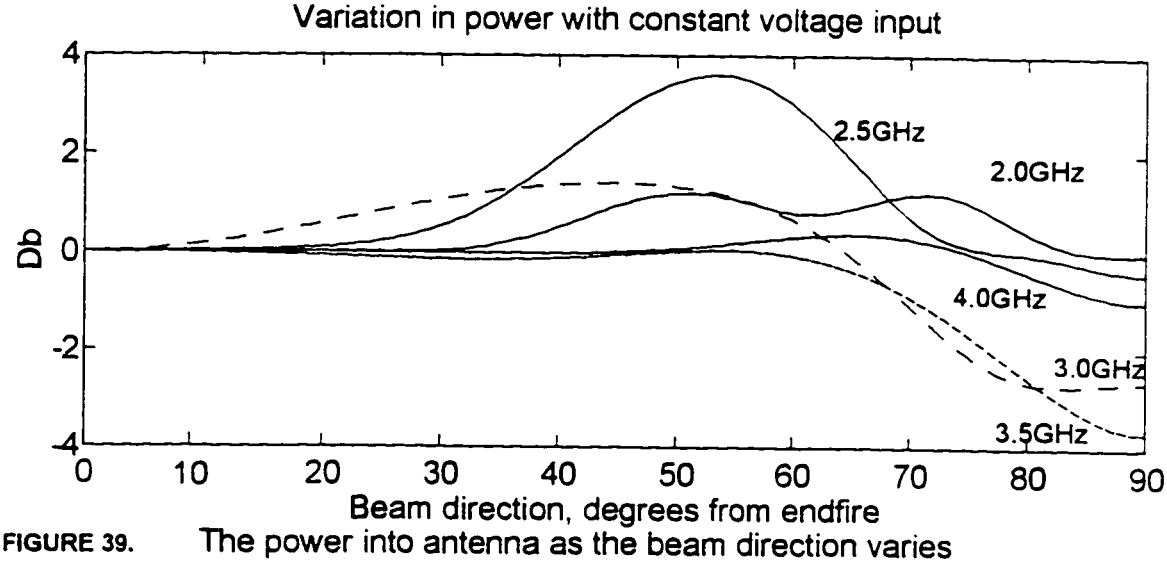

FIGURE 39. The power into antenna as the beam direction varies

10.3 Single Frequency Matching

A useful reference, and perhaps the most straightforward design, is a simple match at a single frequency within the band of the antenna, for a particular receive direction (Figure 40). The design was carried out for a source at 60°, at two frequencies, 2.6GHz and 3.4GHz. All the available power will be extracted from the antenna at the design frequency and for a source at 60°, but for other receive directions or frequencies, the receive performance will suffer.

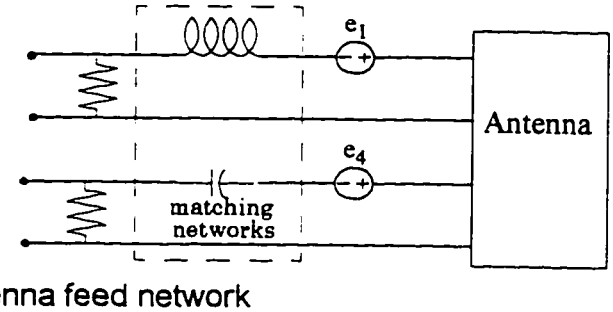

FIGURE 40. The simple antenna feed network

An analysis was performed of the two designs, with frequency varying, for several different source directions. The results are shown in Figure 41.

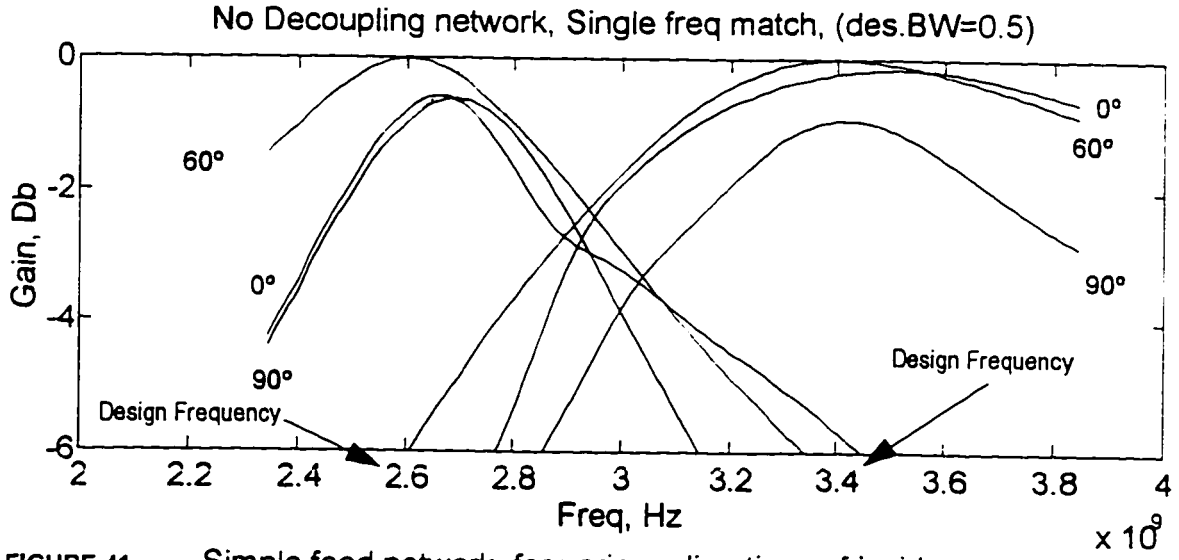

FIGURE 41. Simple feed network, for various directions of incident wave

This antenna does not show much variation in power flow with change in excitation phase, but there is some evidence of it here. At the design frequency, variation of about 1 db in power response is seen as the direction of reception varies. The best power extraction shown here is a perfect match with 60 source direction at the two design frequencies. The bandwidth with gain better than -3 db ranges from 1.35Ghz to 0.62Ghz, depending on source direction.

The antenna excitation for Figure 41 is progressive phase, constant amplitude. If it is assumed that, when transmitting, the antenna has just that excitation on its ports, the transmitting and receiving power graphs will be

identical. As frequency varies, the transmitters will have to adjust their amplitudes and phases to achieve the given antenna port voltage distribution.

10.3.1 Decoupling to improve match at other receive angles

Addition of a transformer network will result in angle-independent matching at the design frequency. This scheme is shown in Figure 42.

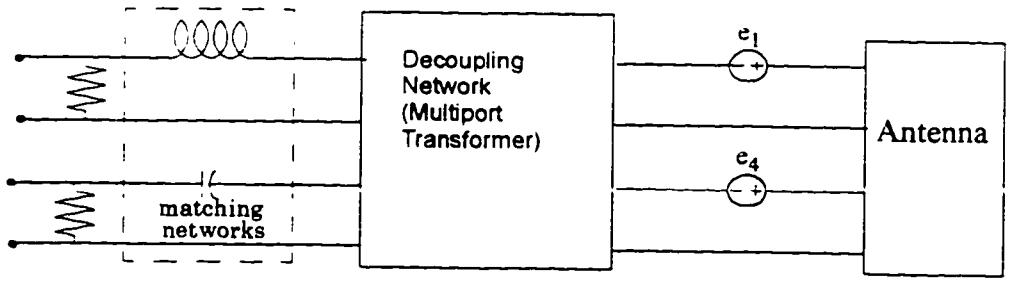

FIGURE 42. Simple matching network, with decoupling network

Simulation of the feed network of Figure 42 under identical conditions used for the network of Figure 40 results in the performance of Figure 43.

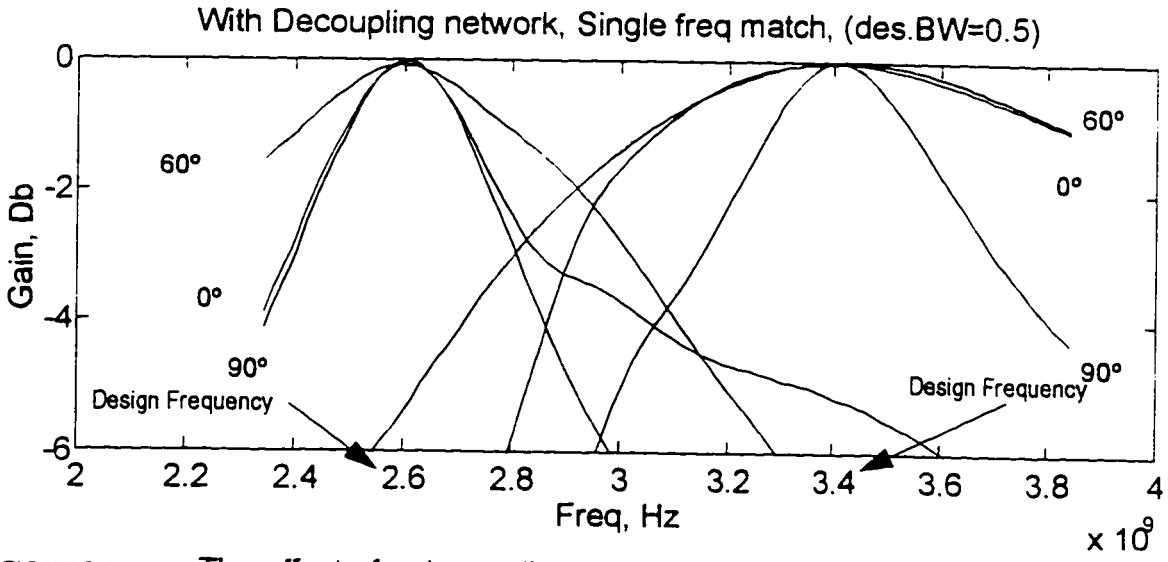

FIGURE 43. The effect of a decoupling transformer

At the design frequency, the reactances in the matching network are chosen to cancel the reactive part of the source's active impedance. At that frequency, with a coupling transformer, the match will be independent of the excitation angle. Thus, all the curves meet at the design frequency in Figure 43. However, at other frequencies, the antenna is no longer close to being conjugate matched, even with the decoupling transformer. In an unmatched situation, the dependence on scan angle reappears, and is not lessened by the transformer.

The transformer used in Figure 43 is derived using the SVD of the antenna admittance data. That the transformer does a good job of decoupling over the band is verified by noticing that, at both design frequencies, there is no scan dependence on power gain.

10.4 Use of sophisticated matching networks

When a decoupling transformer is used, where the match is good, the transducer power gain from the antenna source into each of the loads is equal. Because of this, the power response of the system is not dependent on the angle of the received waves. If a fairly good match could be maintained over a wider bandwidth, similar performance would be expected over that bandwidth. The feed network design of Figure 44 is a combination of broadband matching and broadband decoupling which can provide good power flow over a range of frequencies and scan angles.

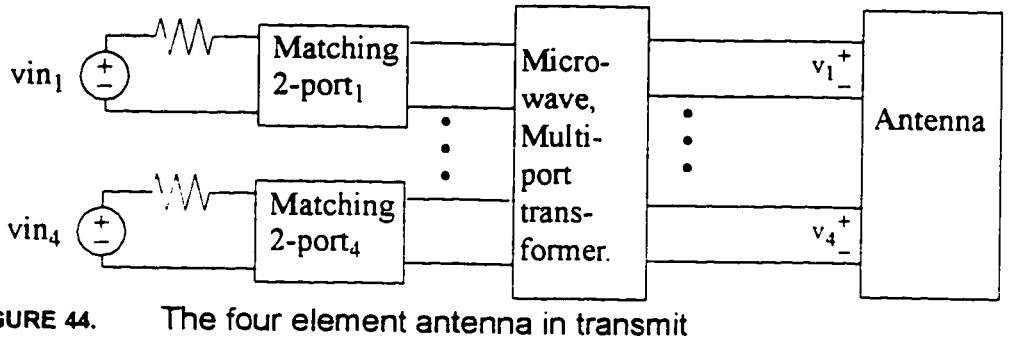

FIGURE 44. The four element antenna in transmit

This is demonstrated in Figure 45. Here, fourth order broadband matching networks are used to match over a 10% bandwidth. The gain of the matching networks is close to unity, because the bandwidth is not that large. In this case, the transformer is effective in removing the angle dependence on gain.

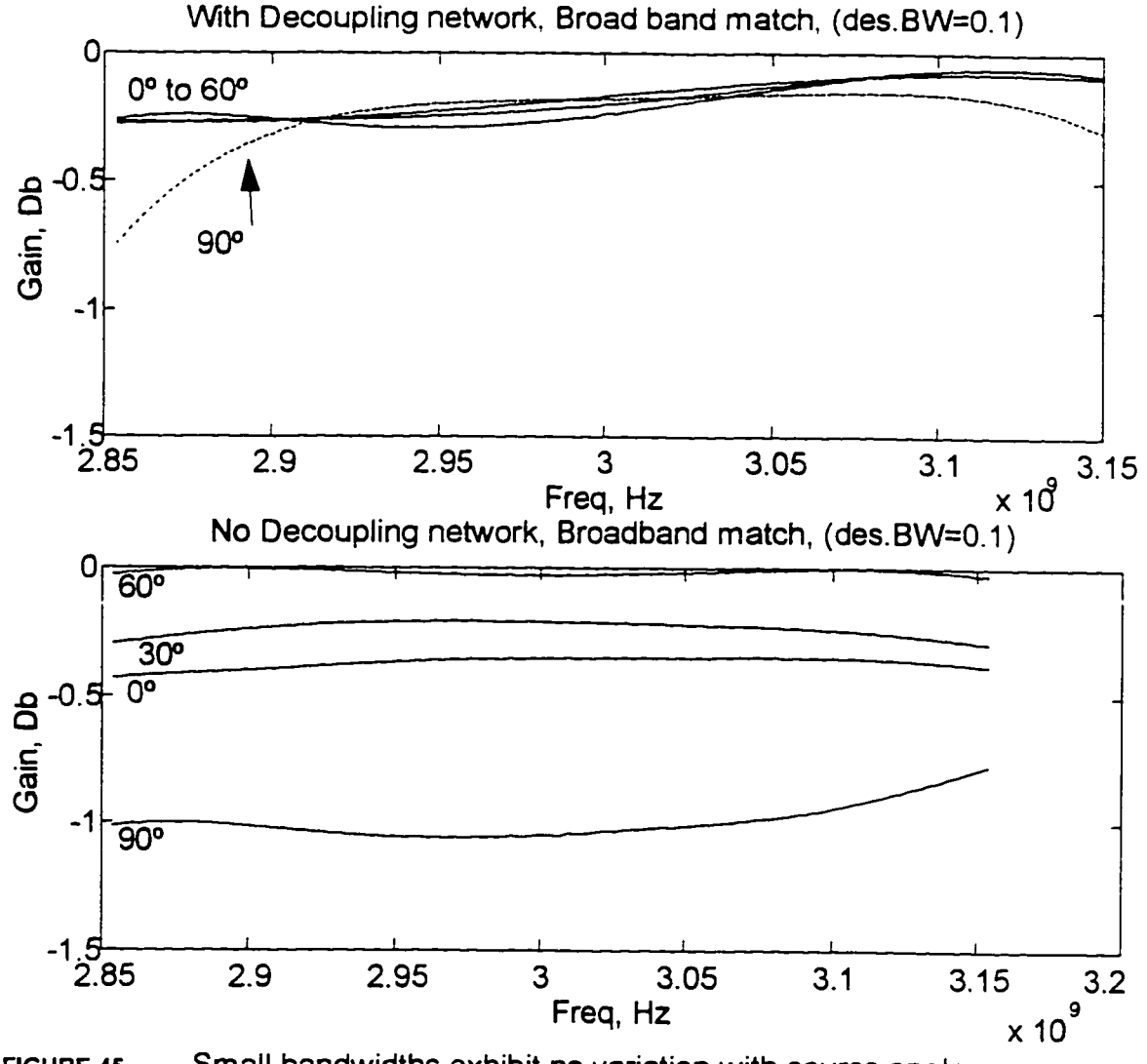

FIGURE 45. Small bandwidths exhibit no variation with source angle

10.5 Gain equalization provides scan-independence

In order to solve the broadband matching problem for antenna feed networks using the theory of section 7.0, the gains of the individual matching networks must be equalized. In this section, the effectiveness of this technique is demonstrated with the four element array example.

Here, the circuit diagram of Figure 44 is still appropriate. After design of the decoupling transformer, and numerical design of individual matching networks, a second numerical optimization is performed. This optimization drives the gains of the separate matches to the gain of the smallest one, equalizing the power flow from each transmitter into the antenna (or, from the antenna to each resistive load, in the receive case).

To drive home the necessity of the gain equalization, and illustrate the trade- offs necessary to accomplish the match, several different designs were performed and analyzed.

Figure 46 shows how effective four, fourth order broadband matching networks can be in broadbanding the antenna response. Here, no decoupling network is used, instead, the optimum diagonal load for the antenna over the frequency band is calculated. Then, the numerical matching technique is used to design matching networks that match to the conjugate of the best diagonal loads. The minimum gain over a 50% bandwidth is between -4.2 and -1.2 db, depending on source angle.

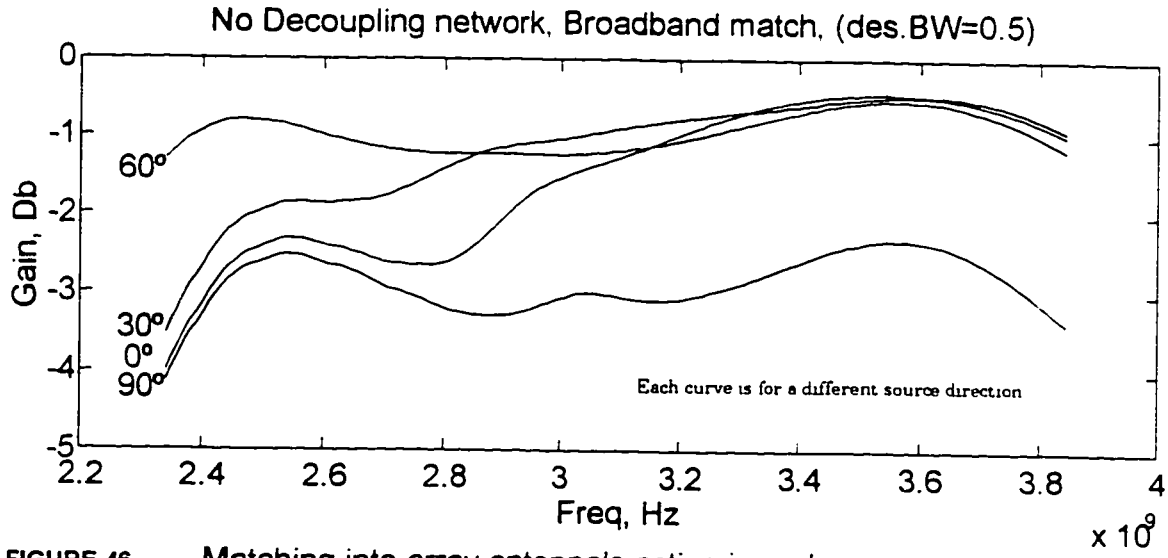

FIGURE 46. Matching into array antenna's active impedance

With a transformer between the matching networks and the antenna, (Figure 47), the dependence on scan angle is not changed much. The matching performance overall is improved negligibly. By introducing the transformer, however, changes in the antenna port excitations can be regarded as moving the power flow from one transmitter port to another. Therefore, if the individual gains of each port can be equalized, the overall power gain into the antenna (on transmit), or out of the antenna (in receive), will no longer change with antenna excitation.

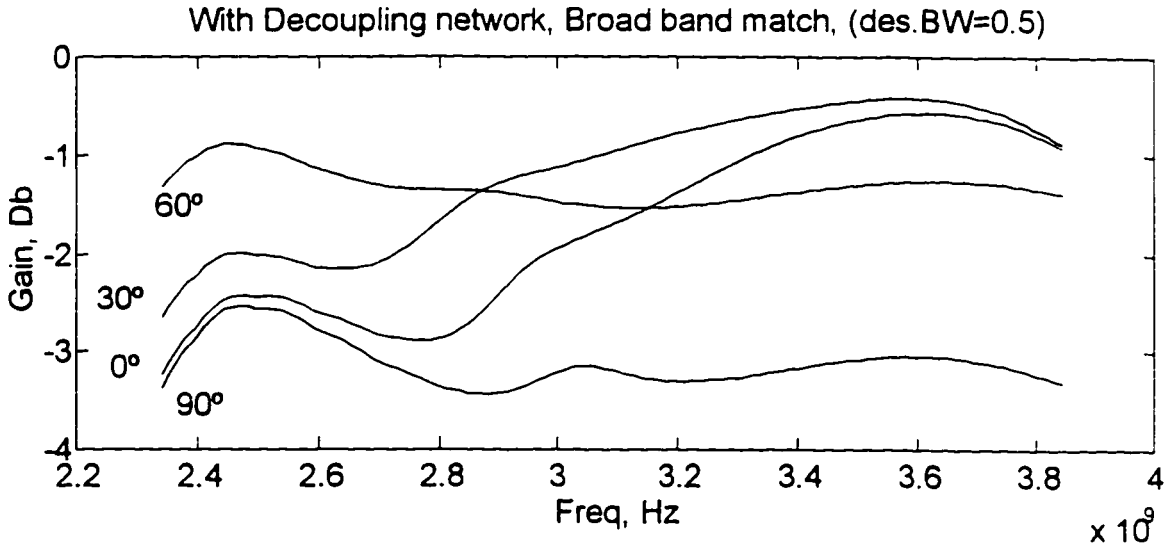

FIGURE 47. Decoupling and broadband matching. No gain equalization.

Numerically equalizing the gains, (by lowering the gain of the higher gain channels to that of the lowest gain channel), removes the scan dependence shown in Figure 47, and results in the performance of Figure 48.

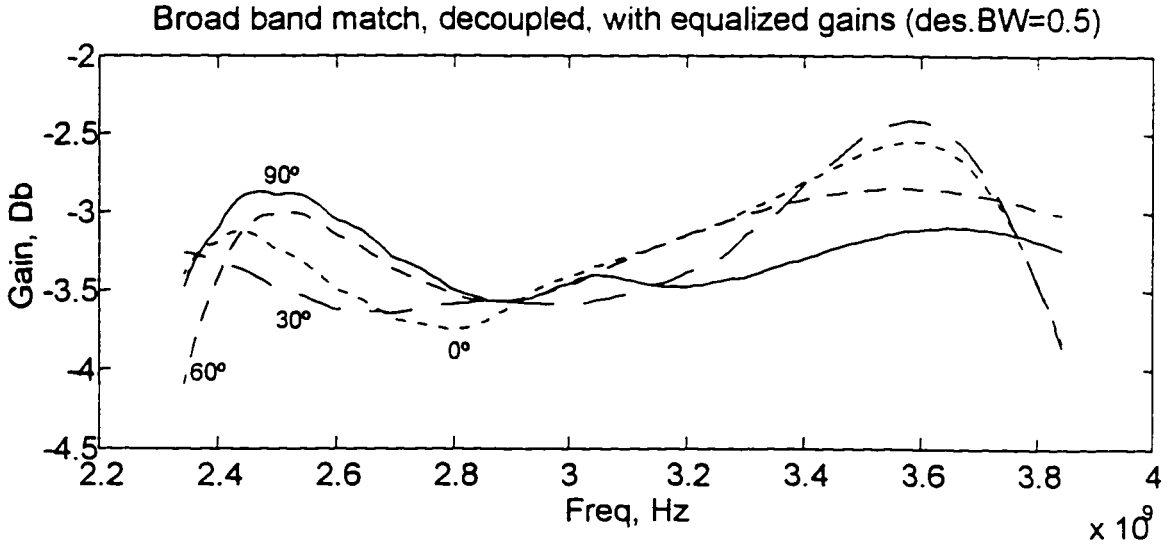

FIGURE 48. Gain equalization removes scan dependence

The price paid for scan independent power flow is a lowering of the individual channel's power gain.

10.6 Broadband, excitation pattern independent power flow

Design by

- Finding a good, frequency independent, congruence transformation for decoupling,
- Broadband matching to the decoupled impedances, and
- Equalizing the gain of the individual matching networks,

was carried out for bandwidths of 10%, 20%, 30%, and 50%, for the example antenna. The performance of the resulting designs is shown in Figure 49. At each bandwidth, a SVD was performed on the antenna data to arrive at the best transformer turns ratios. Then, a fourth order bandpass matching network was designed to match the impedances seen looking into the decoupling transformer. Finally, the matching network gains were equalized to match the lowest gain of the four.

For each design bandwidth, performance at an incident beam angle of endfire, broadside, and 60° was simulated. Overall gains of -0.2, -1, -1.8, and -3.3 db were achieved for bandwidths of 10%, 20%, 30%, and 50%, respectively.

Ripple of less than 1 db within the band and a variation of less than 1 db with beam angle for each design were achieved.

The resulting designs show good power transfer over a band of frequencies, with a variety of antenna excitation patterns. The decoupling networks used can be realized with simple four port power divider structures, and the matching networks used are straightforward fourth order, lumped designs.

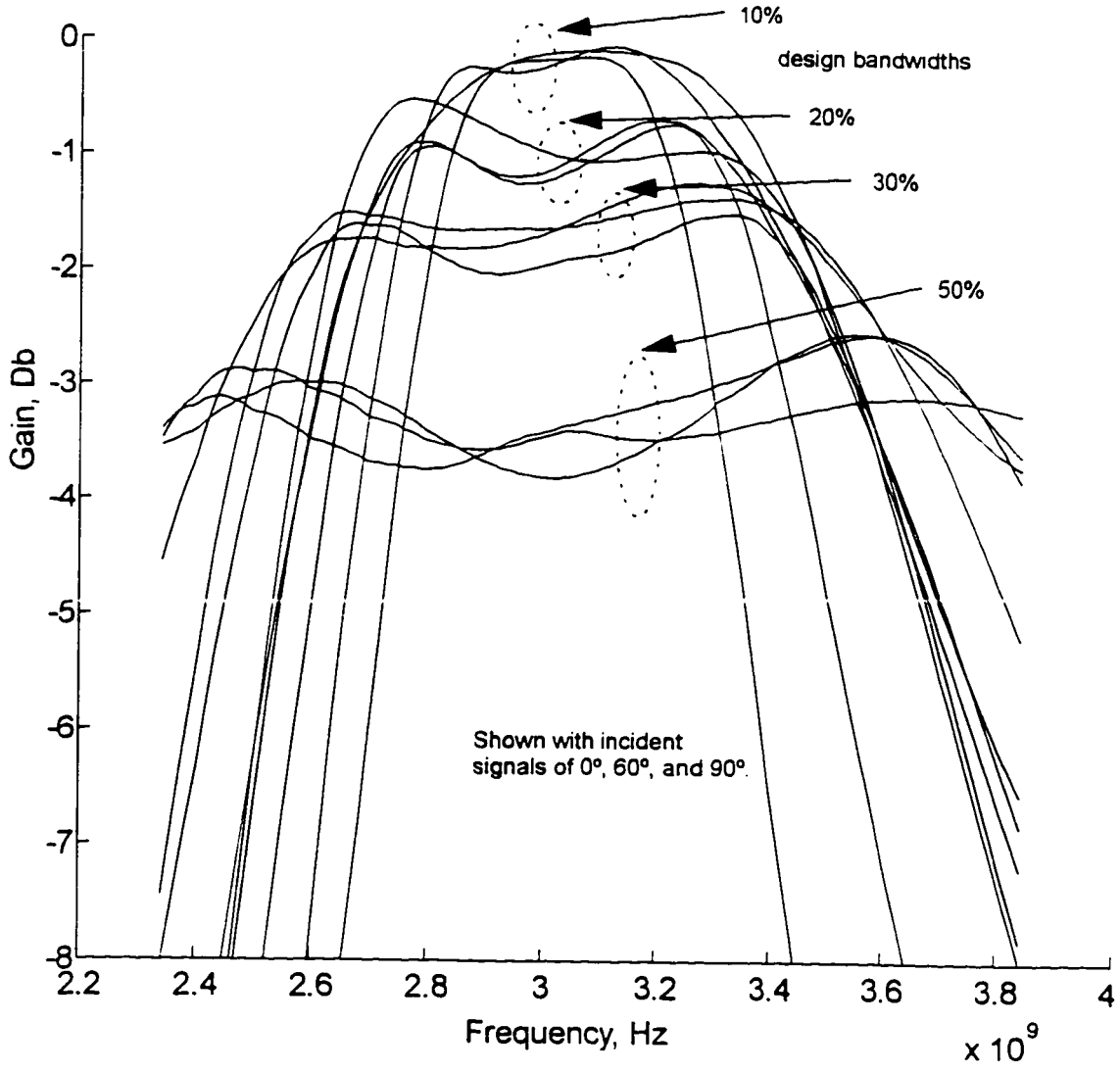

FIGURE 49. Response with equalized matching networks

11.0 Conclusion

In this dissertation, the problem of power transfer between multiport networks has been investigated, with the aim of providing a design procedure for array antenna feed networks. It was shown that simple, isolated matching networks that provide the maximal power transfer at one frequency and excitation can be found by solving for the optimal diagonal load for a multiport. By approximating the optimal diagonal load over a frequency range, broadband power flow can also be achieved with isolated matching networks. There is always a variation of power flow with excitation pattern, or scan angle, with these isolated networks, but the severity of the mismatch depends on the particular multiport being matched to. The variation with excitation, due to the mutual coupling within the multiport, can be reduced by using a network that compensates for this coupling.

A problem in multiport matching was solved in section 6.0 with the aid of a multiport transformer, which is an ideal circuit element that has been known for some time, but regarded as impractical for actual circuit design. It has been shown that, at microwave frequencies, a combination of simple circuit elements can act very much like a multiport transformer of arbitrary turns ratio. Therefore, a multiport transformer can be a practical circuit element in these frequency ranges. The multiport matching problem solved in section 6.0 was for a particular class of multiports, diagonalizable over all frequencies.

Also, the excitation constraints existing in the antenna feed problem were not considered in this multiport matching problem.

It was next shown how, at the expense of some gain, the excitation pattern constraints in the antenna feed network matching problem can be accommodated. The kind of multiports that can be matched using the theory of section 6.0 was extended by developing a numerical technique to find a good diagonalizing transformation over a range of frequencies for arbitrary multiports. This technique makes use of the singular value decomposition of the multiport impedance data.

Single port matching constraints for a pair of new loads, RLC tank circuits and RLC series resonant circuits, were derived using classical matching theory. An existing numerical technique for single port matching was also adapted for use in designing the single port match subproblem of the multiport matching design.

Through the use of a scheme for approximate diagonalizing over a frequency range, and the modification of a single port matching technique to allow for gain equalization, the multiport matching solution with the limitations of section 6.0 was extended to apply to the antenna feed network problem. The resulting designs show a good match over wide frequency ranges, and various excitation patterns.

Impedance data from a four slot linear array designed for 3GHz operation provided concrete examples of the design and the results of several different coupling network design procedures. Designs using the developed "broadband matching with decoupling" procedure were carried out for four different bandwidths, and the resulting performance showed both a good match and insensitivity to scan angle changes over the design frequency ranges.

12.0 References

[1] A. Bloch, "N-Terminal Networks", *Wireless Engineer*, Vol. 33, pp. 295-300, Dec. 1956.

[2] V. Bellevitch, *Classical Network Theory*, San Francisco, Holden-Day, 1968.

[3] D. M. Pozar, *Microwave Engineering*, Chapter 12.1. Reading, Mass.: Addison-Wesley, 1990.

[4] C. R. Curry, and J. Andersen, *Boeing Company Progress Report*, June 19, 1995.

[5] H. Flanders, "On The Maximal Power Transfer Theorem For n-Ports", *Circuit Theory and Applications*, Vol. 4, pp. 319-344, 1976.

[6] V. Bellevitch, "Theory of 2n-terminal networks with applications to conference telephony", *Electrical Communication*, Vol. 27, no. 3, pp. 231-244, Sept., 1950.

[7] W. P. Geren, C. R. Curry, J. Andersen, "A Practical Technique for Designing Passive Lossless N-Port Coupling Networks," *IEEE Trans. On Microwave Theory and Techniques*, March, 1996.

[8] C. A. Desoer, "The maximum power transfer theorem for n-ports," *IEEE Trans. On Circuit Theory*, Vol. CT-20, pp. 328-330, May, 1973.

[9] G. E. Forsythe and C. B. Moler, *Computer Solution of Linear Algebraic Systems*, Prentice-Hall, Englewood Cliffs, N.J., 1967.

[10]G. E. Forsythe, M. A. Malcom, and C. B. Moler, *Computer Methods for Mathematical Computations*, Prentice-Hall, Englewood Cliffs, N.J., 1977.

[11]L. J. Augustine, *On Electrical Equalization of Piezoelectric Transducers to Obtain Optimal Power Transfer and Short Acoustic Bursts*, PhD Dissertation, University of Washington, 1978.

[12] M. Vidyasagar, "Maximum Power Transfer in n ports with passive loads," *IEEE Trans. On Circuits and Systems*, Vol. CAS-21, pp. 327-330, May, 1974.

[13]H. J. Carlin, "A new approach to gain-bandwidth problems," *IEEE Trans. On Circuits and Systems*, Vol. CAS-24, pp. 170-175, April, 1977.

[14]B. S. Yarman, and H. J. Carlin, "A Simplified Real Frequency Technique Applied to Broad-Band Multistage Microwave Amplifiers, *IEEE Trans. On Microwave Theory and Techniques*, Vol. MTT-30, no. 12, pp. 2216-2222, Dec., 1982.

[15]R. Vescovo, "Pattern synthesis with null constraints for circular arrays of equally spaced isotropic elements", *IEE Proc. Microwaves, Antennas, and Propagation.*, Vol. 143 No 2, pp. 103-106, April, 1996

[16]H. Steyskal and J.S. Herd, "Mutual Coupling Compensation in Small Array Antennas", *IEEE Trans. On Antennas and Propagation*, Vol. 38, No. 12, pp. 1971-1975, December, 1990.

[17]P. J. Davis, *Circulant Matrices*, New York: Wiley, 1979.

[18]E. A. Guillemin, *Synthesis of Passive Networks*, New York, Wiley, p. 368, 1957

[19]M. AbuShaaban and S. O. Scanlan "Modal Circuit Decomposition of Lossy Multiconductor Transmission Lines", *IEEE Trans. On Microwave Theory and Techniques*, Vol 44, No. 7, pp. 1046-1057, July, 1996.

[20]M. Wax, and J. Sheinvald, "Direction Finding of Coherent Signals via Spatial Smoothing for Uniform Circular Arrays", *IEEE Trans. On Antennas and Prop.*, Vol 42, no. 5, pp. 613-620, May, 1994.

[21]R. M. Fano, "Theoretical Limitations on the Broadband Matching of Arbitrary Impedances", *J. Franklin Inst.*, Vol 249, pp. 57-83, Jan., 1950; and pp. 139-155, Feb. 1950.

[22]D.C. Youla, "A new theory of broadband matching," *IEEE Trans. Circuits and Systems*, Vol. CT-11, pp. 30-50, Mar., 1964.

[23]R. W. Vogel, "Analysis and Design of Lumped and Lumped Distributed Element Directional Couplers for MIC and MMIC Applications", *IEEE Transactions on Microwave Theory and Techniques*, Vol. 40, no 2, pp. 253-260, Feb., 1992

[24]G. H. Golub, and C.F.Van Loan, *Matrix Computations*, Baltimore: John Hopkins, 1989

[25]R. W. Newcomb, *Linear Multiport Synthesis*. New York: McGraw-Hill, 1964.

[26]P. M. Lin, "Competitive Power Extraction from Linear n-Ports". *IEEE Trans. Circuits and Systems*, Vol. Cas-32, no.2, pp. 185-191, Feb., 1985.

[27]A Cantoni, and P. Butler, "Eigenvalues and Eigenvectors of Symmetric Centrosymmetric matrices", *Linear Algebra and its Applications*, Vol. 13, pp. 275-288, 1976.

[28]R. E. Collin, and F. J. Zucker, *Antenna Theory*. New York: McGraw-Hill. 1969.

[29]R. M. Foster, "A Reactance Theorem", *Bell System Tech. J.*, Vol 3, pp. 259-267, April, 1924.

[30]D.C. Youla, "Direct Single Frequency Synthesis from a Prescribed Scattering Matrix", *IRE Trans. On Circuit Theory*, Vol. CT-6, pp. 340-344, Dec., 1959.

[31]S. Darlington, "Synthesis of Reactance 4-Poles Which Produce Prescribed Insertion Loss Characteristics", *Journal of Mathematics and Physics*. Vol XVIII, no. 4, pp 257-353, Sept., 1939.

[32]R. E. Collin, *Foundations for Microwave Engineering*, N.Y., McGraw- Hill, 1966.

[33]P. G. Rogers, "Application of the Minimum Scattering Antenna Theory to Mismatched Antennas", *IEEE Trans. On Antennas and Prop.*, no 10, Vol AP-34, Oct., 1986

[34]P. W. Hannan, "Proof That a Phased Array Antenna Can Be Impedance Matched for All Scan Angles", *Radio Science*, Vol. 2 (New Series), no. 3, pp. 361-369, March, 1967

[35]P. W. Hannan, D. S. Learner, and G. H. Knittel, "Impedance Matching a Phased-Array Antenna Over Wide Scan Angles by Connecting Circuits", *IEEE Trans. On Antennas and Prop*. Vol AP-13, no. 1, pp 28-33, Jan., 1965

[36]J. B. Andersen, and H. H. Rasmussen, Decoupling and Descattering Networks for Antennas, *IEEE Trans. On Antennas and Propagation*, Vol AP-24, pp. 841-846, Nov., 1976.

[37]D. S. Gao, A. T. Yang, and S. M. Kang, "Modeling and Simulation of Interconnection Delays and Crosstalks in High Speed Integrated Circuits, *IEEE Transactions on Circuits and Systems*, Vol. 37, No. 1, pp. 1-9, January, 1990.

[38]M. T. Ma, *Theory and Application of Antenna Arrays*, New York.: John Wiley, 1974.

[39]W. K. Chen "Explicit formulas for the synthesis of optimum broad-band impedance-matching networks ", *IEEE Trans. Circuits and Systems*, Vol. CAS-24, pp 157-169, April, 1977.

[40]W. K. Chen and K. G. Kourounis "Explicit formulas for the synthesis of optimum broad-band impedance-matching networks II", *IEEE Trans. Circuits and Systems*, Vol. CAS-25, pp. 609-620, Aug, 1978.

[41]W. K. Chen and T. Chaisrakeo, "Explicit formulas for the synthesis of optimum band-pass Butterworth and Chebyshev impedance matching networks ", *IEEE Trans. Circuits and Systems*, Vol. CAS-27, pp 928-942, Oct., 1980.

[42]W. K. Chen and Q. Z. Zha, "The synthesis of Chebyshev broad-band impedance matching networks ", *J. Franklin Institute*, Vol. 327, no. 3, pp 377-402, 1990.

[43]H. J. Carlin, and A. B. Giordano, *Network Theory*, Englewood Cliffs, N.J., Prentice-Hall, 1964.

[44]N. Amitay, V. Galindo, C. P. Wu, Theory and Analysis of Phased Array Antennas, New York: John Wiley, 1972.

Appendix I Power flow between two multiport networks

This derivation of the optimum loading network for a multiport source is central to the problem of feed network design for an array antenna.

Consider a multiport source, represented by ideal voltage sources in series with an N-port network, described by its impedance matrix. For sinusoidal signals, the voltage sources can be expressed as a length n vector of complex numbers, "e", and the network by an n by n matrix of complex numbers, "Z_{source}". [8], [12]

Now consider a multiport load for this source, also described by an impedance matrix. The overall network is shown in Figure 50.

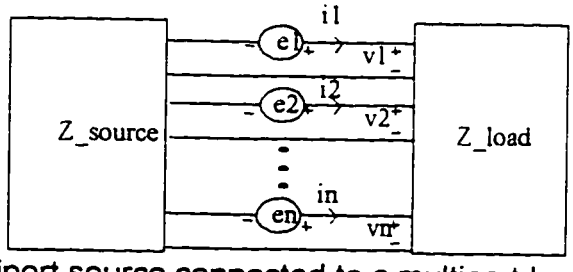

FIGURE 50. A multiport source connected to a multiport load

In this figure, ideal voltage sources are identified as e_1 through e_n. The source network is identified with its describing matrix labeled as Z_{source}, and the load network matrix is labeled Z_{load}. At each port, a current i flows due to the source e. The voltage across the load port can be calculated as

$$v = e - Z_{source} i \quad , \qquad \text{(EQ 54)}$$

where e, v, and i are column vectors. The power delivered to the load is

$$P_{load} = Re(\bar{v}^t i) = \frac{1}{2}(\bar{v}^t i + \bar{i}^t v)$$

$$= \frac{1}{2}(\bar{e}^t i + \bar{i}^t e - \bar{i}^t (Z_{source} + \overline{Z^t_{source}})\, i) \qquad \text{(EQ 55)}$$

where the overbar represents complex conjugate. The aim is to identify the Z_{load} matrices that maximize the power delivered to the load. To accomplish this, the current which brings about maximum power delivered to the load is first found. By differentiating 55 with respect to current, the optimum current can be identified. The derivative goes to zero when the current is such that

$$e - (Z_{source} + \overline{Z^t_{source}})\, i_{opt} = 0 \,. \qquad \text{(EQ 56)}$$

Now, four cases can be identified, depending on the nature of the source impedance.

Case 1. $Z_{source} + \overline{Z^t_{source}}$ is positive definite. Then the current which maximizes the power to the load is

$i_{opt} = (Z_{source} + \overline{Z^t_{source}})^{-1} e$. Since $Z_{source} i + Z_{load} i = e$, then

$$Z_{load} i_{opt} = \overline{Z^t_{source}} i_{opt} \,. \qquad \text{(EQ 57)}$$

The optimum Z_{load} must satisfy 57. One such Z_{load} is $\overline{Z^t_{source}}$.

Case 2. $Z_{source} + \overline{Z^t_{source}}$ is indefinite. No *finite* current which maximizes power to the load can be found in this case.

Case 3. $Z_{source} + \overline{Z^t_{source}}$ is positive semidefinite, and e belongs to the range of $Z_{source} + \overline{Z^t_{source}}$. In this case, the equation

$$e = (Z_{source} + \overline{Z^t_{source}})\, i_{many} \qquad \text{(EQ 58)}$$

has an infinite number of solutions for i_{many}. Any Z_{load} satisfying

$$Z_{load} i_{many} = \overline{Z^t_{source}} i_{many} \qquad \text{(EQ 59)}$$

is optimal.

Case 4. $Z_{source} + \overline{Z^t_{source}}$ is positive semidefinite, and e does not belong to the range of $Z_{source} + \overline{Z^t_{source}}$. In this case, there is no *finite* current which maximizes the power to the load.

In cases 1 and 3, an optimum load impedance matrix exists. From 57 and 59, one can see that the n^2 parameters of Z_{load} are constrained by n equations. Let N_{iopt} denote the $(n^2\text{-}n)$ dimensional subspace consisting of all matrices that map i_{opt} into the zero vector, where i_{opt} is a solution of 57 or 59. The matrices Z_{load} which satisfy these equations can be expressed as

$$(Z_{load} = \overline{Z^t_{source}} + Z_{null}), \quad Z_{null} \in N_{iopt}. \qquad \text{(EQ 60)}$$

One way to find matrices Z_{null} is to set up an orthonormal basis for R^n that includes the excitation vector, i_{opt}, as one of the basis vectors. Then, any linear combination of the other n-1 vectors in the basis, excluding i_{opt}, can be used to form the columns of Z_{null}.

What this means is that, for any particular excitation pattern of currents, there are many (nontrivial) N-port networks which actually end up

with no voltage across their ports when excited with this pattern of currents. Any number of these N ports can be placed in series with any load network and not change the power delivered to the load from the source. Thus, there are an *infinite number of optimum loads for a particular source with a particular excitation* (at one frequency).

However, if a Z_{load} is desired which always extracts the maximum power from the source, regardless of the excitation pattern, the load which has an impedance matrix which equal to the conjugate of the source impedance is the best load.

Appendix II The multiport transformer ideal circuit element

Use of this ideal circuit element is the only way that general multiport networks can be synthesized, as the necessary and sufficient conditions for transformerless synthesis of even purely resistive networks are not known. The equivalence of these transformers and connections of microwave directional couplers allows much of classical network theory to be applied to microwave design problems.

Transformers can change impedance levels. The familiar two port transformer, when loaded with a load Z_{load}, has an input impedance of $n^2 Z_{load}$, where n is the turns ratio, primary over secondary. By employing more complicated transformers, this characteristic can be generalized from single port impedance transformation to multiport impedance transformation.

An (X+Y) port multiport transformer is defined as a network with X input ports and Y output ports. There are Y transformers inside the network, each with X windings on the primary and one secondary. The secondaries of the transformers form the output ports of the network. The input ports are formed by connecting in series one primary winding of each and every one of the transformers, forming a series connection of Y windings for each of the X input ports. A realization of a multiport transformer is shown in Figure 51. Let the turns ratio between the primary connected to port "i" and the secondary

connected to port "j" be t_{ij}. Then the turns ratio matrix is defined as the X x Y matrix of t's.

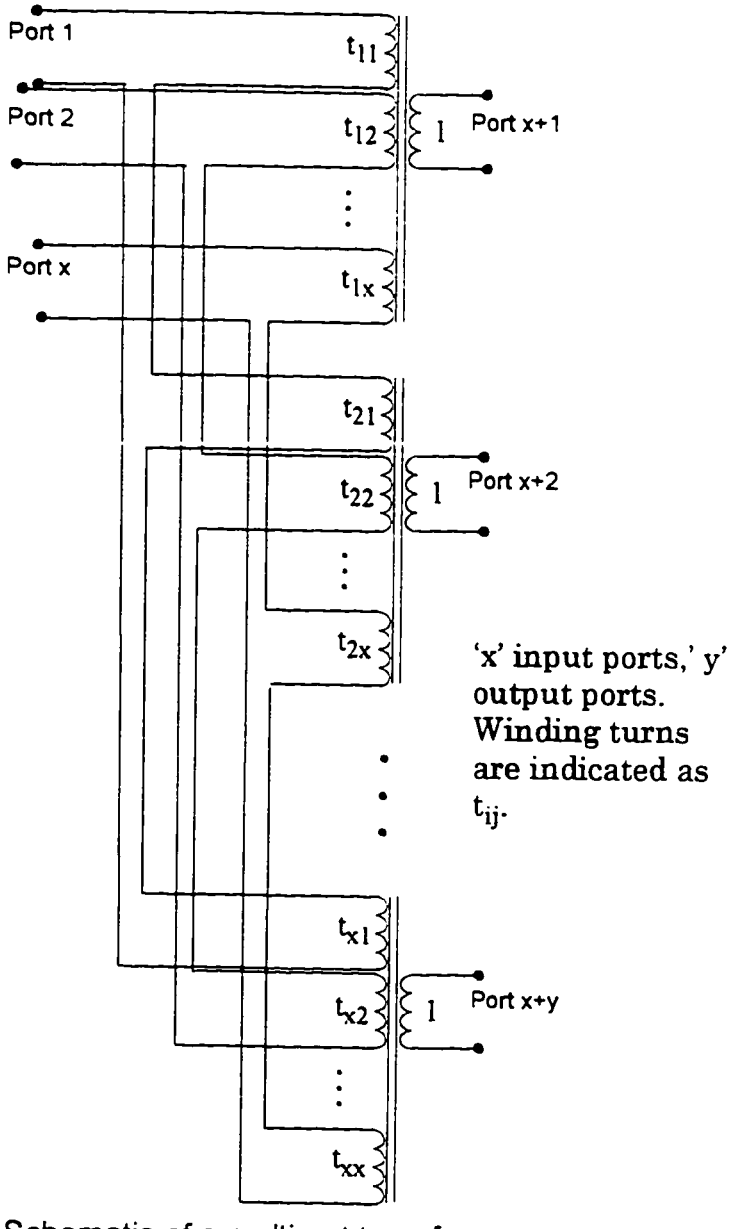

FIGURE 51. Schematic of a multiport transformer.

A multiport transformer loaded by an Y port network with an impedance matrix Z_{load} has an input impedance at its X input ports of

$$Z_{in} = T^t Z_{load} T. \qquad \text{(EQ 61)}$$

Here, Zin is X by X, the turns ratio matrix T is Y by X and the load impedance matrix Zload is Y by Y.

II.1 Multiport network design using ideal transformers

Now, say an impedance matrix is to be realized, but the realization technique is not obvious to the designer. If a constant congruence transformation can be found that converts the matrix into a form whose realization is obvious, the problem is solved by using a multiport transformer. For example, if the matrix can be diagonalized with a congruence transformation, the impedance is formed as the input impedance of a transformer, loaded with isolated, two terminal impedances.

Conditions for matrix diagonalization are discussed in Appendix V.

Appendix III Derivation of the Singular Value Decomposition

III.1 Derivation of the SVD for square matrices [9]

The singular value decomposition is simply the decomposition of a matrix A, into two orthogonal matrices U and V, and a diagonal matrix, with non-negative entries. The singular value decomposition is unique: although there are other ways to decompose a matrix into orthogonal and non-orthogonal parts, there is only one with a diagonal part that has non-negative elements.

AA^t is a symmetric, positive semidefinite matrix. It follows that all its eigenvalues are nonnegative. Let the matrix of eigenvectors of AA^t be an orthogonal matrix U. Then $U^t(AA^t)U = D^2$, where D is a diagonal matrix of the positive square roots of the eigenvalues.

Now consider the matrix U^tA. Another way of writing the above equation is $(U^tA)(U^tA)^t = D^2$. From this equation, one can see that the norm of the i^{th} row of U^tA is the i^{th} eigenvalue of AA^t. Also, the rows of U^tA are orthogonal, since all off diagonal elements of D^2 are zero.

Divide each row of the matrix U^tA by its norm, so that it becomes a unit vector. Call this (now row- orthonormal) matrix, V^T. (If some of the eigenvectors of U^tA are zero, so the division cannot be done, do it to all the rows possible,

then fill out the V^T matrix with orthonormal rows using the Gram-Schmitt process). Now, V such that $U^TA = DV^T$, or, $U^TAV = D$ has been created.

To summarize, the orthogonal matrix U is the eigenvector matrix of AA^T. The singular values are the positive square roots of the eigenvectors of AA^T. The columns of the orthogonal matrix V are constructed from the scaled rows of U^TA.

III.2 Interpretation of the SVD

The "size" of a vector is easy to visualize as its Euclidean length. Coming up with a good definition for the size of a matrix is a little more difficult. Consider a matrix as a mapping of vectors from one space to another. A good size definition with this in mind is to think of the size of a matrix as the maximum stretch it can give to a unit vector, or the size of the largest vector that it maps a unit vector to. Mathematically speaking, let the 2-norm of a matrix be defined as

$$\|A\|_2 = \sup_{x \neq 0} \frac{\|Ax\|_2}{\|x\|_2} \qquad \text{(EQ 62)}$$

where the two norm of a vector is just the familiar square root of the sum of the magnitudes squared, or

$$\|x\|_2 = (x^Tx)^{1/2} \qquad \text{(EQ 63)}$$

Note that

$$\|Ax\|_2^2 = x^TA^TAx. \qquad \text{(EQ 64)}$$

Writing the SVD as $AV = DU$, one can see that the first column of V in the SVD is mapped by the matrix A into the first column of U, scaled by the 2-norm of A, the first singular value. This first column of V is the one vector in R^{nxn} that is mapped to the "biggest" vector by A. Then the space of vectors to be considered is reduced by one dimension, and the next optimizing vector, (in the space orthogonal to the first), becomes the second column of V. The next singular value is then the maximum scaling done by A in this reduced space. The process is continued, until the last singular value, which is the smallest the matrix A scales the orthogonal coordinate system defined by the matrix V.

A unit circle in a two dimensional domain of A defined by unit first and last column vectors of V is mapped into an ellipse by A. The ellipse has semiaxes which are the largest and smallest singular values of A. This is the greatest distortion which can occur to any unit circle in the domain of A. [10]

Appendix IV Diagonalization and properties of circulant matrices

Circulant matrices are matrices where the elements of each row are identical to those of the previous row, but are moved one position to the right and wrapped around. The whole matrix is determined by the first row or column. Circulant matrices are a subset of Toeplitz matrices. Circulant matrices all commute with each other under multiplication, therefore, they are diagonalizable with an orthogonal congruence transform. Symmetric circulant matrices have real eigenvalues and eigenvectors, and for the symmetric case, the diagonalizing matrix, T, for an even number of elements will be [19],

$$T = \frac{1}{\sqrt{n}}\begin{bmatrix} 1 & 1 & \sqrt{2} & 0 & \dots & \sqrt{2} & 0 \\ 1 & -1 & \sqrt{2}\cos\left(\frac{2\pi}{n}\right) & \sqrt{2}\sin\left(\frac{2\pi}{n}\right) & \dots & \sqrt{2}\cos\left(\frac{(n-2)\pi}{n}\right) & \sqrt{2}\sin\left(\frac{(n-2)\pi}{n}\right) \\ 1 & 1 & \sqrt{2}\cos\left(\frac{4\pi}{n}\right) & \sqrt{2}\sin\left(\frac{4\pi}{n}\right) & \dots & \sqrt{2}\cos\left(\frac{2(n-2)\pi}{n}\right) & \sqrt{2}\sin\left(\frac{2(n-2)\pi}{n}\right) \\ 1 & -1 & \sqrt{2}\cos\left(\frac{6\pi}{n}\right) & \sqrt{2}\sin\left(\frac{6\pi}{n}\right) & \dots & \sqrt{2}\cos\left(\frac{3(n-2)\pi}{n}\right) & \sqrt{2}\sin\left(\frac{3(n-2)\pi}{n}\right) \\ 1 & \dots & \dots & \dots & \dots & \dots & \dots \\ 1 & \pm 1 & \sqrt{2}\cos\left(\frac{2(n-1)\pi}{n}\right) & \sqrt{2}\sin\left(\frac{2(n-1)\pi}{n}\right) & \dots & \sqrt{2}\cos\left(\frac{(n-1)(n-2)\pi}{n}\right) & \sqrt{2}\sin\left(\frac{(n-1)(n-2)\pi}{n}\right) \end{bmatrix}. \quad \text{(EQ 65)}$$

The diagonalizing matrix for an odd number of elements is

$$T = \frac{1}{\sqrt{n}}\begin{bmatrix} 1 & \sqrt{2} & 0 & \dots & \sqrt{2} & 0 \\ 1 & \sqrt{2}\cos\left(\frac{2\pi}{n}\right) & \sqrt{2}\sin\left(\frac{2\pi}{n}\right) & \dots & \sqrt{2}\cos\left(\frac{(n-1)\pi}{n}\right) & \sqrt{2}\sin\left(\frac{(n-1)\pi}{n}\right) \\ 1 & \sqrt{2}\cos\left(\frac{4\pi}{n}\right) & \sqrt{2}\sin\left(\frac{4\pi}{n}\right) & \dots & \sqrt{2}\cos\left(\frac{2(n-1)\pi}{n}\right) & \sqrt{2}\sin\left(\frac{2(n-1)\pi}{n}\right) \\ 1 & \sqrt{2}\cos\left(\frac{6\pi}{n}\right) & \sqrt{2}\sin\left(\frac{6\pi}{n}\right) & \dots & \sqrt{2}\cos\left(\frac{3(n-1)\pi}{n}\right) & \sqrt{2}\sin\left(\frac{3(n-1)\pi}{n}\right) \\ 1 & \dots & \dots & \dots & \dots & \dots \\ 1 & \sqrt{2}\cos\left(\frac{2(n-1)\pi}{n}\right) & \sqrt{2}\sin\left(\frac{2(n-1)\pi}{n}\right) & \dots & \sqrt{2}\cos\left(\frac{(n-1)^2\pi}{n}\right) & \sqrt{2}\sin\left(\frac{(n-1)^2\pi}{n}\right) \end{bmatrix}. \quad \text{(EQ 66)}$$

The row, column, entries of Equation 66 can be found as either cosine or sine of $\frac{2\pi}{N}\left(fix\left(\frac{col}{2}\right)(row-1)\right)$, where fix(x) is the integer part of x.

For non-symmetric matrices, the diagonalizing matrix is the same matrix that performs a DFT on a vector, sometimes called the Fourier matrix[17], where for $w = \exp\left(j\frac{2\pi}{N}\right)$, the elements of the conjugate of the Fourier matrix are

$$F^*(i,j) = \frac{1}{\sqrt{N}}(w^{(i-1)(j-1)}). \qquad \text{(EQ 67)}$$

The result, y, of the linear transformation $y = Fx$ is called the discrete Fourier transform of x.

Appendix V Conditions for diagonalization of matrices

If three symmetric real matrices could be simultaneously diagonalized, then all passive lumped element networks could immediately be synthesized with three multiport transformers and resistors, capacitors, and inductors. In general, however, this diagonalization cannot be performed. In this appendix, conditions for diagonalization of many different sets of matrices are presented.

Any Hermitian matrix A with rank r can be diagonalized with a product of elementary transformation matrices T by forming $ct(T) \times A \times T$, where the notation means conjugate transpose [25]. The diagonal form will have r nonzero entries on the diagonal. Real, symmetric, positive definite matrices A can be diagonalized with real orthogonal T, in which case the diagonal terms are the eigenvalues of A.

Two Hermitian matrices A and B, of which one is nonsingular and positive definite, can be diagonalized simultaneously by the same matrix T. The scheme to diagonalize both matrices relies on this strategy:

- a congruence transformation is applied to both matrices that transforms one of the matrices into the unit matrix: then
- An *orthogonal* transformation is applied to the resulting two matrices that diagonalizes the second one. An orthogonal transformation will

leave the unit matrix unchanged. Thus, the combination of the two transformations diagonalizes both matrices.

To provide details, assume it is the A matrix that is Hermitian positive definite. Then an Hermitian matrix, which is like a "square root" matrix, can be found:

$$A = \sqrt{A}\sqrt{A}. \qquad \text{(EQ 68)}$$

Because the A matrix is nonsingular, this square root matrix has an inverse, and it is easy to see that

$$\sqrt{A}^{-1}A\sqrt{A}^{-1} = I. \qquad \text{(EQ 69)}$$

Consider any arbitrary orthogonal matrix T. It will be true that

$$T^t\sqrt{A}^{-1}A\sqrt{A}^{-1}T = T^tIT = I \quad . \qquad \text{(EQ 70)}$$

Now, find the eigenvectors of the Hermitian matrix $\sqrt{A}^{-1}B\sqrt{A}^{-1}$. These eigenvectors can be formed into an orthogonal matrix T. Then

$$T^t\sqrt{A}^{-1}B\sqrt{A}^{-1}T = Diagonal, \qquad \text{(EQ 71)}$$

because T is formed from the eigenvectors, and

$$T^t\sqrt{A}^{-1}A\sqrt{A}^{-1}T = I = Diagonal, \qquad \text{(EQ 72)}$$

which is Equation 70. So, evidently, both A and B can be diagonalized by the matrix $\sqrt{A}^{-1}T$.

Also, if both are positive semi definite, they can be simultaneously diagonalized, even if they are both singular. [2]

The four matrices A, B, C, and D, with A strictly positive definite, can be simultaneously diagonalized iff [19]

$$\begin{aligned} BA^{-1}C &= CA^{-1}B \\ BA^{-1}D &= DA^{-1}B \\ DA^{-1}C &= CA^{-1}D \end{aligned} \qquad \text{(EQ 73)}$$

As a corollary, if D is zero, then the three matrices A, B, C, with A strictly positive definite, can be simultaneously diagonalized if

$$BA^{-1}C = CA^{-1}B. \qquad \text{(EQ 74)}$$

A group of real symmetric matrices are simultaneously diagonalizable with an *orthogonal* T iff all of the matrices commute under multiplication.

Appendix VI Diagonalizing symmetric, Toeplitz, tri-diagonal matrices

The elements of the diagonalizing matrix can be computed as [37]

$$t_{i,j} = \frac{\Phi_{i-1}(u_j)}{\delta_j}, \qquad \text{(EQ 75)}$$

where $\Phi_i(u) = (u\Phi_{i-1}(u) - \Phi_{i-2}(u))$ $i \geq 2$, and $\Phi_0(u) = 1$, and $\Phi_1(u) = u$, where

$u_i = \left(-2\cos\left(\frac{i\pi}{N+1}\right)\right)$ $i = 1, \ldots N$, and $\delta_j^2 = \sum_{i=1}^{N} (\Phi_{i-1}(u_j))^2$.

Appendix VII Singular value decomposition design example

For example, let the antenna data be collected at the five frequencies 2.5, 2.8, 3.1, 3.4, and 3.7 GHz.

Equation 41 takes the form

$$\begin{bmatrix} 0.61-j2.44 & -0.18-j0.16 & 0.12+j0.45 & -0.08+j0.10 \\ 0.82-j0.96 & -0.28-j0.09 & 0.14-j0.08 & -0.15+j0.11 \\ 1.09+j0.48 & -0.36+j0.04 & 0.03-j0.19 & 0.12+j0.05 \\ 1.45+j1.96 & -0.38+j0.24 & -0.15-j0.18 & 0.10-j0.13 \\ 1.93+j3.56 & -0.31+j0.46 & -0.29+j0.00 & -0.12-j0.16 \end{bmatrix} = \begin{bmatrix} Y_{1a} & Y_{2a} \\ Y_{1b} & Y_{2b} \\ Y_{1c} & Y_{2c} \\ Y_{1d} & Y_{2d} \\ Y_{1e} & Y_{2e} \end{bmatrix} \begin{bmatrix} a1 & a2 & a3 & a4 \\ b1 & b2 & b3 & b4 \end{bmatrix}, \quad \text{(EQ 76)}$$

where Y1, Y2, the a's and b's are unknown.

Equation 42, the SVD, for the example takes the form of

$$SVD\left(\begin{bmatrix} 0.61 & -0.18 & 0.12 & -0.09 \\ 0.82 & -0.28 & 0.14 & -0.15 \\ 1.1 & -0.36 & 0.03 & 0.12 \\ 1.45 & -0.38 & -0.15 & 0.09 \\ 1.93 & -0.31 & -0.30 & -0.12 \\ -2.4 & -0.16 & 0.04 & 0.01 \\ -0.96 & -0.09 & -0.08 & 0.11 \\ 0.48 & 0.45 & -0.19 & 0.05 \\ 1.96 & 0.24 & -0.18 & -0.13 \\ 3.56 & 0.46 & 0.00 & -0.16 \end{bmatrix}\right) = \begin{bmatrix} 0.11 & -0.19 & 0.37 & 0.39 \\ 0.14 & -0.32 & 0.44 & 0.13 \\ 0.19 & -0.44 & 0.23 & -0.39 \\ 0.25 & -0.49 & -0.16 & -0.30 \\ 0.34 & -0.39 & -0.46 & 0.53 \\ -0.43 & -0.10 & -0.06 & 0.33 \\ -0.17 & -0.09 & -0.24 & -0.26 \\ 0.08 & 0.01 & -0.41 & -0.26 \\ 0.34 & 0.21 & -0.30 & 0.18 \\ 0.63 & 0.44 & 0.2 & -0.05 \end{bmatrix} \begin{bmatrix} 5.64 & 0 & 0 & 0 \\ 0 & 0.89 & 0 & 0 \\ 0 & 0 & 0.43 & 0 \\ 0 & 0 & 0 & 0.23 \end{bmatrix} \begin{bmatrix} 0.99 & 0.02 & -0.03 & -0.03 \\ -0.02 & 0.98 & 0.08 & -0.15 \\ 0.03 & -0.08 & 0.99 & -0.02 \\ -0.02 & -0.15 & -0.03 & -0.98 \end{bmatrix}$$

(EQ 77)

The data vectors are expressible as a combination of the columns of U. The first data vector (for example), is expressible as a weighted combination of the four columns of U:

$$\begin{bmatrix}0.61\\0.82\\1.1\\1.45\\1.93\\-2.4\\-0.96\\0.48\\1.96\\3.65\end{bmatrix} = 5.64\,(0.99)\begin{bmatrix}0.11\\0.14\\0.19\\0.25\\0.34\\-0.43\\-0.17\\0.08\\0.34\\0.63\end{bmatrix} + 0.89\,(-0.02)\begin{bmatrix}-0.19\\-0.32\\-0.44\\-0.49\\-0.39\\-0.10\\-0.09\\0.01\\0.21\\0.44\end{bmatrix} + 0.43\,(0.03)\begin{bmatrix}0.37\\0.44\\0.23\\-0.16\\-0.46\\-0.06\\-0.24\\-0.41\\-0.30\\0.20\end{bmatrix} + 0.23\,(-0.02)\begin{bmatrix}0.39\\0.13\\-0.39\\-0.30\\0.53\\0.33\\-0.26\\-0.26\\0.18\\-0.05\end{bmatrix} \quad \text{(EQ 78)}$$

The largest singular value, S(1,1), which is 5.64, always multiplies the first column of U when used to reconstruct the data. For the first data vector, above, the total weighting of the first column of U, which is 5.63, happens to dominate the contributions from the other vectors, but this will not always be true.

Therefore, the two basis vectors are[1]

$$\begin{bmatrix}Y_1 & Y_2\end{bmatrix} = U(:,1{:}2) = \begin{bmatrix}0.11 & -0.19\\0.14 & -0.32\\0.19 & -0.44\\0.25 & -0.49\\0.34 & -0.39\\-0.43 & -0.10\\-0.17 & -0.09\\0.08 & 0.01\\0.34 & 0.21\\0.63 & 0.44\end{bmatrix} = \begin{bmatrix}0.11-j0.43 & -0.19-j0.10\\0.14-j0.17 & -0.32-j0.09\\0.19+j0.08 & -0.44+j0.01\\0.25+j0.34 & -0.49+j0.21\\0.34+j0.63 & -0.39+j0.44\end{bmatrix}. \quad \text{(EQ 79)}$$

The weights are

1.The notation A(:,1:2) means all the rows, and columns 1 and 2 of matrix A. Similarly, the notation V(1:2,:) means all the columns, and rows 1 and 2 of matrix V. This notation is defined by Golub [24], and is also used in the computer program MATLAB.

$$\begin{bmatrix} a1 & a2 & a3 & a4 \\ b1 & b2 & b3 & b4 \end{bmatrix} = SV^{T}(1{:}2,:) = \begin{bmatrix} 5.63 & 0.13 & -0.18 & -0.16 \\ -0.02 & 0.87 & 0.07 & -0.14 \end{bmatrix}. \quad \text{(EQ 80)}$$

Through the use of SVD, j-axis values of two admittances that most closely can approximate the four impedances that comprise the original data have been found. It is more important, though, that the set of weights for the two admittances have been found. These eight weights are the entries in the matrices of Equation 39, which now takes the form

$$Y_{ANTENNA} = \begin{bmatrix} Y_{11} & Y_{12} & Y_{13} & Y_{14} \\ Y_{12} & Y_{11} & Y_{12} & Y_{13} \\ Y_{13} & Y_{12} & Y_{11} & Y_{12} \\ Y_{14} & Y_{13} & Y_{12} & Y_{11} \end{bmatrix} = \begin{bmatrix} 5.63 & 0.13 & -0.18 & -0.16 \\ 0.13 & 5.63 & 0.13 & -0.18 \\ -0.18 & 0.13 & 5.63 & 0.13 \\ -0.16 & -0.18 & 0.13 & 5.63 \end{bmatrix} Y_1(s) + \begin{bmatrix} -0.02 & 0.87 & 0.07 & -0.14 \\ 0.87 & -0.02 & 0.87 & 0.07 \\ 0.07 & 0.87 & -0.02 & 0.87 \\ -0.14 & 0.07 & 0.87 & -0.02 \end{bmatrix} Y_2(s).$$

(EQ 81)

VII.1 How the Diagonalization is performed

The entire admittance matrix of the antenna has now been parameterized with two constant matrices. Both matrices can be simultaneously diagonalized with a congruence transformation. This mathematical operation corresponds to the physical act of adding a lossless coupling network to the front of the antenna. (This network is ideally a multiport transformer). A transformation matrix, "Trans", is found such that

$$Trans^{t} Y_{ANTENNA} Trans = \begin{bmatrix} 1 & 0 & 0 & 0 \\ 0 & 1 & 0 & 0 \\ 0 & 0 & 1 & 0 \\ 0 & 0 & 0 & 1 \end{bmatrix} Y_1(s) + \begin{bmatrix} 0.25 & 0 & 0 & 0 \\ 0 & -0.13 & 0 & 0 \\ 0 & 0 & 0.09 & 0 \\ 0 & 0 & 0 & -0.25 \end{bmatrix} Y_2(s). \quad \text{(EQ 82)}$$

Here,

$$Trans^{t} = \begin{bmatrix} -0.15 & -0.25 & -0.25 & -0.15 \\ -0.25 & 0.15 & 0.15 & -0.25 \\ 0.25 & 0.13 & -0.13 & -0.25 \\ 0.15 & -0.26 & 0.26 & -0.14 \end{bmatrix} . \qquad \text{(EQ 83)}$$

If a transformer with a turns ratio matrix given by "Turns" is loaded with a network that has an admittance matrix "Y_L", the admittance looking into the transformer is

$$Y_{in} = Turns^{-1} Y_L (Turns^{t})^{-1} \qquad \text{(EQ 84)}$$

Therefore, the antenna admittance matrix can be approximately diagonalized with a multiport transformer coupling network. The multiport transformer should have a turns ratio of

$$Turns = (Trans^{t})^{-1} = \begin{bmatrix} -0.85 & -1.41 & 1.51 & 0.78 \\ -1.44 & 0.88 & 0.84 & -1.42 \\ -1.44 & 0.88 & -0.84 & 1.42 \\ -0.85 & -1.41 & -1.51 & -0.78 \end{bmatrix} . \qquad \text{(EQ 85)}$$

This multiport transformer does not exactly diagonalize the antenna. However, the mutual coupling effects are greatly reduced.

Appendix VIII S-matrix representation of an impedance example

For example, if it is known that the input impedance of the overall network is

$$Z_{in} = \frac{0.96s^3 + 1.543s^2 + 1.551s + 0.9803}{s^2 + 1.608s + 0.9803} \qquad \text{(EQ 86)}$$

This happens to be the impedance of a ladder network:

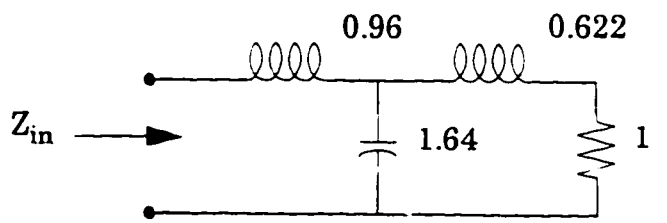

FIGURE 52. A ladder network used in this example.

the input reflection coefficient must be

$$\Gamma_{in} = \frac{s^3 + 0.5661s^2 - 0.05923s}{s^3 + 2.649s^2 + 3.29s + 2.042} \qquad \text{(EQ 87)}$$

The reflection coefficient has no common factors, so tran will not be of any higher degree than necessary. The transfer scattering parameter is proportional to

$$tran(s)tran(s) = (-s^6 + 0.439s^2 - 0.00351s^2 + 4.17) - (-s^6 + 0.439s^4 - 0.00351s^2)$$
$$tran(s) = 2.04 \qquad \text{(EQ 88)}$$

Tran can be scaled larger or smaller by multiplying the numerator and denominator of the reflection coefficient functions by any constant. The lossless scattering matrix corresponding to a transfer numerator of 2.04 is

$$\begin{bmatrix} \frac{s^3 + 0.5661s^2 + -0.05923s}{s^3 + 2.649s^2 + 3.29s + 2.042} & \frac{2.042}{s^3 + 2.649s^2 + 3.29s + 2.042} \\ \frac{2.042}{s^3 + 2.649s^2 + 3.29s + 2.042} & \frac{s^3 + -0.5661s^2 + -0.05923s}{s^3 + 2.649s^2 + 3.29s + 2.042} \end{bmatrix} \quad \text{(EQ 89)}$$

Before the broadband matching can start, the numerator of the s12 entry of a lossless scattering matrix needs to be chosen. Practically, a numerator of the form s^x, which leads to a ladder network, would be the choice. Here we choose x=0, so the matching network takes the form of a low pass ladder.

If this tran(s)=1 is used, the overall s-matrix of the lossless network that can be terminated in a one ohm resistor is

$$\begin{bmatrix} \frac{0.4896s^3 + 0.277s^2 - 0.029s}{0.4896s^3 + 1.2972s^2 + 1.611s + 1.0} & \frac{1}{0.4896s^3 + 1.2972s^2 + 1.611s + 1.0} \\ \frac{1}{0.4896s^3 + 1.2972s^2 + 1.611s + 1.0} & \frac{(-0.4896)s^3 + 0.277s^2 + 0.029s}{0.4896s^3 + 1.2972s^2 + 1.611s + 1.0} \end{bmatrix} \quad \text{(EQ 90)}$$

Appendix IX A derivation of Equation 17.

The power into a network with a Toeplitz describing matrix is a weighted sum of cosines, where each weight is proportional to one of the diagonals of the Toeplitz matrix.

The real power into a multiport is given by the quadratic form of Equation 12. If each diagonal of the admittance matrix is separated out into its own summation, (writing the diagonals above the main diagonal first, and then the ones below the main diagonal,

$$Power = \sum_{i=1}^{N} Y_{i,i}|v_i|^2 + \sum_{i=1}^{N-1} Y_{i,i+1}v_i^*v_{i+1} + \sum_{i=1}^{N-2} Y_{i,i+2}v_i^*v_{i+2} + \ldots + Y_{1,N}v_1^*v_N +$$

$$\sum_{i=1}^{N-1} Y_{i+1,i}v_{i+1}^*v_i + \sum_{i=1}^{N-2} Y_{i+2,i}v_{i+2}^*v_i + \ldots + Y_{N,1}v_N^*v_1 \qquad \text{(EQ 91)}$$

For a symmetric Toeplitz matrix, though, $Y_{i,i+a} = Y_{i+a,i} = Y_{a+1}$, as indicated in Equation 15, and also $v_i^*v_{i+a} = v_iv_{i+a}\exp(j\theta(a))$, as indicated in Equation 16. Therefore Equation 91 becomes

$$Power = Y_1\sum_{i=1}^{N}|v_i|^2 + Y_2\sum_{i=1}^{N-1}(v_iv_{i+1}\exp(j\theta) + v_iv_{i+1}\exp(-j\theta)) +$$

$$Y_3\sum_{i=1}^{N-2}(v_iv_{i+2}\exp(j2\theta) + v_iv_{i+2}\exp(-j2\theta)) +$$

$$\ldots + Y_N(v_iv_{i+1}\exp(j(N-1)\theta) + v_iv_{i+1}\exp(-j(N-1)\theta)) \qquad \text{(EQ 92)}$$

But, each of the terms in Equation 92 are of the form

$a\exp(jb) + a\exp(-jb) = a(\exp(jb) + \exp(-jb)) = 2a\cos(b)$, yielding the purely real expression of Equation 17.

Appendix X A multiport power flow example.

Consider a phased array radar. To transmit a beam in a particular direction, the phasing of the excitation is varied so that the transmitted wavefronts all line up in that direction. The antenna represents a multiport network that must be driven by the transmitter to produce a particular voltage on its ports, so the antenna pattern is the desired one.

For example, assume the positive real resistive four port with an admittance matrix of

$$Y = \begin{bmatrix} 0.522 & 0.981 & 0.939 & 0.368 \\ 0.981 & 2.16 & 2.22 & 0.920 \\ 0.939 & 2.22 & 2.54 & 1.08 \\ 0.368 & 0.920 & 1.08 & 0.463 \end{bmatrix}, \quad \text{(EQ 93)}$$

represents the antenna. This network exhibits and interesting effect: when the phasing between its ports gets above a certain limit: it accepts very little current, and so the power into it is very small. Figure 1 demonstrates that, with one volt on each of its ports, the network accepts 18 watts when driven all in phase, and about a tenth of a watt when the phasing between ports approaches exactly antiphase.

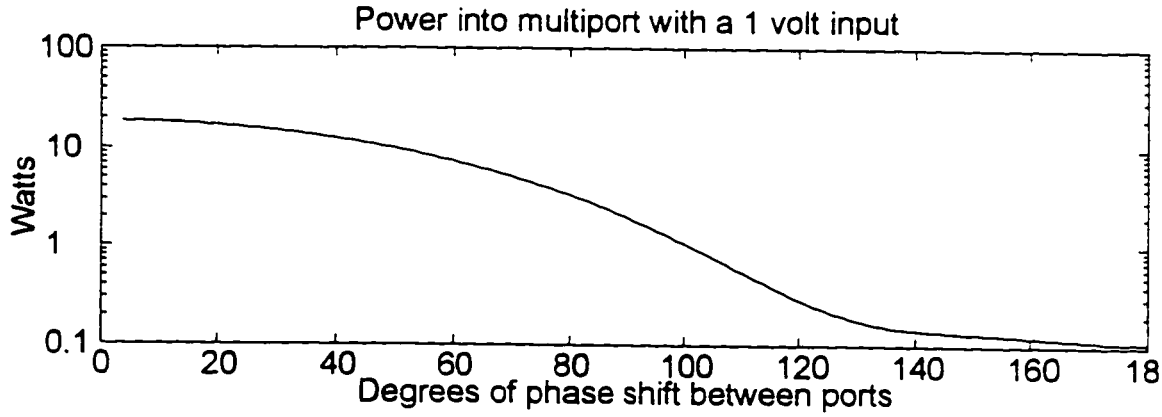

FIGURE 53. Power, driven by a progressive phase source.

If it is desired to deliver a constant power to network, regardless of the input phasing, (for an antenna, if the transmitted power is to remain the same as the beam is steered), a lot more voltage drive will be needed as the phase shift between ports increases.

Figure 54 shows the electrical characteristics of the network when one watt is delivered to the network, with a uniform voltage and a range of progressive phasing applied., Note that the power, and the real part of the impedance, are actually negative for some ports at some phasing.

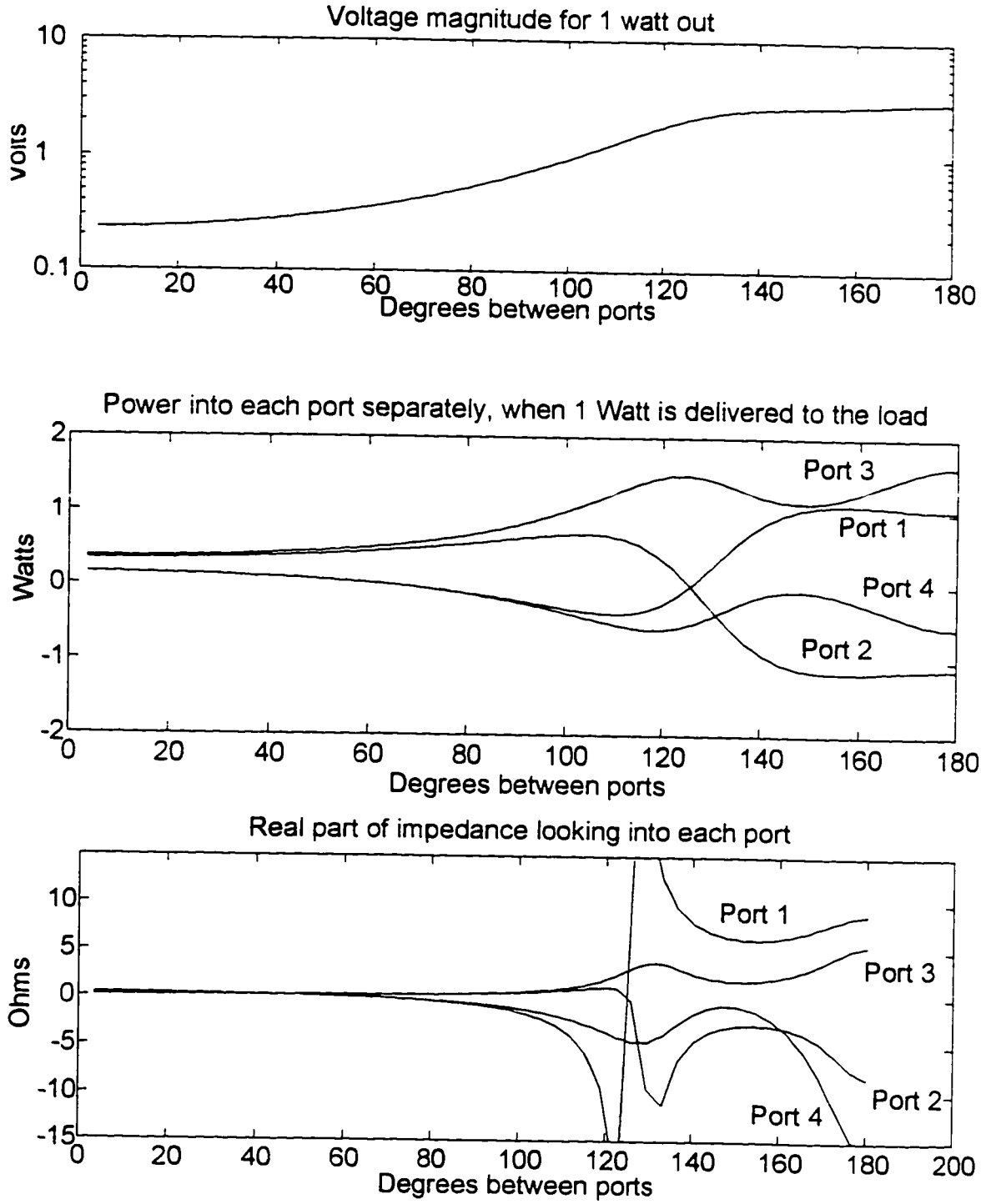

FIGURE 54. Electrical characteristics of the multiport load

The behavior of the load with phasing difference makes it difficult to design a source to deliver the desired signal to the load. The source must be able to sink power as well as source it, and remain stable with all kinds of load impedances.

If a coupling network is placed between the source and the load, and this coupling network has a scattering matrix given by

$$S_{coupling} = \begin{bmatrix} -0.94 & 0 & 0 & 0 & -0.24 & 0.23 & -0.12 & 0.02 \\ 0 & -0.998 & 0 & 0 & 0.01 & 0 & -0.02 & 0.05 \\ 0 & 0 & -0.62 & 0 & -0.50 & -0.34 & 0.40 & 0.28 \\ 0 & 0 & 0 & 0.69 & 0.20 & 0.45 & 0.49 & 0.20 \\ -0.24 & 0.01 & -0.50 & 0.20 & 0.69 & -0.37 & -0.20 & -0.04 \\ 0.23 & 0 & -0.34 & 0.45 & -0.37 & 0.25 & -0.61 & -0.24 \\ -0.12 & -0.02 & 0.40 & 0.49 & -0.20 & -0.61 & 0.12 & -0.39 \\ 0.02 & 0.05 & 0.28 & 0.20 & -0.04 & -0.24 & -0.39 & 0.82 \end{bmatrix}, \quad \text{(EQ 94)}$$

The coupling network can be driven by a source to produce the same voltages on the load as before. At the input to the coupling network, Figure 55 describes the electrical characteristics.

The coupling network of Equation 94 cancels out the mutual coupling of the load, so that looking into the coupling network, the source sees four, isolated, one ohm resistors. The impedance at each port, seen by the source, is a resistive 1 ohm, no matter what the excitation.

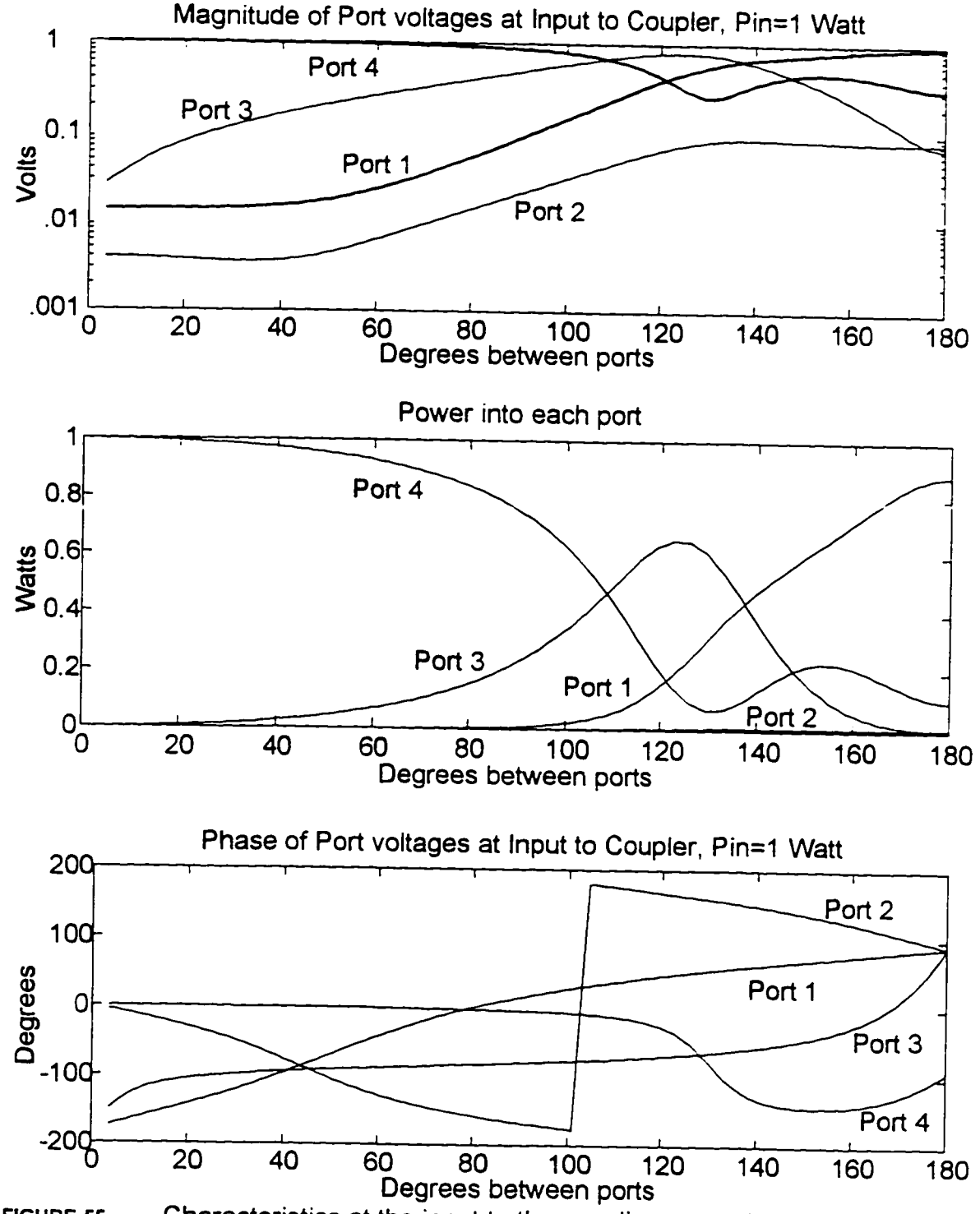

FIGURE 55. Characteristics at the input to the coupling network,.

To demonstrate that the coupling network of Equation 94 is not an impossible idealization, Figure 56 indicates, (roughly,) what the coupling network might look like, where it implemented at microwave frequencies.

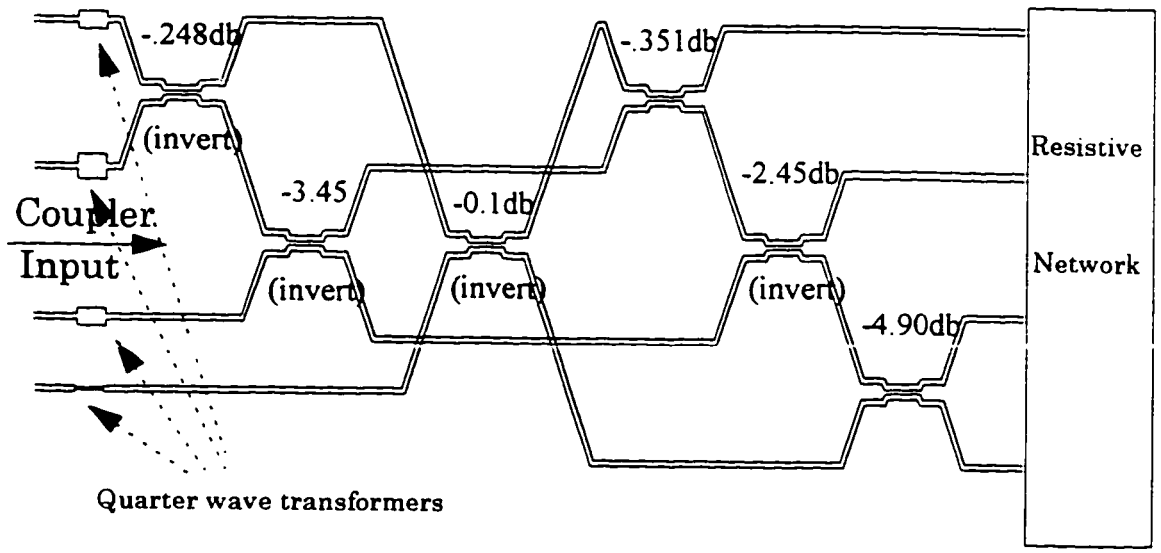

FIGURE 56. A possible printed circuit layout for the coupling network

Appendix XI Matching constraints for series and parallel RLC loads.

The load in question is a parallel resonant circuit:

$$Z = \frac{1}{C}\frac{s}{\left(s^2 + \frac{w_0}{Q}s + w_0^2\right)} \qquad \text{(EQ 95)}$$

The squared magnitude of Z is a function of frequency squared, and is given by

$$|Z|^2 = \frac{Q^2 X}{(CQ)^2 X^2 + (Cw_0)^2(2Q^2 - 1)X + (CQw_0^2)^2}. \qquad \text{(EQ 96)}$$

Here, X is radian frequency squared.

The parameters of Equation 96 can be found from the measured curve of the magnitude of Z. To do this, notice that the impedance magnitude reaches a maximum at

$$X = w_0^2. \qquad \text{(EQ 97)}$$

The value of the impedance at this frequency is

$$|Z(X)|^2|_{max} = \left(\frac{Q}{Cw_0}\right)^2. \qquad \text{(EQ 98)}$$

At two frequencies on either side of the center, the impedance squared is half this minimum. The difference in X at these two frequencies is

$$freq_{high} - freq_{low} = \frac{w_0}{Q}.$$

By measuring the maximum frequency, the bandwidth, and the maximum impedance, The following parameters result

$$w_0 = maximum \text{ frequency}$$

$$Q = \frac{w_0}{\text{difference in freqencies}}$$

$$C = \frac{Q}{w_0 maximum \text{ impedance}} \qquad \text{(EQ 99)}$$

XI.1 Matching characteristics for the parallel resonance

The even part of the load is given by

$$r2 = Ev(Z) = \frac{w_0}{CQ} \frac{s^2}{s^4 + \frac{2(w_0 Q)^2 - w_0^2}{Q^2} s^2 + w_0^4} \qquad \text{(EQ 100)}$$

The zeros of transmission of the load are given by the RHP zeros of

$$W = \frac{Ev(Z)}{Z} = \frac{w_0 s}{Qs^2 + w_0 s + Q w_0^2} \qquad \text{(EQ 101)}$$

There is a order 1 zero at zero, where Z is zero. Therefore this is a class 2 zero.

There is also an order 1 zero at infinity, where Z is zero. This is also a class 2 zero.

The A function is constructed from the RHP poles of Z(-s). These are at the points

$$s_{\text{transmission zero}} = \frac{w_0}{2Q}(1 \pm \sqrt{1 - 4Q^2}) \qquad \text{(EQ 102)}$$

Therefore A is simply

$$A = \frac{s^2 - \frac{w_0}{Q}s + w_0^2}{s^2 + \frac{w_0}{Q}s + w_0^2} \quad \text{(EQ 103)}$$

The A function can be expanded about zero, where its first few terms are

$$A_0 = 1, A_1 = -\frac{2}{w_0 Q}, and, A_2 = \frac{2}{(Qw_0)^2}. \quad \text{(EQ 104)}$$

The A function expanded around infinity yields the terms

$$A_0 = 1, A_1 = -\frac{2w_0}{Q}, and, A_2 = \frac{2w_0^2}{Q^2}. \quad \text{(EQ 105)}$$

The F function is 2*r2*A, which is

$$F = \frac{numer}{denom}, \text{ where}$$

$$numer = (-2q^2w0s^4 + 2qw0^2s^3 + -2q^2w0^3s^2), \text{ and}$$

$$denom = cq^3s^6 + cq^2w0s^5 + (3cw0^2q^3 - cw0^2q)s^4 + (2cw0^3q^2 - cw0^3)s^3 + ((3cw0^4q^3 - cw0^4q)s^2 + cw0^5q^2s + cw0^6q^3) \quad \text{(EQ 106)}$$

The F function can be expanded around zero, where its first few terms are

$$F_0 = 0, F_1 = 0, and, F_2 = -\frac{2}{Qw_0^3 C}. \quad \text{(EQ 107)}$$

Also, the F function can be expanded around infinity, where its first few terms are

$$F_0 = 0, F_1 = 0, and, F_2 = -\frac{2w_0}{QC}. \quad \text{(EQ 108)}$$

Let p_1 be the first term in the expansion of the reflection coefficient at the back end of the matching network. Then Youla's first constraints are that the reflection coefficient go to total reflection where there is no power gain, at DC and s=infinity. The other coefficient constraints for the class 2 zeros are

$$\frac{(A_1 - p_1)}{F_2} \equiv \frac{-\frac{2}{w_0 Q} - p1}{-\frac{2}{Q w_0^3 C}} \geq 0, \text{ or } p_{zero1} \geq \frac{-2}{Q w_0}, \text{ at s = zero, and}$$

$$\frac{-\frac{2w_0}{Q} - p1}{-\frac{2w_0}{QC}} \geq 0 \text{ , or } p_{inf1} \geq \frac{-2w_0}{Q}, \text{ at } s = \infty \qquad \text{(EQ 109)}$$

The power gain function, which determines the reflection coefficient, is constrained by these equations. Now, matching constraints can be determined for any power gain function. To determine the constraints, (for bandpass types of power gains), only two things about the reflection coefficient must be known: the slope at s=zero and the slope at s=infinity.

Consider a bandpass reflection coefficient, expressed as a rational function. Choosing a monic denominator does not loose generality. The reflection coefficient goes to unity at DC and at infinity. This means that the highest coefficient of the numerator must be unity, and that the lowest coefficients of numerator and denominator must be equal. Therefore the reflection coefficient could be written

$$\rho(s) = \frac{s^n + b_{n-1}s^{n-1} + b_{n-2}s^{n-2} + \ldots + b_3 s^3 + b_2 s^2 + b_1 s + x}{s^n + a_{n-1}s^{n-1} + a_{n-2}s^{n-2} + \ldots + a_3 s^3 + a_2 s^2 + a_1 s + x} \quad \text{(EQ 110)}$$

Now, limit the reflection coefficient to one that comes from the low pass to band pass transformation, with the center frequency of the transformation equal to unity. The transformation is

$$s \rightarrow \frac{s^2 + 1}{BWs}, \quad \text{(EQ 111)}$$

therefore, a polynomial of the form $a_n s^n + a_{n-1}s^{n-1} + \ldots + a_2 s^2 + a_1 s + a_0$, after scaling, becomes a polynomial $As^{2n} + Bs^{2n-1} + Cs^{2n-2} + \ldots + C + Bs + A$. In this case, the transformation always creates polynomials that are symmetrical about their centers. A reflection coefficient derived with this transformation then has the form

$$\rho(s) = \frac{s^n + b_{n-1}s^{n-1} + b_{n-2}s^{n-2} + \ldots + b_{n-2}s^2 + b_{n-1}s + 1}{s^n + a_{n-1}s^{n-1} + a_{n-2}s^{n-2} + \ldots + a_{n-2}s^2 + a_{n-1}s + 1}. \quad \text{(EQ 112)}$$

Expanding this reflection coefficient around zero and infinity yields the same result for the first few terms. In particular, the first non-constant term, the slope of the response, is simply

$$\rho_1 = a_{n-1} - b_{n-1} \quad \text{,around zero and around infinity.} \quad \text{(EQ 113)}$$

To proceed, the two coefficients of Equation 113 must be known.

For any reflection coefficient derived from a known all pole low pass prototype like a Butterworth or Chebyshev function, the minimum phase

reflection coefficient is fairly easy to find from tables of the prototype coefficients. The denominator coefficients come directly from the tables (or from the table, through the low pass to band pass transform for the bandpass case). If the reflection coefficient is minimum phase, then the numerator coefficients can be calculated from the denominator coefficients and the gain factor of the match. There are two possible added complexities, though:

- Some of the lhp zeros of the minimum phase reflection coefficient could be moved to the RHP, causing no change in the denominator, but changing the numerator.

- An all pass function can be multiplied into the reflection coefficient, increasing the degree of both the numerator and denominator, but not changing the j-axis behavior of the reflection coefficient, or the power gain of the resulting design.

XI.2 Chebyshev reflection coefficients

For the minimum phase band pass reflection coefficient, the reflection coefficient defined by Chen[41,Equation 94] is used. With n the degree of the low pass prototype,

$$p(s) = \frac{As^{2n} + Bs^{2n-1} + \ldots + Bs + A}{Cs^{2n} + Ds^{2n-1} + \ldots + Ds + C} \cdot \qquad \text{(EQ 114)}$$

Where

$$A = C = 1$$

$$D = \frac{\sinh\left(\frac{1}{n}\operatorname{asinh}\frac{1}{\varepsilon}\right)}{\delta \sin\frac{\pi}{2n}}$$

$$B = \frac{\sinh\left(\frac{1}{n}\operatorname{asinh}\frac{\sqrt{(1-K)}}{\varepsilon}\right)}{\delta \sin\frac{\pi}{2n}}$$

(EQ 115)

Here ε is the Chebyshev ripple factor, and δ is the reciprocal of the / bandwidth of the power gain. Then the slope of the reflection coefficient at both zero and infinity becomes

$$\rho_1 = B - D = \frac{1}{\delta \sin\frac{\pi}{2n}}\left(\sinh\left(\frac{1}{n}\operatorname{asinh}\frac{\sqrt{(1-K)}}{\varepsilon}\right) - \sinh\left(\frac{1}{n}\operatorname{asinh}\frac{1}{\varepsilon}\right)\right)$$

(EQ 116)

The gain can be computed when $X = \frac{-2}{Qw_0}$ or $\frac{-2w_0}{Q}$ is known, then the maximum gain is given by the lesser of

$$\Phi = \operatorname{asinh}\left(\sinh\left(\frac{\operatorname{asinh}\varepsilon^{-1}}{n}\right) + X\delta\sin\left(\frac{1}{2}\frac{\pi}{n}\right)\right)$$

$$Gain_{max} = 1 - (\varepsilon \sinh(n\Phi))^2$$

(EQ 117)

The conditions for a possible match are revealed by considering when a positive, non-zero gain results from Equation 117. A match is possible as the bandwidth of Chebyshev power gain gets larger and larger, (the gain just gets smaller and smaller). However, surprisingly, as the bandwidth of the power gain gets smaller and smaller, the gain, after rising to unity, also begins to be

forced smaller. The bandwidth must be larger than the limits given in Equation 118, or no match is possible at all.

$$Bandwidth > \frac{\sinh\frac{\operatorname{asinh}\frac{1}{\varepsilon}}{n}}{\frac{w_0}{Q}\sin\frac{\pi}{2n}}$$

$$Bandwidth > \frac{\sinh\frac{\operatorname{asinh}\frac{1}{\varepsilon}}{n}}{\frac{1}{Qw_0}\sin\frac{\pi}{2n}} \qquad \text{(EQ 118)}$$

Now, a reflection coefficient with second order real regular all pass[41, Equation 99] is considered;

$$p(s) = \frac{As^{2n+2} + Bs^{2n+1} + \ldots + Bs + A}{Cs^{2n+2} + Ds^{2n+1} + \ldots + Ds + C} \qquad \text{(EQ 119)}$$

where,

$$A = C = 1$$

$$D = \frac{\sinh\left(\frac{1}{n}\operatorname{asinh}\frac{1}{\varepsilon}\right)}{\delta\sin\frac{\pi}{2n}} + \frac{\sigma}{\delta}$$

$$B = \frac{\sinh\left(\frac{1}{n}\operatorname{asinh}\frac{1}{\frac{\varepsilon}{\sqrt{(1-K)}}}\right)}{\delta\sin\frac{\pi}{2n}} - \frac{\sigma}{\delta} \qquad \text{(EQ 120)}$$

and sigma (non-negative), is the low pass prototype all pass zero frequency.

Then the slope of the reflection coefficient at both zero and infinity becomes

$$\rho_1 = B - D = \frac{1}{\delta \sin\frac{\pi}{2n}}\left(\sinh\left(\frac{1}{n}\operatorname{asinh}\frac{\sqrt{(1-K)}}{\varepsilon}\right) - \sinh\left(\frac{1}{n}\operatorname{asinh}\frac{1}{\varepsilon}\right)\right) \qquad \text{(EQ 121)}$$

The gain can be computed when $X = \frac{-2}{Qw_0}$ or $\frac{-2w_0}{Q}$ is known, then the maximum gain is given by whichever X leads to the smaller of

$$\Phi = \operatorname{asinh}\left(2\sigma \sin\frac{\pi}{2n} + \sinh\left(\frac{\operatorname{asinh}\varepsilon^{-1}}{n}\right) + X\delta \sin\frac{\pi}{2n}\right)$$

$$Gain_{max} = 1 - (\varepsilon \sinh(n\Phi))^2 \qquad \text{(EQ 122)}$$

The gain now depends on the right half plane zero location. The addition of the right half plane zero generally lowers the gain when the bandwidth is wide, but it also allows more gain for narrow bandwidth matches. When sigma is non-zero, a match can no longer be made for an arbitrarily wide bandwidth of Chebyshev power response. The bandwidth of the power gain is now limited as indicated in Equation 123. However, as the bandwidth gets smaller and smaller, a sigma can always be chosen to allow full gain for that bandwidth.

$$\frac{\frac{w_0}{Q}}{\sigma} > Bandwidth > \frac{\frac{w_0}{Q}\sin\frac{\pi}{2n}}{\sinh\frac{\operatorname{asinh}\frac{1}{\varepsilon}}{n} - 2\sigma\sin\frac{\pi}{2n}}$$

and

$$\frac{\frac{1}{w_0 Q}}{\sigma} > Bandwidth > \frac{\frac{1}{w_0 Q}\sin\frac{\pi}{2n}}{\sinh\frac{\operatorname{asinh}\frac{1}{\varepsilon}}{n} - 2\sigma\sin\frac{\pi}{2n}} \qquad \text{(EQ 123)}$$

For a particular w0, q of the load, the gain can be maximized by choosing a particular sigma. A stationary point for sigma that leads to the best gain is

$$\sigma_{best} = \frac{2\frac{w_0}{Q}\delta \sin\frac{\pi}{2n} - \sinh\frac{\operatorname{asinh}\frac{1}{\varepsilon}}{n}}{2\sin\frac{\pi}{2n}} \quad \text{(EQ 124)}$$

The positive best sigma only exists, though, if

$$Bandwidth < \frac{2\frac{w_0}{Q}\sin\frac{\pi}{2n}}{\sinh\frac{\operatorname{asinh}\frac{1}{\varepsilon}}{n}}$$

and

$$Bandwidth < \frac{2\frac{1}{w_0 Q}\sin\frac{\pi}{2n}}{\sinh\frac{\operatorname{asinh}\frac{1}{\varepsilon}}{n}} \quad \text{(EQ 125)}$$

If there is a best sigma, it is chosen using Equation 124 and the gain in this case will be one. Otherwise, the right half plane point does no good, sigma is set to zero and the gain is calculated from Equation 122.

XI.3 Bandpass matching constraints for a series RLC load.

The series case is dual to the parallel one.

The load in question is a series resonant circuit.

$$Z = \frac{L}{s}\left(s^2 + \frac{w_0}{Q}s + w_0^2\right) \quad \text{(EQ 126)}$$

The squared magnitude of Z is a function of frequency squared, and is given by

$$|Z|^2 = \frac{(LQ)^2X^2 - (Lw_0)^2(2Q^2-1)X + (LQw_0^2)^2}{Q^2X} \quad \text{(EQ 127)}$$

Where X is radian frequency squared.

The parameters of Equation 126 can be found from the measured curve of the magnitude of Z. To do this, notice that the impedance magnitude reaches a minimum at

$$X = w_0^2. \quad \text{(EQ 128)}$$

The value of the impedance at this frequency is

$$|Z(X)|^2|_{min} = \left(\frac{Lw_0}{Q}\right)^2. \quad \text{(EQ 129)}$$

At two frequencies on either side of the center, the impedance squared is twice this minimum. The difference in X at these two frequencies is

$$freq_{high} - freq_{low} = \frac{w_0}{Q}.$$

So, by measuring the minimum frequency, the bandwidth, and the minimum impedance, The following parameters result

$$w_0 = \text{minimum frequency}$$

$$Q = \frac{w_0}{\text{difference in freqencies}}$$

$$L = \text{minimum impedance } \frac{Q}{w_0}$$

(EQ 130)

XI.4 Matching characteristics

The even part of the load is given by

$$r2 = Ev(Z) = L\frac{w_0}{Q}. \qquad \text{(EQ 131)}$$

The zeros of transmission of the load are given by the RHP zeros of

$$W = \frac{w_0 s}{Qs^2 + w_0 s + Qw_0^2}. \qquad \text{(EQ 132)}$$

There is a order 1 zero at zero, where Z is infinite. Therefore this is a class 4 zero.

There is also an order 1 zero at infinity, where Z is infinite. This is also a class 4 zero.

The residue of Z at zero is Lw_0^2. The residue of Z at infinity is L.

The A function is constructed from the RHP poles of Z(-s). There are none of these. Therefore A is simply unity. The F function is 2*r2*A, which is

$2r2 = 2L\frac{w_0}{Q}$.

The coefficient constraints are

$$\frac{F_0}{A_1 - p_1} \equiv \frac{2L\frac{w_0}{Q}}{0 - p_1} \geq L w_0^2, \text{ or } 0 > p_{zero1} \geq \frac{-2}{Q w_0}, \text{ at s = zero, and}$$

$$\frac{2L\frac{w_0}{Q}}{0 - p_1} \geq L \text{ , or } 0 > p_{inf1} \geq \frac{-2w_0}{Q}, \text{ at } s = \infty$$

(EQ 133)

Not surprisingly, these constraints are very similar to those for the parallel case. The only difference is that the reflection coefficient slope is limited from above: it must be negative at both DC and infinity, while there was no upper limit for the parallel case.

The parallel results are applicable here, as might be expected. Since the series load is dual to the parallel case, a dual, (or reciprocal), matching network derived for the parallel case could be used directly for the series case.

The design of the matching network follows the determination of the gain of the match and the zero frequency of any extra all pass function. To complete the design,

- The low pass Chebyshev power gain function with gain=1 is created from Chebyshev polynomials of the first kind.

- This is converted to a band pass response, using the low pass to band pass transformation, with the center frequency=1.

- A reflection coefficient is formed from 1 minus the power gain, scaled by the gain parameter, which is determined by the above coefficient constraints.

- If an all pass function is used, it is multiplied into the reflection coefficient.

- The back end impedance of the matching network is determined from the reflection coefficient and the load impedance.

- The matching network is realized as a lossless network terminated in a resistor using cascade synthesis.

XI.5 Butterworth reflection coefficient constraints

The minimum phase, Butterworth, bandpass reflection coefficient defined by Larry Augustine[11] is used here. With n the degree of the low pass prototype,

$$p(s) = \frac{As^{2n} + Bs^{2n-1} + \ldots + Bs + A}{Cs^{2n} + Ds^{2n-1} + \ldots + Ds + C} \qquad \text{(EQ 134)}$$

Where

$$A = C = 1$$

$$D = a_{n-1} Bandwidth$$

$$B = a_{n-1} Bandwidth \; d \qquad \text{(EQ 135)}$$

Where Bandwidth is the bandwidth of the low pass to band pass transformation, or the bandwidth of the desired power gain, $d = (1 - gain)^{\frac{1}{2n}}$ and $a_{n-1} = \frac{1}{\sin\left(\frac{\pi}{2n}\right)}$ is the coefficient of the s^{n-1} th term of the Butterworth lowpass denominator polynomial. Then the slope of the reflection coefficient at both zero and infinity becomes

$$\rho_1 = B - D = \frac{1}{\sin\left(\frac{\pi}{2n}\right)} Bandwidth\left((1 - gain)^{\frac{1}{2n}} - 1 \right) \quad \text{(EQ 136)}$$

The gain can be computed when $X = \frac{-2}{Qw_0}$ or $\frac{-2w_0}{Q}$ is known, then the maximum gain is given by

$$gain = 1 - \left(\frac{X \sin\left(\frac{\pi}{2n}\right) + Bandwidth}{Bandwidth} \right)^{2n} \quad \text{(EQ 137)}$$

As the bandwidth gets larger, the gain falls off. However, the bandwidth must be greater than

$$Bandwidth > \frac{w_0 \sin\frac{1}{2n}}{Q}$$

$$and$$

$$Bandwidth > \frac{\sin\frac{1}{2n}}{Qw_0} \quad \text{(EQ 138)}$$

for any match at all to be made. It is likely that the use of an all pass function in the reflection coefficient will remove this limitation. To this end, we can use the Butterworth bandpass coefficient with an all pass function given

by Chen[41, Equation. 23]. There, the coefficient of the 1/s term in the expansion of the reflection coefficient about infinity is given as

$$\rho_1 = \frac{1}{\sin\left(\frac{\pi}{2n}\right)} Bandwidth\left((1 - gain)^{\frac{1}{2n}} - 1 \right) - 2\sigma \quad \text{(EQ 139)}$$

Where Bandwidth is the bandwidth of the low pass to band pass transformation, and sigma is the right half plane zero location of the low pass all pass function. Again, the all pass function allows matching for very small bandwidths, as in the Chebyshev case. The gain is now given by

$$gain = 1 - \left(\frac{X \sin\left(\frac{\pi}{2n}\right) + Bandwidth + 2\sigma \sin\left(\frac{\pi}{2n}\right)}{Bandwidth} \right)^{2n} \quad \text{(EQ 140)}$$

Which, for larger bandwidths, will be less than Equation 137, but allows a match for smaller bandwidths than Equation 137. To find the value of sigma that maximizes the gain, the derivative of Equation 140 can be set to zero, and it is found that

$$\sigma_{best} = -\frac{1}{2}\left(\frac{X \sin\left(\frac{1}{2n}\right) + Bandwidth}{\sin\left(\frac{1}{2n}\right)} \right), \quad \text{(EQ 141)}$$

which leads to unity gain when sigma is positive.

Once the gain is known, a series of steps similar to those for the Chebyshev matching can be followed to determine the matching network.

Vita

Clifford R. Curry was born in Wichita, KS. He received the B. S. E. E. degree from the University of Illinois in 1975 and M. S. E. E. degree from Wichita State University, Wichita, KS., in 1977.

Form 1978 to 1980 he was a Design Engineer at John Fluke Manufacturing Company in Everett, WA. From 1980 to 1984 he designed ultrasonic imaging medical equipment for Advanced Technology Laboratories in Bellevue, WA. From 1985 to 1990 he was Principal Engineer at Quinton Instrument Company in Seattle, WA, designing patient monitoring instrumentation for cardiology applications. Since 1991 he has been a Research Assistant the University of Washington.